AN ANALYSIS OF PLUTONIUM RECYCLE FUEL ELEMENTS IN SAN ONOFRE - I

MASSACHUSETTS INSTITUTE OF TECHNOLOGY
DEPARTMENT OF NUCLEAR ENGINEERING
CAMBRIDGE, MASSACHUSETTS 02139

AN ANALYSIS OF PLUTONIUM RECYCLE FUEL ELEMENTS IN SAN ONOFRE-I

by

Bruce F. Momsen
David D. Lanning
Edward E. Pilat *

May 1974

MITNE-161

---

* Yankee Atomic Electric Co.

AN ANALYSIS OF PLUTONIUM RECYCLE FUEL ELEMENTS IN SAN ONOFRE - I

by

Bruce F. Momsen
David D. Lanning
Edward E. Pilat

ABSTRACT

A method has been developed to allow independent assessment of the use of plutonium recycle assemblies in operating reactors. This method utilizes Generalized Mixed Number Density (GMND) cross sections (based on Breen's Mixed Number Density cross sections) and the spectrum code LASER.

LASER is modified to form LASER-M by adding ENDF/B-II thermal cross sections for the plutonium isotopes; adding edits to output GMND cross sections, approximate microscopic removal and transport cross sections; and increasing LASERs compatibility with commonly used diffusion theory codes such as PDQ.

Plutonium critical experiments for a number of lattices of 1.5 w/o and 6.6 w/o plutonium are analysed with LASER-M which is found to give better criticality agreement than LASER (without the ENDF/B-II plutonium cross sections) and other published data.

Unit assembly power distributions are calculated for a uranium assembly and a constant and graded enrichment plutonium assembly both surrounded by uranium assemblies. The use of LASER-M with GMND cross sections is found to give excellent agreement with the published calculations of power distributions for the uranium assembly and good agreement for the plutonium assemblies.

A quarter core depletion calculation of the San Onofre reactor containing four plutonium recycle demonstration assemblies is performed using the diffusion theory computer code PDQ-7. Use of PDQ-7 with GMND cross sections from LASER-M is shown to give excellent agreement with quasi experimental power distributions at cycle burnups of 0 MWD/MTM, 3342 MWD/MTM, and 6045 MWD/MTM. Also, the calculated value of k-eff versus cycle burnup is determined to be in excellent agreement with the actual operating condition of k-eff = 1.000.

ACKNOWLEDGEMENTS

The work described in this report has been performed primarily by the principal author, B. F. Momsen, who has submitted substantially the same report in partial fulfillment of the requirements for the Nuclear Engineer and Master of Science degrees at M.I.T.

The principal author gratefully acknowledges the financial support received for this study. The majority of the computer and related costs of this study, as well as a summer Research Assistantship for the principal author, were shared equally by the NUS Corporation and Southern California Edison. Additionally, the principal author gratefully acknowledges the timely and generous financial support of the Yankee Atomic Electric Company which provided funds for the costly quarter core depletion.

The principal author would like to thank Bill Flournoy of SCE for his work in the processing of the ENDF/B-II cross sections, and his constant willingness to supply the principal author with information required to complete this study. The principal author would also like to thank Alex Deng and Steve Bauer of SCE and Ray Sullivan of NUS for their assistance in this study.

Additionally, special thanks go to Brian Kirschner of Yankee Atomic whose valuable assistance in the final quarter core depletion was greatly appreciated.

The principal author wishes to express his appreciation to the many typists who have assisted in the completion of the final manuscript and a special word of thanks to Joan Johnson whose help was greatly appreciated.

Finally, the principal author would like to express his very special gratitude and appreciation to his wife, Ms. Linda Foster Momsen, whose life the principal author can now share in much more than while completing this study.

TABLE OF CONTENTS

LIST OF FIGURES

FIGURE PAGE

LIST OF TABLES

TABLES PAGE

CHAPTER 1

INTRODUCTION

1.1 Project Description

With the rapid growth of the nuclear power industry, increasing quantities of plutonium are quickly becoming available in the U. S. The importance of plutonium as an energy source for thermal reactors has been recognized by various groups who have included plutonium utilization in their power planning. In addition to the economic incentive, the available plutonium can constitute a significant fraction of the light water reactor (LWR) fuel required to meet future energy demands.[1] Additionally, the timely utilization of plutonium can delay the need for additional uranium enrichment capacity in the U. S.

Neutronic design methods which have been developed for use in uranium fueled LWRs cannot be applied, a priori, to reactors utilizing recycled plutonium. Government laboratories in several nations, as well as private industry, have carried out extensive programs to study and demonstrate the feasibility of plutonium recycle. To date, the most current review and analysis of the available experimental reactor physics data related to problems

of plutonium recycle is given by Uotinen, et al.[2] As a result of these experimental and calculational neutronics studies good progress has been made in assessing expected design method uncertainties.

In the present study an analysis of the four plutonium recycle fuel elements which were in the San Onofre pressurized water reactor (PWR) during cycles 2 and 3 was carried out. These assemblies were 14 by 14, graded enrichment mixed oxide (MOX) assemblies with an average of 3.53 w/o plutonium mixed with natural uranium in the form of dished pellets as described in Ref. 3. Figure 1.1 shows a quarter of the MOX assembly and the specifications of the plutonium and uranium fuel rods are given in Table 1.1 with supplementary data in Appendix A.

1.2 Research Objectives

The Edison Electric Institute (EEI) and Westinghouse Electric Corporation have published results of their analysis of the four plutonium assemblies which can be compared to the published results as well as to experimental power distributions in the plutonium assemblies for cycle 2.

In the Westinghouse analysis, an improved version of the spectrum code LEOPARD[4] was used. However, it has been shown by a number of independent workers (Mertens,[5] Celnik, et al.,[6] and Taylor[7]) that the

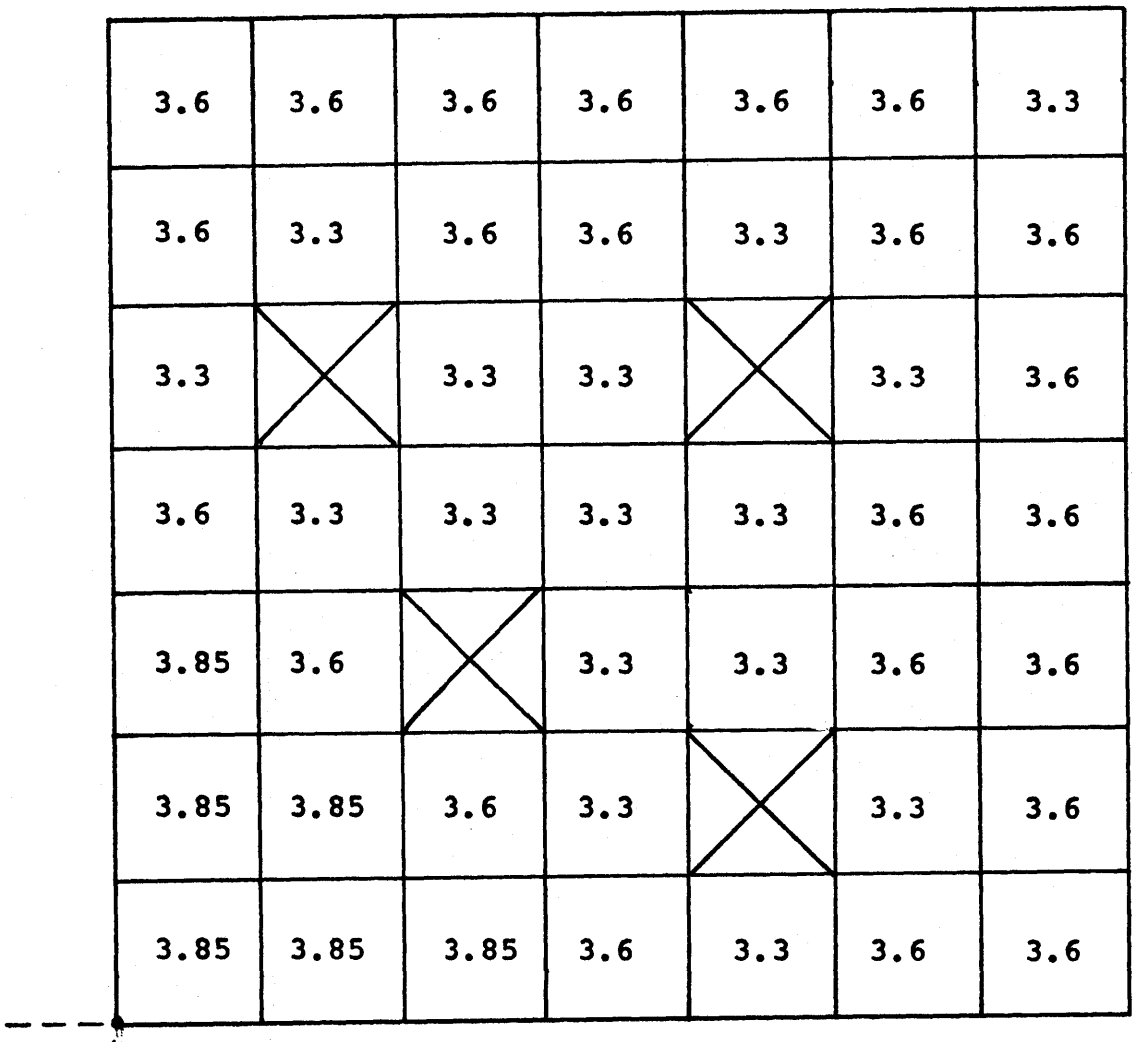

Figure 1.1

Enrichment Pattern for a Quarter of the San Onofre Plutonium Assembly (Ref. 3)

TABLE 1.1

DESIGN PARAMETERS FOR SAN ONOFRE REGION 4 PLUTONIUM AND URANIUM ASSEMBLES (Ref. 3)

Fuel Assemblies	Region 4-Pu Assemblies	Region 4-U Assemblies
Number	4	48
Rod Array	14 X 14	14 X 14
Rods per Assembly (fueled)	180	180
Rod Pitch (in.)	0.556	0.556
Number of Grids per Assembly	7	7
Fuel Rods		
Clad Material	Zircaloy-4	304 SS
Outside Diameter, in.	0.422	0.422
Diametral Gap, in.	0.0075	0.0055
Clad Thickness, in.	0.0243	0.0165
Fuel Length, in.	119.4	120.0
Fuel Pellets		
Diameter, in.	0.3659	0.3835
Material	PuO_2-UO_2	UO_2
Density (% of Theoretical)	91	93
Enrichment - rods/assembly (total)	3.3 w/o - 64 3.6 w/o - 92 3.85 w/o - 24	4.0 w/o - 180
Nominal Isotopics (fresh fuel), a/o		
Pu-239	80.6	
Pu-240	13.4	
Pu-241	5.2	
Pu-242	0.8	

spectrum code LASER[8] shows better agreement than LEOPARD or similar codes when analysing plutonium cells. Therefore, the basic objective of this research is to develop an analysis procedure using LASER which will be as good or better than the Westinghouse analysis.

Since the published results are almost totally limited to power distribution calculations in the plutonium assemblies and surrounding uranium assemblies described in Section 1.1, the analysis carried out in the present work will deal almost exclusively with the power distributions given in Ref. 3. Although power distribution predictions are certainly considered to be of major concern in reactors utilizing plutonium recycle assemblies,[9] other considerations (not analysed here) such as reactivity lifetimes, control requirements, and numerous safety considerations are also of importance.

1.3 Benchmarks

1.3.1 Introduction

The specific benchmarks used for comparative purposes in the present work are briefly discussed in the following subsections. A good compact discussion of almost all presently available neutronics benchmarks for plutonium fuel is contained in Ref. 2 which should be consulted for more detailed benchmark information.

1.3.2 Critical experiments

As discussed in Chapter 3, cross section modifications were carried out in LASER. Because of these modifications and the desire to further ensure that LASER yielded acceptable results when analysing plutonium, a number of critical experiments were analysed. A detailed description of the experimental design and calculated results is discussed in Chapter 4.

1.3.3 Calculated Power Distributions

A major effort of this work was to match the assembly power distributions which were published in the "reference WCAP" report (WCAP-4167-2)[3] for the plutonium recycle fuel elements used in the San Onofre PWR.

The reference WCAP report contains cell powers in

1. a UO_2 quarter assembly containing 4 w/o U-235 in an infinite sea of like assemblies,
2. a quarter of a PuO_2 - UO_2 assembly with a constant enrichment of 3.6 w/o PuO_2 surrounded by UO_2 assemblies with 4 w/o U-235,
3. a quarter of a PuO_2 - UO_2 assembly with enrichment variations (as shown in Fig. 1.1) surrounded by UO_2 assemblies containing 4 w/o U0235.

Additionally, the reference WCAP report contains quarter core power and burnup distributions during cycle 2 (which was the first cycle the plutonium assemblies were present) for the San Onofre PWR.

It should be noted that the power distributions in the reference WCAP report are sometimes misleading and contain information which could not be explained by the calculations done in the present work. A discussion of adjustments to the cell power distributions is presented in Chapter 6 and difficulties in using the quarter core power distributions is discussed in Chapter 8. It is also important to point out that since these power distributions are calculated instead of experimental, the fact that these results are

reproduced by independent calculations does not necessarily mean that the independent calculations are correct. However, since the basic objective of this research was to demonstrate that the results given in the reference WCAP report could be reproduced, these results were used as benchmarks.

1.3.4 "Experimental" Power Distributions

Southern California Edison (SCE) has provided experimental assembly power data for various times during cycle 2 of the San Onofre PWR. This data was used with the quarter core power distributions during cycle 2 calculated by Westinghouse to produce quasi-experimental assembly powers for each assembly in the quarter core. These quasi-experimental power distributions were then used as benchmarks and compared to the calculated assembly power distributions in the quarter core. This procedure is similar to the one normally used to determine the accuracy of calculated assembly power distributions in an operating PWR. A detailed discussion of the procedure is contained in Chapter 8.

1.4 Basic Methods and Assumptions

1.4.1 General Comments on Neutronic Analysis of Plutonium Fuel

In general, neutronic analysis of LWRs fueled with plutonium-enriched rods is expected to be less accurate than an analysis of LWRs fueled with uranium-enriched rods. Basically, this is because more isotopes are present in plutonium-enriched than in uranium-enriched fuel. In addition, the neutron cross sections of the plutonium isotopes have significant resonances at thermal and near thermal energies. This resonance structure complicates the important calculation of the neutron spectra in the plutonium-fueled reactors. Also, in mixed-oxide fuels the interaction of the resonances of uranium and plutonium isotopes in the resonance energy region further complicates the spectrum calculation. Finally, since plutonium dioxide exists in the form of particles in mixed oxide fuel, neutron self-shielding effects due to this particulate form also add to the calculational problems.

In practice, various assumptions and approximations are made which simplify the calculational problems. Some of these assumptions and approximations are inherent in the computer code being used and others

result from uncertainties in input parameters. It has been found that, on the average, the errors due to various approximations act in opposite directions resulting in cancellation of errors. It is obvious that one would like to know the error to be expected when using a certain calculational procedure, but it is usually very difficult to accurately assess. Some information, however, can be obtained from a review of a report by Liikala, et al.,[10] who give a fairly detailed assessment of errors which they expected in their analysis of the numerous critical experiments reported in Ref. 11. These include three enrichments (1.8 w/o, 2.0 w/o, and 5.0 w/o) of plutonium in aluminum - plutonium alloy fuels and five enrichments (2.0 w/o Pu with 8%, 16% and 24% Pu-240; 4 w/o Pu; and 1.5 w/o Pu) of plutonium in uranium dioxide-plutonium dioxide fuels. To this base they added a series of lattice experiments containing UO_2 - 6.6 w/o PuO_2 fuel rods which were done at Westinghouse.[7] Additionally, a number of slightly enriched UO_2 lattice criticals and some aqueous solution critical experiments were analysed to gain further insight into possible systematic errors.

Table 1.2 presents a summary of the approximations analyzed by Liikala as well as the effect they are expected to have on the calculation of k_{eff} for the

various criticals analysed. Whenever possible, the numbers presented in Table 1.2 are those quoted by Liikala for mixed oxide criticals only. The sign of the bias and the method used to arrive at its magnitude are explained in the report by Liikala, but the signed numbers contained in Table 1.2 are given simply to show the relative magnitudes of the errors and the possible cancellation of those errors.

Although the bias values listed in Table 1.2 are intended mainly to illustrate the relative magnitudes of potential errors, it is interesting to note that if midrange values are used for the bias values a total bias of only -0.25% in k_{eff} is obtained (without considering uncertainties in cross section, definition of diffusion coefficient, and use of diffusion theory) illustrating how the errors will often tend to cancel. Translating the information given in Table 1.2 to the San Onofre plutonium assemblies or the criticals calculated in Chapter 4 is, at best, a very uncertain process. However, a rough estimate of the bias in k_{eff} can be obtained by making use of any trends in error and translating the approximations in the codes used in this work (Liikala's codes were fairly similar to those used in

Table 1.2

AREAS OF CALCULATIONAL UNCERTAINTY AND ESTIMATES OF RESULTING BIAS IN THE CALCULATED K_{eff}. (Ref. 10)

AREAS OF CALCULATIONAL UNCERTAINTY	BIAS IN K_{eff} (%)
1. Slowing Down Calculation	
Spatial fast effect neglected	-0.2 to - 0.5
Resonance overlap neglected.	0.0 to - 0.5
2. Thermalization calculation	
Reflecting cell boundary condition assumed	-0.5 to - 0.1
Energy detail	+ 0.1
Upper energy limit of thermalization calculation (Effect of Upscattering Model)	- 0.7
Approximation of anisotropy.	Negligible
3. Leakage Calculation	
Axial leakage representation	0.25
Spatial detail	1.0
Energy detail	-0.5
Diffusion theory assumed accurate.	Suspect*
4. Assumptions Regarding the Geometric Detail of Assemblies	
Fuel assumed homogeneous	0.1 to 0.7
Lattice hardware ignored.	Less than 0.2
5. Uncertainties in Physical Parameters	
Nuetron cross sections of the isotopes	±1.0 to ± 2.0
Definition of diffusion coefficient	±0.5
Axial buckling used to describe the axial leakage	Negligible
Manufacturing tolerances (dimensions, contents, etc) of fuel rods and lattice components.	Assumed to Cancel (randomly distributed)

*NOTE: Since the criticals analysed were all small, high leakage systems, diffusion theory may itself be introducing errors. Liikala concludes that diffusion theory tends to overestimate the leakage for the critical experiments (thus yielding values of K_{eff} which are smaller than transport theory values) but no firm estimate of bias in k_{eff} for mixed oxide criticals was given.

this work). By proceeding along these lines a rough estimate of the bias in k_{eff} of -0.45% for the San Onofre fuel and -0.65% for the 1.5 w/o Pu criticals analysed in Chapter 4 is obtained.

By using these already rough estimates an even more approximate value of error can be obtained by comparing the bias of -0.65% for the 1.5 w/o Pu criticals to the value of 0.541% actually calculated in Chapter 4. If one assumes that the difference in the estimated and calculated values of bias is due to the uncertainties in cross sections and definition of diffusion coefficient (not considered to this point) an estimate of the bias in k_{eff} of 0.75% is obtained for the San Onofre fuel. That is, the analysis of the plutonium cells done in the present study are estimated to yield values of k_{eff} which are 0.75% too high. It should again be emphasized that this is a very rough estimate. Additionally, since lifetime calculations were not an integral part of this work the accuracy of the calculation of k_{eff} is not of paramount importance and enters only through its effect on the relative powers in the various cells and assemblies.

It is instructive to further consider the major differences between uranium and plutonium fueled LWRs. Basically, the much larger thermal

absorption cross sections of the plutonium iostopes yields a harder (i.e. higher average neutron energy) thermal spectrum and a lower total thermal flux in a plutonium fueled reactor than in a uranium fueled reactor. Additionally, the increased resonance structure of the plutonium isotopes results in a more negative Doppler coefficient and the depletion characteristics of a plutonium core differ from those of a uranium core. The effect of these differences on important design parameters is listed in Table 1.3 which also gives a capsule comparison of the differences between uranium and plutonium fueled LWRs. For a more detailed discussion of the problems involved in analysing plutonium-enriched fuel and the general differences in plutonium and uranium fuel the reader should consult Refs. 2, 6, 9, and 10.

1.4.2 Neutron Spectrum Calculation

By far the most commonly used method to solve the neutronics problem in nuclear reactors today is to use diffusion theory with two to four energy groups to calculate the neutron behavior in the various region of the reactor. In order to do the diffusion calculation, varying degrees of cell homogenization and spectrum averaging must be carried out to obtain the group averaged cross sections, $\bar{\sigma}$ or $\bar{\Sigma}$, and volume

TABLE 1.3

CAPSULE COMPARISON OF URANIUM AND PLUTONIUM NUCLEAR DESIGN CHARACTERISTICS (Ref. 3)

PARAMETER	PLUTONIUM CORE	REASON FOR DIFFERENCE
Moderator Temperature Coefficient	More Negative	Increased resonance absorption and spectrum shift
Doppler Coefficient	More Negative	Pu-240 resonances
Cold-to-hot Reactivity Swing	Increased	Larger moderator temperature coefficient
Installed Reactivity	Reduced	Reduced depletion rate - Reactivity saturates
Control Rod Requirement	Increased	Larger moderator and Doppler coefficients
Control Rod Worth	Reduced	Thermal flux reduced
Boron Worth	Reduced	Thermal flux reduced
Xenon Worth	Reduced	Thermal flux reduced
Fission Product Poisons	Increased	Increased yields- Increased resonance absorptions
Local Power Peaking	Increased	Increased water worth

averaged atom number densities, $\bar{N}$s, required as input. The purpose of the neutron spectrum calculation is to determine the energy dependence of the neutron flux, $\phi(E)$, such that group averaged cross sections may be obtained by flux weighting the various cross sections. In general, the group averaged cross sections, $\bar{\sigma}$, which are input to various diffusion codes are calculated in spectrum codes using

$$\bar{\sigma} = \frac{\int_{E_g} \sigma(E)\,\phi(E)\,dE}{\int_{E_g} \phi(E)\,dE} \qquad (1.1)$$

where E_g is the energy range of group g.

From the above it is obvious that the most basic assumption in this method is that the space and energy dependence of the flux are separable since the spectrum (energy) calculation and the diffusion (spatial) calculation are carried out separately.

The neutron spectrum calculation can be done with a wide variety of computer codes which are described in Refs. 12 and 13. Perhaps the most widely used codes in the commercial nuclear power industry are LEOPARD [4] and LASER [8], which are described in Sections 2.3 and 2.1, respectively. These codes have cross section libraries which, in general, contain absorption, fission, and scattering cross sections as well as resonance parameters for the various nuclides at many different energy points. It is im-

portant to note that these cross section libraries are generated from experimental data by flux weighting the experimental data with an assumed neutron spectrum. Then, in the spectrum codes, the neutron spectrum is calculated with varying degrees of rigor and the group averaged cross sections are obtained.

In both LEOPARD and LASER the unit cell which is modeled is assumed to be in an infinite sea of like cells (since zero net current boundary conditions are used) and the fast flux is assumed spatially flat across the cell.

As mentioned in Section 1.2, LASER has been found to calculate plutonium cells more accurately than LEOPARD. Basically, this is because of the difference in the thermal calculation since both codes employ MUFT[14] in the fast region. In the thermal energy range LASER actually calculates, using integral transport theory, the neutron spectrum at up to 14 space points in the cylindrically modeled unit cell, whereas LEOPARD is essentially a zero-dimensional calculation.

In plutonium cells, this spatial calculation is very importnat due to the strong spatial dependence of the plutonium isotopes with burnup. Celnik, et al.,[6] show results for the 6.6 w/o PuO_2- UO_2 Saxton fuel burned to 25,000 MWD/MTM which illustrates this effect. In Celnik's figures, variations in plutonium number densities from the center to the edge of the fuel are shown to be about 20% for Pu-239, 14% for Pu-240, and 110% for Pu-241. Celnik also

states, however, that the errors in representing spatial depletion tend to be canceled by the softer spectrum of the zero-dimensional calculation, with both LEOPARD and LASER giving essentially identical reactivity data as a function of burnup for the Saxton fuel. It should be pointed out that this by no means implies that isotopics (nuclide concentrations of the various isotopes) versus burnup in the two codes also show good agreement (see Sections 4.5 and 7.2 for further discussion).

Another advantage in using LASER lies in the fact that it has an upper thermal energy cutoff of 1.855 eV versus LEOPARDs cutoff of 0.625 eV, allowing the huge Pu-240 resonance at 1.056 eV to be more precisely treated in the thermal region.

In conclusion, it is a generally accepted fact that LASER will more accurately calculate plutonium systems and for that reason LASER was used as the basic spectrum code in this work.

1.4.3 Generalized Mixed Number Density (GMND) Cross Sections

1.4.3.1 Basis of Theory

The Generalized Mixed Number Density (GMND) cross sections were developed by Mertens[5] at M. I. T. and are an extension of the Mixed Number Density (MND) cross section theory developed by Breen.[15] Breen points out that the standard procedure of using regionwise thermal constants with flux and current continuity in diffusion calculations results in a calculated discontinuity of activation at boundaries between dissimilar media.

This is caused by the assumption that the microscopic cross section has an abrupt change in value at the boundary which is a result of doing separate asymptotic spectrum calculations (as discussed in Section 1.4.2) for the various regions. In additional, since the regionwise constants do not account for a softening of spectrum approaching a water gap, the peaking with the normal model may be under estimated by as much as 20%.[15]

Breen shows that the one-group diffusion equation,

$$-D\nabla^2\bar{\phi} + \bar{\Sigma}_t\bar{\phi} = S, \tag{1.2}$$

where $\bar{D}$ and $\bar{\Sigma}_t$ are spectrum averaged values of the diffusion coefficient and macroscopic total cross section, respectively, and S is the thermal source term, may be written as

$$-\frac{\bar{D}}{(\overline{1/v})}\nabla^2\bar{n} + \frac{\bar{\Sigma}_t}{(\overline{1/v})}\bar{n} = S, \tag{1.3}$$

where v = neutron velocity

$\bar{n}$ = spectrum averaged neutron density.

Writing the one-group diffusion equation as in Eq. 1.3 imposes continuity of neutron density and current and thus, for a 1/v absorber, implies that activation continuity ($\sigma\phi$) is obtained.

Breen observed that while the discontinuity of the thermal activation is eliminated by using Eq. 1.3, the calculated activation shapes within a region are essentially those obtained using the normal method (Eq. 1.2) since the characteristic diffusion length

is the same in both cases.

This problem is centered around the fact that the spectrum averaged diffusion coefficient, $\bar{D}$, is more properly defined when averaged over the gradient spectrum ($\nabla\phi(E)$) than the normal flux spectrum ($\phi(E)$). Additionally, comparison to a more rigorous calculation showed that the gradient spectrum seemed to be very near a maxwellian distribution. By using these observations Breen proposed modifying Eq. 1.3 to obtain the diffusion equation of the form

$$-\frac{\bar{D}_{Max}}{(\overline{1/v})_{Max}}\nabla^2\bar{n} + \frac{\Sigma_t}{(\overline{1/v})}\bar{n} = S, \tag{1.4}$$

where the coefficients for the leakage term are averaged over a maxwellian spectrum and the coefficients for the absorption term are averaged over a flux spectrum. Breen states that using Eq. 1.4 results in "quite successful" duplication of activation shapes calculated by more rigorous means.

Equation 1.4, then, is the basis of the MND method. It should be noted that the LEOPARD code includes a calculation of MND cross sections using Breen's method. That is, in LEOPARD,

$$\bar{\Sigma}_a^{MND} = \frac{\bar{\Sigma}_a}{(\overline{1/v})}, \quad \bar{\Sigma}_f^{MND} = \frac{\bar{\Sigma}_f}{(\overline{1/v})} \tag{1.5}$$

and $$\bar{D}^{MND} = \frac{\bar{D}^{Max}}{\overline{(1/v)}^{Max}}, \qquad (1.6)$$

where $\bar{\Sigma}$ = flux spectrum averaged macroscopic cross section

$\overline{(1/v)}$ = flux spectrum averaged 1/v for the cell

$\bar{D}^{Max}$ = maxwellian spectrum averaged diffusion coefficient

$(1/v)^{Max}$ = maxwellian spectrum averaged 1/v for the cell.

Basically, Mertens' GMND method does not automatically assume that the gradient spectrum is close to a maxwellian since in using the method an approximate gradient averaged velocity is calculated. The GMND method is based on the diffusion equation written as

(1.7)

$$- \frac{\bar{D}\nabla^2\bar{n}}{\overline{(1/v)}_g} + \frac{\bar{\Sigma}_t\bar{n}}{\overline{(1/v)}} = S,$$

where the diffusion coefficient, $\bar{D}$, is again averaged over the flux spectrum and $\overline{(1/v)}_g$ is the inverse of the neutron velocity averaged over an approximate gradient spectrum. It should be pointed out that although it would be more proper to average D over a gradient spectrum, this would involve detailed reprogramming of most commonly used codes since they do not calculate the gradient

spectrum in the thermal energy range. To obtain $\overline{(1/v)}_g$, however, one does not require a detailed gradient spectrum since it can be approximated as shown below.

By definition,

$$\overline{(1/v)}_g \equiv \frac{\int \frac{1}{v(E)} \nabla\phi(E)\,dE}{\int \nabla\phi(E)\,dE} , \tag{1.8}$$

and since

$$\nabla\phi(v,E) \cong \frac{\phi(r_1,E) - \phi(r_2,E)}{r_1 - r_2} , \tag{1.9}$$

one can write

$$\overline{(1/v)}_g \cong \frac{\int \frac{\phi(r_1,E)\,dE}{v(r_1,E)} - \int \frac{\phi(r_2,E)\,dE}{v(r_2,E)}}{\int \phi(r,E)\,dE - \int \phi(r_2,E)\,dE} . \tag{1.10}$$

Also, by definition,

$$\bar{\phi}(r) \equiv \int \phi(r,E)\,dE , \tag{1.11}$$

and

$$\bar{n}(r) \equiv \int \frac{\phi(r,E)\,dE}{v(r,E)} . \tag{1.12}$$

Substitution of Eqs. 1.11 and 1.12 into Eq. 1.10 yields

$$\overline{(1/v)}_g \cong \frac{\bar{n}(r_1) - \bar{n}(r_2)}{\phi(r_1) - \phi(r_2)} \tag{1.13}$$

where $\bar{n}(r)$ is the total, spectrum averaged neutron density at point r and $\bar{\phi}(r)$ is the total, spectrum averaged neutron flux at point r.

Although it is not generally true that the average of an inverse of a function is equal to the inverse of the average it is a simple matter (by using the definition of the total flux as the neutron density times the neutron velocity) to show that

$$(\overline{1/v}) = 1/\bar{v} \ , \tag{1.14}$$

so that Eq. 1.13 can be written as

$$\bar{v}_g \cong \frac{\phi(r_1) - \phi(r_2)}{\bar{n}(r_1) - \bar{n}(r_2)} \ , \tag{1.15}$$

where points r_1 and r_2 should be chosen to reflect the change in $\bar{\phi}(r)$ and $\bar{n}(r)$ in the moderator of the cell.

It should be pointed out that the GMND method can be applied using information calculated by LASER since it edits the pointwise total thermal flux and neutron density required to calculate the gradient spectrum average velocity by Eq. 1.15. Additionally, LASER edits pointwise averaged neutron velocity (averaged over the flux spectrum) as well as the cell average of the neutron velocity required for the GMND cross sections. FIGURES 1.2 and 1.3 show the total thermal flux and total neutron density (normalized to one at the center of the cell) for various points in typical plutonium

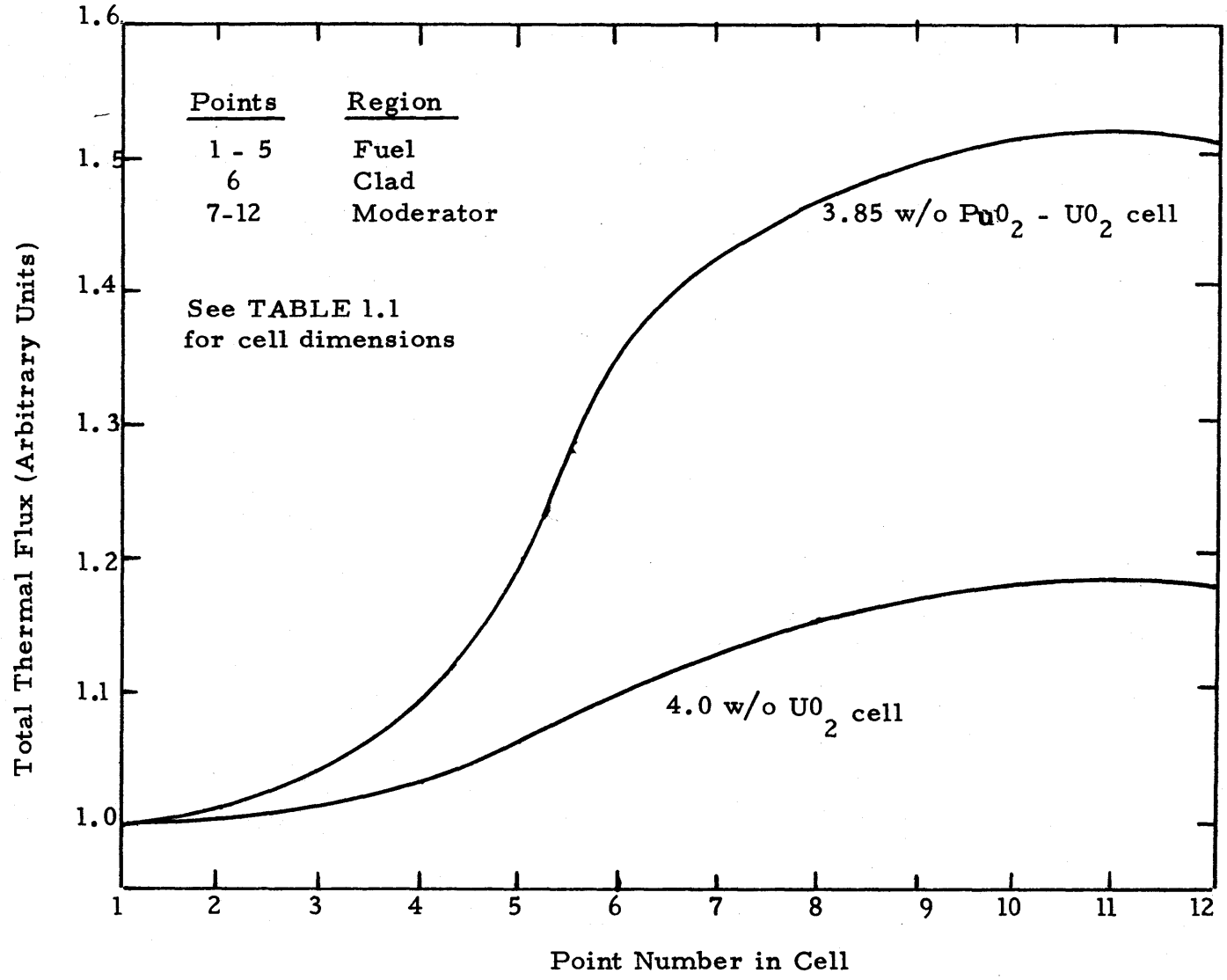

FIGURE 1.2 Total Thermal Flux versus Position in cell for Pu and U cells.

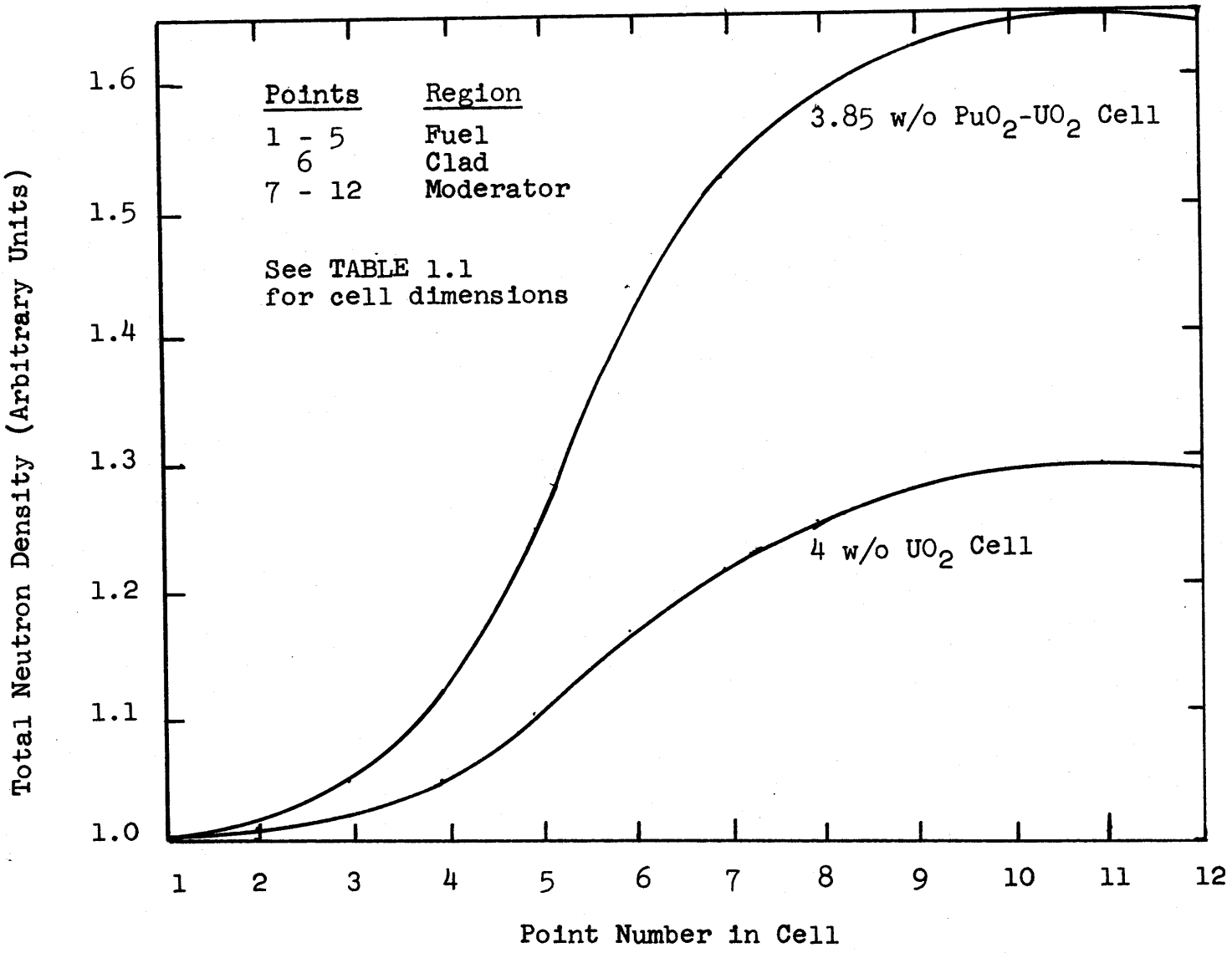

FIGURE 1.3 Total Neutron Density versus Position in Cell for Pu and U Cells

and uranium cells.

It is readily seen from these figures that the plutonium cell shows a much larger flux gradient than the uranium cell. More specifically, by using points 7 and 11 of the moderator in Eq. 1.15 it is found that $\bar{v}_g$ in the uranium is 1.494 (in units of 2200 m/sec) and $\bar{v}_g$ in the plutonium is 1.965 (a 32% difference). FIGURE 1.4 shows how the neutron velocity varies in the plutonium and uranium cell and it is seen that although the plutonium cell has a harder spectrum (higher neutron velocity) the change in velocity with position in the cells is almost identical.

1.4.3.2 General Application

By using Eq. 1.14, Eq. 1.7 can be written as

$$-\bar{D}\,\bar{v}_g\,\nabla^2\,\bar{n} + \bar{\Sigma}_t\bar{v}\bar{n} = S, \tag{1.16}$$

where $\bar{v}$ is the cell average neutron velocity. Modifications to LASER have been done in this study (see subsection 3.3.7) to calculate the GMND cross sections given by

$$\bar{D}^{GMND} = \bar{D}\,\bar{v}_g \tag{1.17}$$

$$\bar{\Sigma}^{GMND} = \bar{\Sigma}\,\bar{v}\quad, \tag{1.18}$$

such that use of GMND cross sections is now a simple matter.

It is easy to show (using the standard two-group diffusion equation) that the units of $\bar{v}_g$ and $\bar{v}$ are completely arbitrary. Thus,

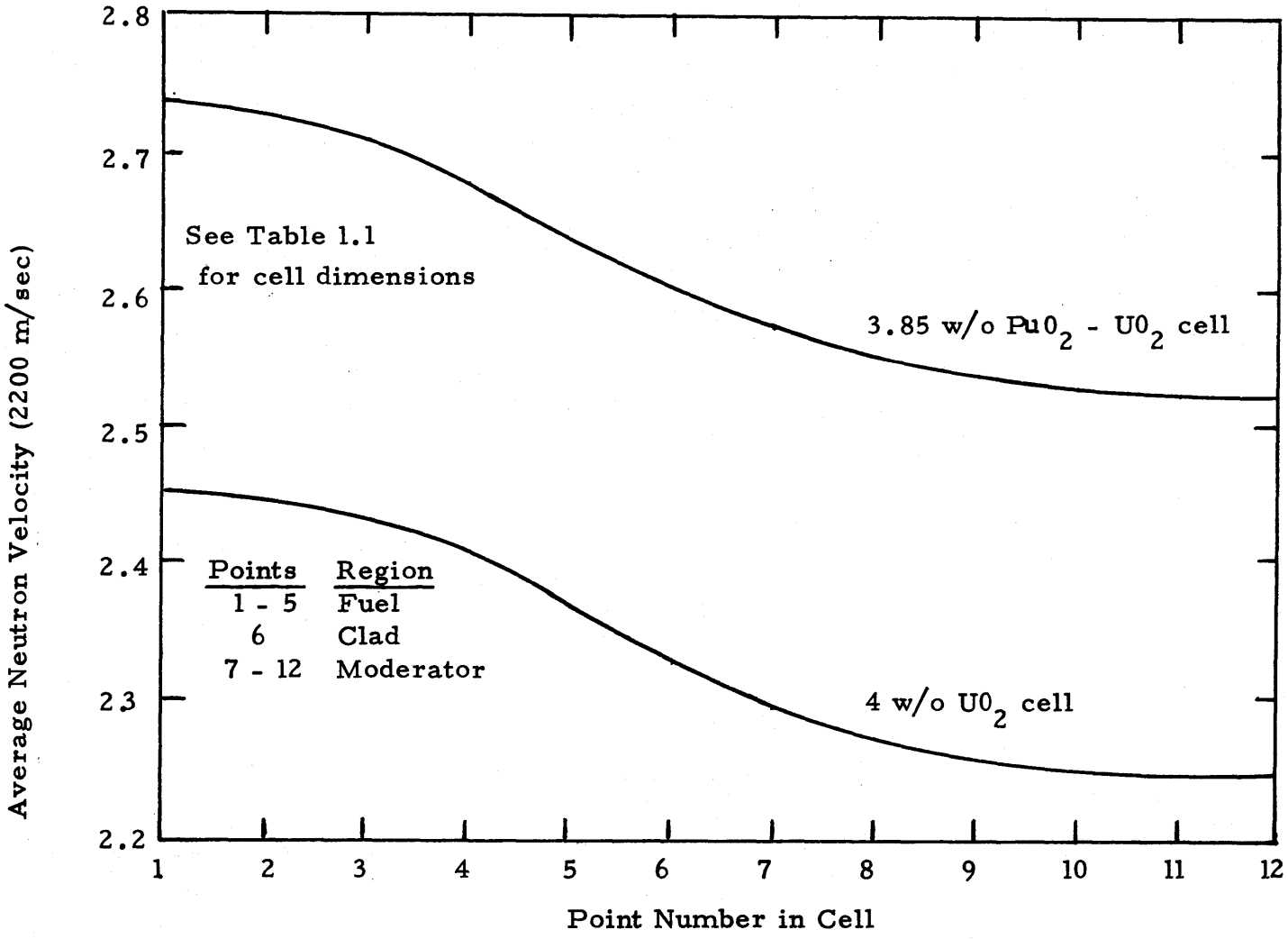

FIGURE 1.4 Average Neutron Velocity versus Position in cell for Pu and U cell.

when using GMND cross sections in diffusion theory codes, they are employed in the thermal group only in a manner completely analgous to the normal cross sections and the effect is to more accurately calculate the power peaking at fuel-water interfaces. It should be noted, however, that the normalization on the thermal flux is also affected such that the cell averaged thermal flux when using GMND cross sections is reduced approximately by a factor of $\bar{v}$.

Mertens also extended the GMND method in an attempt to account for power peaking at the mixed- oxide (MOX) - uranium cell interface. By using arguments similar to those used to obtain Eq. 1.15, it can be shown that the gradient spectrum averaged velocity for a MOX - UO_2 interface, $\bar{v}_{g,Int.}$, can be obtained from

$$\bar{v}_{g,Int.} \cong \frac{\bar{\phi}^{cell}_{UO_2} - \bar{\phi}^{cell}_{Mox}}{\bar{n}^{cell}_{UO_2} - \bar{n}^{cell}_{Mox}} , \qquad (1.19)$$

where $\bar{\phi}^{cell}$ and $\bar{n}^{cell}$ are the cell averaged total flux and neutron density of the individual cells (both cells having the same power). For the plutonium and uranium cells discussed in subsection 1.4.3.1, a value of 2.0202 is obtained for $\bar{v}_{g,Int.}$ by using Eq. 1.19. It is interesting to note that this value is less than 3% higher than $\bar{v}_g$ for the plutonium cell. This implies that to have any effect on the cal-

culation, $\bar{v}_{g,Int.}$ should be used to obtain the GMND diffusion coefficient in the uranium adjacent to the plutonium.

In conclusion, Mertens has shown that by using GMND cross sections the power peaking at fuel-water and MOX-UO_2 interfaces shows reasonable agreement with more rigorous calculations. For this reason, GMND cross sections have been used in this work. It should be pointed out that MND cross sections are used by at least one reactor manufacturer[12] as well as other analysis groups in the U. S.

CHAPTER 2

DESCRIPTION OF COMPUTER CODES

2.1 LASER

The LASER program [8] is a multi-energy, one-dimensional (cylindrical) unit cell burnup program. The specific nature of the physical problem solved and the mathematical formulation of the model, together with the most complete discussion of the output of LASER, is found in Ref. 16. LASER is based on modified versions of the slowing down program MUFT[14] and the thermalization transport theory program THERMOS[17] and performs a calculation of the neutron spectrum in a uniform lattice made up of cylindrical rods, cladding, and surrounding moderator with a thermal energy cutoff of 1.855 eV. An isotropic scattering ring surrounding the cell is automatically provided in LASER. Honeck[18] has shown that the inclusion of the so called white scattering ring eliminates, to a large extent, the errors introduced by cylindricizing the unit cell.

LASER will, at option, perform a burnup calculation for the cell explicitly calculating the spatial distribution of the various nuclides as the cell is burned.

LASER uses different treatments in the thermal energy range (0.0 to 1.855 eV) and in the epithermal (1.855 eV to 5.53 keV) and fast (5.53 keV to 10 MeV) energy ranges.

In the thermal range, LASER solves the integral transport equation subject to isotropic scattering. In the epithermal and fast energy ranges, LASER solves the consistent B-1 approximation to the transport equation.

LASER has been modified in this study and renamed LASER-M. Most of the modifications were of a fairly minor nature and none of the basic mathematics of LASER were altered. A complete discussion of the modifications is given in Chapter 3 and further discussion of LASER is contained in Appendix G.

2.2 LIBP-IV

The thermal cross section library for LASER is formed by use of the LIBP-IV program originally written by Honeck.[17] Basically, LIBP takes preprocessed data and simply puts this data into the form required in the thermal library. To obtain the data for input to LIBP the user must process experimental cross section values using the computer code SIG1 (described briefly in Ref. 8), ETOT,[21] or other similar codes. The thermal library was modified in this work by using ETOT and LIBP. The procedure is discussed in subsection 3.2.1. It is important to note that the input instructions to LIBP-IV are essentially those found in the THERMOS manual[17] as modified by the information given in the LASER manual.[8] Appendix D contains a brief discussion of the input to LIBP as well as a listing of the cards used to change the thermal library.

2.3 LEOPARD

The LEOPARD code[4] is a zero-dimensional spectrum code which determines fast and thermal spectra using only basic geometry, composition, and temperature data as input. LEOPARD is based on modified versions of the MUFT[14] and SOFOCATE[22] computer programs. The code will, optionally, perform a depletion calculation for the unit cell.

In the fast energy region (above 0.625 eV) a MUFT calculation is performed similar to that described in Appendix G for LASER. Also, LEOPARD provides an optional U-238 L factor search as well as a critical buckling and poison search almost identical to those described for LASER.

Basically, the major difference between LEOPARD and LASER is in the thermal calculation where LEOPARD calculates a Wigner-Wilkins spectrum. Since LEOPARD has a 0.625 eV thermal cutoff, it is not as effective for analysing plutonium fuel as LASER. Also, since LEOPARD performs a zero-dimensional calculation, an approximate method of treating space-energy effects by means of multigroup disadvantage factors is used. In this approach, disadvantage factors are computed using the method of Amouyal, Benoist, and Horswitz[23] (the ABH method) for each of the 172 thermal energy groups. Flux and volume weighted macroscopic cross sections are then determined at each energy. These energy-dependent macroscopic cross sections are used in a normal spectrum calculation for a homogeneous medium, and spectrum averaged cross sections are computed.

LEOPARD edits flux weighted number densities, $(\overline{g\ N})^i$, as well as volume weighted number densities, $\bar{N}^i$, and their ratio, $(\overline{g\ N})^i / \bar{N}^i$. This ratio, defined here as $\bar{g}^i$, is actually a mean disadvantage factor which varies from nuclide to nuclide reflecting absorption profiles as well as the geometric location of the nuclide. LEOPARD also edits region averaged microscopic cross sections for three fast energy groups (10 MeV to 0.823, 0.823 MeV to 5.53 KeV, and 5.53 KeV to 0.625 eV), for one fast group (10 MeV to 0.625 eV), and for the thermal energy group (0.0 to 0.625 eV). LEOPARD does not, however, edit effective thermal microscopic cross sections, $\bar{\sigma}^i_{eff}$, as defined in Appendix G. To obtain the effective cross sections the user must multiply the region averaged cross section, $\bar{\sigma}^i$, by the mean disadvantage factor, $\bar{g}^i$, so that

$$\bar{\sigma}^i_{eff} = \bar{g}^i\ \bar{\sigma}^i. \qquad (2.3)$$

Alternately, region averaged cross sections may be entered in the diffusion codes such as PDQ along with thermal self-shielding factors, used as disadvantage factors, such that PDQ calculates the effective thermal cross sections. Although there is no mention of the fact in the LEOPARD manual, it can be shown that the thermal macroscopics are calculated using the flux weighted number densities (equivalent to using effective microscopic cross sections) and the fast macroscopics are computed using the volume averaged number densities (since a flat fast flux is assumed).

An advantageous feature of LEOPARD is the capability of designating a fictitious extra region in addition to the fuel, clad, and moderator region of the unit cell. This allows the user to model as extra region those parts of a fuel assembly or core which are not in a unit cell(i.e. water holes, control rod followers, assembly cans, structure, etc.). However, care must be taken when using the extra region since the number densities and macroscopic parameters output by LEOPARD in this case are for the whole "super cell" (the unit cell plus the extra region).

Additional features of LEOPARD are the use of a built-in polynomial fit to the pseudo fission product cross section as a function of burnup and the output of the Mixed Number Density (MND) cross section discussed in subsection 1.4.3.1.

The basic version of LEOPARD has been modified at M.I.T. by Spierling[29] and Farrar.[25] The work by Spierling is of special interest in this study since he modified LEOPARD to better handle plutonium fuel. Although Mertens[5] found Spierling's version of LEOPARD (designated LEOPARD-R) to still be somewhat lacking when compared to LASER, LEOPARD-R was used as a secondary tool in this work for comparision to a number of LASER calculations. A primary difficulty of comparing the results of two spectrum codes is assuring that a similar set of basic library data is used.

Appendix B contains a comparison of spectrum averaged

cross sections from LEOPARD -R and LASER-M as well as values of ν (neutrons per fission) and κ (energy per fission). Unfortunately, it is seen that significant differences (not totally explained by the difference in spectrum calculation) are present.

2.4 PDQ-7/HARMONY

The PDQ-7 computer program[26] solves the neutron diffusion-depletion problem in one, two, and three dimensions. Up to five energy groups are permitted, with the thermal neutrons represented by a single group or a pair of overlapping groups. Adjoint and boundary value calculations may be performed and the depletion may be by point or block. The geometries available are rectangular, cylindrical, or spherical in one dimension; rectangular, cylindrical, or hexagonal in two dimension; and rectangular or hexangonal in three dimension. All geometries provide for variable mesh spacing in all dimensions and zero-current, zero-flux, and rotational symmetry boundary conditions are available.

The two overlapping thermal groups may be used in one- or two dimensional problems to describe a spatially dependent thermal-neutron spectrum as a linear combination of overlapping hard and soft spectra.

The PDQ-7 code permits downscatter to only the next lowest energy group, and flux weighted average values of region-dependent parameters are edited as well as regionwise and pointwise flux and power distributions.

The macroscopic data and depletion calculations automatically utilize the HARMONY computer code.[27] Any of the cross sections or self-shielding factors (obtained from a spectrum code) used in the spatial or depletion calculation may be represented as time dependent. Isotopic depletion and fission product chains are specified by the user as discussed in Chapter 8. The total number of depletable isotopes is limited only by the computer storage requirements. Provision has been made in HARMONY to adjust the thermal flux level at specific times within the basic interval to approximate constant-power operation. Compositions may be replaced at any time in a depletion study to investigate the effects of fuel rearrangements.

The PDQ-7 and HARMONY code input is described in Refs. 26 and 27, respectively. However, it should be noted that PDQ-7 at M.I.T. has been revised by the Aerojet Nuclear Corporation for operation on an IBM computer. The revised input to PDQ-7/HARMONY is excellently summarized in ANCR-1061[28] which should be used in conjunction with the original manuals when using PDQ-7 at M.I.T.

As a further note, the large flexibility of problem description in PDQ-7 can lead to fairly complicated input requirements. The users should thoroughly familiarize themselves with the unique terminology (summarized in Ref. 27) used in the PDQ-7/HARMONY code system before attempting to run the code. Some of the basics of the input are discussed further in Chapters 5 and 8.

CHAPTER 3

MODIFICATIONS TO LASER CONTAINED IN LASER-M

3.1 Introduction

As discussed in Appendix G, the standard Argonne version of LASER has a number of major limitations. The scope of the present study did not include the modification of LASER to eliminate these major limitations. However, numerous minor changes discussed in the following sections were incorporated into LASER to form a version designated LASER-M.

LASER has been modified by at least one other worker at M.I.T. (C. S. Rim) and for the sake of completeness these modifications will be discussed here. Rim[29] inserted additional data in LASER to account for the Doppler broadening effect on the Pu-239 resonance at 0.296 eV. The resonance parameters given in TABLE 3.1, were used in Rim's modification to evaluate the line shape function for the 0.296 eV resonance and the virtual level (See Ref. 29 for further discussion).

TABLE 3.1

RESONANCE PARAMETERS USED TO EVALUATE THE LINE SHAPE FUNCTIONS FOR Pu-239 RESONANCES (Ref. 29)

	E_o(eV)	σ_o(b)	Γ(eV)	Γ_f/Γ_a
Pu-239	0.296	2.120 + 3*	9.9 - 2	1.539
	-0.40	1.569 + 2	2.20 - 1	9.695

* NOTE 2.120 + 3 = 2.12E+3 = 2.120×10^3

σ_o is the capture cross section at the resonance energy E_o, Γ the total width, Γ_f the fission width, and Γ_a is the absorption width.

Rim also normalized the thermal U-235 and Pu-239 cross sections to the 2200 m/sec parameters reported by Sher, et al.,[30] and the thermal Pu-241 data to the 2200 m/sec values which Westcott, et al.,[31] presented at the 1964 Geneva Conference. It should be noted that the modifications listed here were the only changes to LASER made by Rim.[32]

3.2 Cross Section Changes

3.2.1 Thermal Cross Section Library

Early in this work it was decided to revise the thermal cross section library of LASER to incorporate the most recent Evaluated Nuclear Data File (ENDF)[33] cross section for the plutonium isotopes. The ENDF/B-II cross sections for Pu-239,

Pu-240, Pu-241, and Pu-242 were processed by Bill Flournoy at Southern California Edison (SCE) using ETOT.[21] In these runs the weighting function was 1/E joined to a Maxwellian Distribution, the cross sections were group averaged, and no resonance parameters were calculated. The cross sections output from ETOT (in the form of punched cards) were then used as input to LIBP (the LASER and THERMOS thermal library generation code discussed in Section 2.2 and Appendix D) to update the thermal library tape of LASER.

The thermal group structure, group-wise microscopic absorption (σ_a) and fission (σ_f) cross sections and the constant thermal values of nu (ν) neutrons per fission for the four plutonium isotopes are listed in Appendix C.

As a first basis of comparison, the ENDF/B-II 2200 m/sec values of σ_a, σ_f, and ν for plutonium which were input to LASER-M are listed in TABLE 3.2 along with the 2200 m/sec values used in the old LASER library and other often referenced values. For completeness U-235 is also included.

3.2.2 Thermal Resonance Parameters

The resonance parameters for the Pu-240 1.056 eV resonance were also changed. These parameters were obtained in a manner analogous to that for the thermal cross sections except that ETOM[35] was used to process the ENDF/B-II cross sections.

TABLE 3.2

CROSS SECTION PARAMETERS AT 2200 m/sec FOR VARIOUS CROSS SECTION SETS (All cross sections are in barns)

QUANTITY	LASER OLD c/s SET	LASER-M SET (ENDF/B-II PU)	SHER[30] (See Note 1)	WESTCOTT[3.4] (See Note 2)
U-235				
σ_a	678.98	678.98	678.2	679.9
σ_f	577.98	577.98	577.1	579.5
ν	2.442	2.442	2.442	2.430
Pu-239				
σ_a	1015.0	1013.0	1014.5	1008.1
σ_f	741.98	742.1	740.6	742.4
ν	2.8980	2.880	2.898	2.871
Pu-240				
σ_a	272.59	290.1		
σ_f	2.9976-2 (See Note 4)	5.785-2		
ν	2.8866	2.8900		
Pu-241				
σ_a	1376.0	1375.0		1391.
σ_f	1013.0	1008.0		1009.
ν	2.9779	2.9360		2.969
Pu-242				
σ_a	18.598	30.01 (See Note 3)		

NOTES:

1. There are two cross section sets generally referred to as "Sher" sets. One set appears in BNL 722(1962) but that data has been updated by a revision to BNL 722 published in 1965 (BNL 918, Ref. 30).

Table 3.2 (continued)

2. There are also two cross section sets generally referred to as "Westcott" sets (or "1964 Geneva Conference" sets). See Ref. 31 and 3.4. It should be noted that the values presented by Westcott at the 1964 Geneva Conference [31] were "preliminary results" and are slightly changed in the final report.[34] The results in the final report "are to be considered as superseding the [1964 Geneva Conference] results."

3. Uotinen, et al.,[2] points out that this value should be about 19 barns. (See Section 4.5).

4. This notation will be used throughout where 2.9976-2 = 2.9976E-2 = 2.9976×10^{-2}.

The major options used in ETOM were as follows:

1. The weighting function was 1/E joined to a U-235 fission spectrum.
2. Extra resonances were added to the smooth cross section.
3. The Grueling-Geortzel parameter was calculated from data on the ENDF/B tape.
4. The N-2N cross section was added half to fission, and half to inelastic scattering.
5. The ingroup inelastic scattering was added to the smooth scattering.
6. The excess scattering was lumped into the highest group.

Data for the Pu-240 1.056 eV resonance obtained for the ETOM run is given in TABLE 3.3.

TABLE 3.3

ENDF/B-II RESONANCE PARAMETER DATA FOR THE Pu-240 1.056 eV RESONANCE (Ref. 36)

Parameter	Value
E_o, eV	1.056
Γ_n, eV	2.44-3
Γ_γ, eV	2.986-2
Γ_f, eV	5.70-6
m	5.3111+3
r	1.7361+5
α	1.9085-4

Definitions of the parameters output from ETOM are given in Ref. 35. They are as follows:

$$r = \frac{\sigma_o(\Gamma_a)}{\Gamma} \tag{3.1}$$

$$m = \frac{\sigma_o(\Gamma_a)}{E_o} \quad , \tag{3.2}$$

and

$$\alpha = \frac{\Gamma_f}{\Gamma_a} = \text{fission to absorption ratio,} \tag{3.3}$$

where the total width, Γ, is given by

$$\Gamma = \Gamma_n + \Gamma_a \quad , \tag{3.4}$$

and

$$\Gamma_a = \Gamma_\gamma + \Gamma_f \quad ,$$

with Γ_n = neutron width

Γ_γ = capture width

Γ_a = absorption width

Γ_f = fission width.

By using Eq. 3.1 to 3.4 and the data in TABLE 3.3 the parameters input to LASER-M (Subroutine DOPL) were obtained (for a more detailed discussion see Ref. 37, p. 115). These parameters are listed in TABLE 3.4 along with the variable name used in DOPL.

TABLE 3.4

RESONANCE PARAMETERS FOR Pu-240 RESONANCE INPUT TO LASER-M

PARAMETER	VARIABLE NAME	VALUE INPUT
σ_o	SIGO	1.86225+5 barns
E_o	EO	1.056 eV
Γ_n	GAMMAN	2.44-3 eV
Γ_γ	GAMMAC	2.986-2 eV
α	GF	1.9085-4

3.2.3 Fast Cross Section Library

Because of the format complexity of the fast cross section library in LASER it was decided not to make any changes in it. It should be noted, however, that the cards and printed output from the ETOT and ETOM runs have been placed in the Nuclear Engineering Code Library to enable future users of LASER-M to further modify the cross section libraries.

3.2.4 Validation of Modifications

As discussed in Chapter 4, the cross section changes made to LASER were checked against criticals and show good agreement. It is important to note that for all modifications

discussed in this Chapter, sample problems were run to insure that the code was working properly and, when possible, hand calculations or comparisons to LEOPARD output were done to verify the results.

3.3 Output Edit Additions

3.3.1 Introduction

In general, LASER prints out more information than its counterpart, LEOPARD, and a great deal of the LASER output is only required in very special cases. Additionally, some required parameters are not edited, thus requiring the user to perform tedious hand calculations to obtain the information. These two facts lead to numerous, but relatively simple, modifications to LASER. Output reduction options and miscellaneous changes to LASER are discussed in Section 3.4, whereas changes to LASER to calculate additional parameters are discussed below.

The major edit additions in LASER-M are as follows:

1. Calculation of an approximate microscopic transport cross section for all groups.
2. Calculation of an approximate microscopic removal cross section for non-thermal groups.
3. Calculation of a thermal diffusion coefficient averaged over the moderator only.

4. Calculation of a spectrum averaged fast and epithermal nu (neutrons per fission) for all fissionable nuclides.
5. Calculation of a spectrum averaged macroscopic kappa fission ($\overline{K\Sigma}_f$) where kappa is the energy per fission of the fissioning nuclides.
6. Calculation of the neutron velocity averaged over an approximate gradient spectrum ($\overline{V}_g$) in the cell.
7. Calculation of all Generalized Mixed Number Density (GMND) microscopic and macroscopic cross sections.
8. Calculation of cell volume fractions and a cell averaged equivalent thermal microscopic cross section for oxygen.
9. A condensed output edit for the microscopic cross sections (in PDQ input form) was added.

Each of these edit changes are described in the following subsections. Note that the approximate values given by these edits are intended for use with light water systems in which hydrogen is the dominant moderator and scattering material.

3.3.2 Approximate Microscopic Transport Cross Section

The standard version of LASER does not edit microscopic transport cross sections, σ_{tr}, which were required in this study. After a great deal of consideration, it was decided to use a relatively simple formulization to obtain a σ_{tr} which would allow PDQ calculations to easily reproduce the diffusion coefficient, D, originally calculated by LASER. This formulization, which has been programmed into LASER-M, was suggested by A.F. Henry[50] and is as follows:

By using the definition of the transport cross section in an absorbing medium

$$\bar{\sigma}_{tr} = \bar{\sigma}_a + (1 - \bar{\mu})\ \bar{\sigma}_s, \qquad (3.5)$$

where $\bar{\sigma}$ = spectrum averaged values of transport, absorption and scattering cross section.

$\bar{\mu}$ = average value of the cosine of the scattering angle,

and the definition of a macroscopic cross section

$$\bar{\Sigma}_{tr} = \sum_i \bar{N}^i\ \bar{\sigma}^i_{tr}\ ; \qquad i - \text{all nuclides} \qquad (3.6)$$

where $\bar{N}^i$ = volume averaged atom density of nuclide i

and combining Eq. 3.5 and 3.6, one obtains

$$\Sigma_{tr} = \sum_i \left[\bar{N}^i \{\bar{\sigma}^i_a + (1 - \bar{\mu}_i)\ \bar{\sigma}^i_s\} \right] . \qquad (3.7)$$

Eq. 3.7 can be written as

$$\Sigma_{tr} = \bar{N}^H \tilde{\sigma}_{tr,s} + \sum_i \bar{N}^i \bar{\sigma}^i_a \; ; \quad i = \text{all nuclides}, \qquad (3.8)$$

where $\bar{N}^H$ = volume averaged hydrogen atom density and $\tilde{\sigma}_{tr,s}$ can be considered to be the total scattering component of the transport cross section (similar to $(1 - \bar{\mu})\sigma_s$) and has been multiplied by the volume averaged hydrogen atom density for convenience.

Now, since

$$\sum_i \bar{N}^i \bar{\sigma}^i_a = \Sigma_a \qquad \text{(output in LASER)}, \qquad (3.9)$$

and

$$\Sigma_{tr} = 1/3D \qquad \text{(D output in LASER)}, \qquad (3.10)$$

Eq. 3.8 can be solved for $\tilde{\sigma}_{tr,s}$ to obtain

$$\tilde{\sigma}_{tr,s} = [1/3D - \Sigma_a]\ [1/\bar{N}^H] \; . \qquad (3.11)$$

Therefore, since only the "scattering" component of the transport cross section is in $\tilde{\sigma}_{tr,s}$ the approximate transport cross section is formed as follows:

$$\tilde{\sigma}^H_{tr} = \tilde{\sigma}_{tr,s} + \bar{\sigma}^H_a \; , \qquad (3.12)$$

so, finally,

$$\tilde{\sigma}^{H}_{tr} = [1/3D - \Sigma_a]\ [1/\overline{N}^{H}] + \overline{\sigma}^{H}_{a} \quad . \tag{3.13}$$

It should be noted that when $\tilde{\sigma}^{H}_{tr}$ was input to PDQ as the transport cross section for hydrogen, and $\overline{\sigma}_a$ was input for the transport cross section of all other nuclides, the correct D for each group was obtained.

As mentioned above, this method is to be considered an approximate method to reproduce D using microscopic parameters. Also, since the scattering of the depletable isotopes is roughly the same (about 10 barns), $\tilde{\sigma}^{H}_{tr}$ remains approximately constant during burnup. For a further discussion of the use of $\tilde{\sigma}^{H}_{tr}$ see Sections 5.3 and 7.3.

3.3.3 Approximate Microscopic Removal Cross Section

The approximate microscopic removal cross section was obtained in a manner analogous to that for $\tilde{\sigma}^{H}_{tr}$. Since the term $\phi g\ \Sigma^{g}_{r}$ is defined in LASER as the rate (per unit volume) at which neutrons leave group g through processes other than absorption or leakage, the removal cross section, Σ_r, can be considered a macroscopic scattering cross section. Since hydrogen is by far the most effective scatterer, an approximate microscopic removal cross section for hydrogen can be obtained by attributing all of the scattering to hydrogen.

That is, $\tilde{\sigma}^H_{tr}$ becomes

$$\tilde{\sigma}^H_r = \Sigma_r / \bar{N}^H \quad , \tag{3.14}$$

with the removal cross sections of all other nuclides set to zero. LASER-M now edits $\tilde{\sigma}^H_r$ formed in this manner for each group.

3.3.4 Diffusion Coefficient Averaged Over the Moderator Only

LASER-M has been modified to edit D over the moderator only to allow its use in an unfueled region of the reactor. Since the epithermal and fast calculation in LASER is done on a homogeneous cell (i.e. there is no spatial dependence), the thermal diffusion coefficient is the only one edited over the moderator.

Basically, the modification used existing variables in subroutine EDIT to perform the integration over the moderator region only. Analogous to the calculation of D_{th} shown in Eq. 19 and 20 of Ref. 8, the formation of D_{mod} is given by

$$\Sigma_{tr}(E) = \frac{\int_r d\bar{r}\ \Sigma_{tr}(\bar{r},E)\ \phi(\bar{r},E)}{\int_r d\bar{r}\ \phi(\bar{r},E)} \quad ; \ \bar{r} \text{ for moderator only,} \tag{3.15}$$

and

$$D_{mod}^{th} = \frac{\frac{1}{3}\int_0^{E^*} dE \left[\Sigma_{tr}(E)\right]^{-1} \int_{\bar{r}} d\bar{r}\ \phi(\bar{r},E)}{\int_0^{E^*} dE \int_{\bar{r}} d\bar{r}\ \phi(\bar{r},E)} \quad ; \quad \bar{r} \text{ for moderator only,} \tag{3.16}$$

where E^* is the thermal cutoff energy.

Finally, an approximate microscopic transport cross section for the moderator only is calculated. It is given by

$$\tilde{\sigma}_{tr}^{H,mod} = [1/3D_{mod} - \Sigma_a^{th,mod}]\ [1/N^{H,mod}] + \bar{\sigma}_a^H \tag{3.17}$$

3.3.5 Spectrum Averaged NU ($\bar{\nu}$) and Kappa Fission ($\overline{K\Sigma}_f$)

Since spectrum averaged values of ν and $K\Sigma_f$ are required as input to PDQ, LASER was modified to edit them. Since the thermal value of ν for each nuclide is taken as constant in LASER there is no need to perform a spectrum average calculation for the thermal group. The modifications, done in subroutine BONE, were as follows:

$$\bar{\nu}_i^g = \frac{\overline{\nu\sigma}_{f,i}^g}{\bar{\sigma}_{f,i}^g} \quad ; \quad \begin{array}{l} i \text{ all fissionable nuclides,} \\ g \text{ all non-thermal energy groups,} \end{array} \tag{3.18}$$

and

$$\overline{K\Sigma}_f^g = \sum_i K_i \bar{N}_i \bar{\sigma}_{f,i}^g \quad ; \quad g = \text{all energy groups}, \qquad (3.19)$$

where K_i = energy (in watt-sec) per fission for nuclide i

$\bar{N}_i$ = volume averaged atom density of nuclide i

$\bar{\sigma}_{f,i}^g$ = effective microscopic fission cross section of nuclide i for energy group g.

3.3.6 Neutron Velocity Averaged Over the Gradient Spectrum ($\bar{v}_g$).

As discussed in Section 1.4 $\bar{v}_g$ is required to calculate GMND cross sections. Since LASER edits pointwise total neutron flux and density it is a simple matter to calculate $\bar{v}_g$ using Eq. 1.15 of Section 1.4.3.

Since five space points are normally assigned to the fuel and a sixth to the clad, space point seven in LASER is usually the first in the moderator. Also, since the flux increases near the boundary of the cell (space point 12) it was decided to use space points eleven and seven to calculate the gradient spectrum.

LASER-M now calculates $\bar{v}_g$, where

$$\bar{v}_g = \frac{\bar{\phi}(11) - \bar{\phi}(7)}{\bar{n}(11) - \bar{n}(7)} \times \frac{1}{2.2 \times 10^5} , \qquad (3.20)$$

where $\bar{\phi}(r)$ = total neutron flux at point r

$\bar{n}(r)$ = total neutron density point r.

The value of $\bar{v}_g$ calculated is in units of 2200 m/sec to be consistent with other velocities output by LASER. It should be noted that $\bar{v}_g$ calculated from other points or from average values as discussed by Mertens[5] does not differ significantly from the method used by LASER-M.

3.3.7 Generalized Mixed Number Density (GMND) Cross Sections

As discussed in Section 1.4, GMND cross sections are formed by multiplying all thermal cross sections by the cell averaged neutron velocity ($\bar{v}_{cell}$), and multiplying the thermal diffusion coefficient by the neutron velocity averaged over the gradient spectrum ($\bar{v}_g$).

Thus, to form macroscopic GMND parameters LASER-M uses the following formulas:

$$\bar{\Sigma}_\alpha^{GMND} = (\bar{\Sigma}_\alpha^{th})(\bar{v}_{cell}); \quad \alpha = \text{absorption and fission}, \qquad (3.21)$$

and

$$\bar{D}^{GMND} = (\bar{D}^{th})(\bar{v}_g). \qquad (3.22)$$

The microscopic GMND parameters are formed in a similar fashion,

$$\bar{\sigma}^{GMND}_{\alpha,i} = (\bar{\sigma}^{th}_{\alpha,i})(\bar{v}_{cell}) \; ; \quad \begin{matrix} \text{nuclide } i, \\ \text{reaction } \alpha, \end{matrix} \tag{3.23}$$

and

$$\bar{\sigma}^{GMND}_{tr} = \bar{\sigma}^{th}_{tr}/\bar{v}_g \; . \tag{3.24}$$

3.3.8 Other Miscellaneous Changes

LASER-M now edits volume fractions for the fuel, clad, and moderator as well as an effective cell averaged thermal absorption cross section for oxygen calculated by the following formula,

$$\bar{\sigma}^{Oxy}_{a,th} = \frac{f_f N^{Oxy}_f \bar{\sigma}^{Oxy}_{a,f} + f_m N^{Oxy}_m \bar{\sigma}^{Oxy}_{a,m}}{\bar{N}^{Oxy}} \; , \tag{3.25}$$

where f_f and f_m = volume fractions of the fuel and moderator, respectively

N^{Oxy}_f and N^{Oxy}_m = atom density of oxygen in the fuel and moderator, respectively

$\bar{\sigma}^{Oxy}_{a,f}$ and $\bar{\sigma}^{Oxy}_{a,m}$ = effective absorption cross section of oxygen in the fuel and moderator, respectively

$\bar{N}^{Oxy}$ = cell volume averaged atom density of oxygen.

A condensed two group (fast plus epithermal and thermal or GMND thermal) output edit of all parameters required as input to PDQ has also been added to LASER-M.

3.4 Elimination of Errors, Output Reduction, Changes to Input

3.4.1 Elimination of Errors

The standard version of LASER gives numerous divide check errors (dividing by zero) as a matter of course during a calculation. These errors were traced and found to have no effect on the calculation. However, since they are annoying, the code was modified to bypass the calculation when the errors would result. Also, when LASER is used with a buckling search that results in a negative buckling, a number of error statements were printed. These errors were also traced and eliminated.

3.4.2 Output Reduction

As discussed above, LASER's output is much more extensive than the usual spectrum code. Because much of this output is not required in most cases, LASER was modified to give the user various options of reducing the output.

Basically, these options are as follows:

1. NOFLUX - Eliminates pointwise and energywise flux output.
2. NORATE - Eliminates the extensive reaction rate output.
3. NO625 - Eliminates the 0.625 eV thermal edit.
4. NOMISC -Eliminates the pointwise cross sections, and various other miscellaneous output.
5. NODECK -Eliminates a continuous deck from being punched at the end of a depletion run.
6. MINBRN -Minimizes the data output for a burnup step.
7. NOPDQ -Eliminates the special PDQ output discussed in Section 3.3.8 above.

For more information on exactly what each variable eliminates, the listing of the subroutines which have been changed in LASER-M (included as Appendix E) should be consulted. Additionally, LASER-M will only punch out a continuation deck at the end of a depletion problem instead of every time a step as done in LASER.

3.4.3 Changes in Input

The input to LASER-M is completely compatable with that of LASER and the only difference is on card number 4 where the format has been extended to 20I2. The variables discussed in Section 3.4.2 are entered on this card through column 38. If a 1 is entered it implies the specific type of output will not appear. A zero or a blank will yield the full output.

CHAPTER 4

COMPARISON OF LASER-M CALCULATIONS WITH PLUTONIUM CRITICAL EXPERIMENTS

4.1 Introduction

As discussed in Chapter 3 the standard Argonne version of LASER has been modified at M.I.T. by a number of independent workers. The most important modification done in this work (from the standpoint of effecting the various parameters calculated) was the updating of the thermal cross sections for all plutonium isotopes. In order to evaluate the effects of the cross section modification, as well as the changes made by other workers, a number of plutonium critical and approach to critical experiments were analyzed.

4.2 Experiments Using 1.5 W/O PuO_2-UO_2 Lattices

An analysis was carried out on experiments done at Battelle, Pacific Northwest Laboratories using the Critical Approach Facility (CAF) [11, 38] for 1.5 w/o PuO_2-UO_2 rods in hexagonal lattices of 0.55, 0.60, and 0.71 inch pitch. A thorough discussion of these and other experiments is contained in Ref. 11. Basically, each lattice was taken close to critical and the buckling and reflector savings for the critical configuration were determined. Basic data for the 1.5 w/o PuO_2 experiments is presented in Table 4.1.

TABLE 4.1

BASIC DATA FROM 1.5 w/o PuO_2 EXPERIMENTS (HANFORD EXPERIMENTS)

(Ref. 11 and 38)

Fuel Rod OD, in	0.426
Fuel OD, in	0.372
Clad Thickness (Zr-2), in	0.027
Fuel Height, in	48.5
PuO_2 in UO_2 (.16 a/o U-235), w/o	1.5
Fuel weight per rod, g	828.
PuO_2 weight per rod, g	12.42

Pu isotopics, a/o

Pu-239	91.41
Pu-240	7.83
Pu-241	0.73
Pu-242	0.03

Hexangular Lattice Spacing, in	H/Pu Atom Ratio	H_2O/Rod Volume Ratio	Measured Buckling, m^{-2}
0.55	230	0.8382	48.0 ± 1.2
0.60	326	1.187	65.1 ± 1.8
0.71	567	2.063	78.5 ± 0.3

Average Temperature, 25°C

4.3 Experiments Using 6.6 w/o PuO_2-UO_2 Lattices

Critical experiments carried out at the Westinghouse Reactor Evaluation Center (WREC) were analyzed [7, 39]. These experiments utilized 6.6 w/o PuO_2-UO_2 (natural) fuel rods in a square lattice of 0.52, 0.56, and 0.735 inch pitch. Basic data from these experiments (given most completely in Ref. 6) is presented in Table 4.2.

4.4 Results of Calculations and Comparison to Other Calculations

In analyzing all the experiments discussed above, the measured buckling was input as the geometric buckling; (materials buckling was not searched); the Nelkin kernal was used; the U-238 L-factor was searched; and the temperature of each experiment was input as accurately as LASER allows.

Table 4.3 contains the results of LASER-M calculations of K_{eff} (as well as the spread in K_{eff} (ΔK) and the average error in K_{eff}) for the Hanford criticals. Also listed in Table 4.3 are the results of analyses done by Westinghouse using LASER with the Nelkin kernal and a standard version of LEOPARD.

Table 4.4 contains the results of the LASER-M calculations for the WREC criticals as well as the results obtained using the M.I.T. version of LASER without the revised

TABLE 4.2

BASIC DATA FOR 6.6 w/o PuO_2 EXPERIMENTS (WREC EXPERIMENTS)
(Table 13, Ref. 6)

Fuel Pellet OD, in	0.337
Clad (Zr-4) ID, in	0.345
Clad Thickness, in	0.023
Fuel Height, in	36.6
PuO_2 in UO_2 (natural U), w/o	6.6
Weight of MOX per rod, g	546.6

Pu isotopics, w/o

Pu-239	90.49
Pu-240	8.57
Pu-241	0.89
Pu-242	0.04

Square Lattice Pitch, in	H/Pu Atom Ratio	Moderator/ Fuel Volume Ratio	Experimental Buckling, m^{-2}	Water Temp. oC
0.52	76	1.68	108.8	25.8
0.56	98	2.16	121.5	16.4
0.753	211	4.70	159.6	24.1
0.56 with 337 wppm Boron	98	2.16	112.3	18.0

TABLE 4.3

RESULTS OF CALCULATIONS ON THE HANFORD (1.5 w/o PuO_2) EXPERIMENTS
(Experimental K_{eff} = 1.00000 in all cases)

Pitch (in)	K_{eff} LASER-M	K_{eff} LASER*	K_{eff} LEOPARD*
0.55	0.992180	1.00666	1.01652
0.60	0.993183	1.01123	1.02397
0.71	0.998409	1.01761	1.03144
ΔK	0.00623	0.01095	0.01492
Average Error	0.541%	1.183%	2.398%

* Note: Westinghouse Calculations, Ref. 7

TABLE 4.4

RESULTS OF CALCULATIONS ON THE WREC (6.6 w/o PuO_2) CRITICALS

(Experimental K_{eff} = 1.00000 in all cases)

Pitch (in)	LASER-M	K_{eff} LASER (old Pu c/s)	LEOPARD*
0.52	1.00006	1.00754	0.9890
0.56	1.01553	1.02363	1.0103
0.735	1.01149	1.01953	1.0128
0.56 w/337 wppm Boron	1.01968	1.02776	1.0148
ΔK	0.01962	0.02022	0.0258
Average Error	1.169%	1.962%	1.2225%

* Note: Westinghouse Calculations, Ref. 7

plutonium cross sections. Additionally, values obtained by Westinghouse using a revised version of LEOPARD with cross sections reported by Westcott [31] at the 1964 Geneva Conference are given.

The revised version of LEOPARD contains a number of small changes from that used by Westinghouse to calculate the Hanford experiments. The changes include the removal of the K bias, a revised Dancoff calculation, a revised SOFOCATE integration, and a correction in a U-235 cross section. The net effect on the calculated K_{eff} due to these changes is reported as small [7].

As seen from Table 4.3 the LASER-M calculations of K_{eff} for the 1.5 w/o PuO_2 fuel rods yield appreciably better values than the Westinghouse LASER and LEOPARD calculations. The average error in K_{eff} is 0.541%, 1.183%, and 2.398%, respectively. Another important basis of comparison is the spread in the calculated value of K_{eff} for the various lattice pitches studied. LASER-M again gives a much better (lower) value (0.00623) than the two Westinghouse calculations (0.01095 and 0.01492, respectively).

From Table 4.4 it is again seen that LASER-M calculations of K_{eff} for the 6.6 w/o PuO_2 fuel rods yield better values than the M.I.T. version of LASER without thermal ENDF/B-II plutonium cross sections and the revised LEOPARD calculations done by Westinghouse. The average error in K_{eff} for the three codes is 1.169%, 1.962%, and 1.2225%, respectively, with the spread in K_{eff} being 0.01962, 0.02022, and 0.0258, respectively. It should be noted that the LASER calculations with the old cross sections yielded worse values of K_{eff} than either the LASER-M or LEOPARD results, but the spread in K_{eff} was about 30% better (lower) than LEOPARD and was essentially equal to the LASER-M values.

4.5 Conclusions

The data presented in this chapter shows that the revised version of LASER (LASER-M) containing ENDF/B-II plutonium cross sections yields better values of K_{eff} when analyzing criticals than LASER without the revised cross sections. LASER-M also yields better values of K_{eff} when compared with other published data. Additionally, the spread in K_{eff} for the various lattice pitches analyzed was lower in LASER-M than the other calculations.

It is important to note that it is not possible to conclude, a priori, from this data that the ENDF/B-II cross sections are more accurate. As discussed in

Section 1.4, Liikala, et al., [10] thoroughly consider the many assumptions and uncertainties in spectrum calculations. It is apparent from this discussion that if all other errors are somehow taken out of the calculation, the ENDF/B-II cross section set may give worse results than other sets. In fact, Liikala obtains better results when using BNWML cross section data than when using ENDF/B-II data and Uotinen, et al., [2] point out a number of discrepancies in the ENDF/B-II plutonium cross sections. Generally, however, the ENDF/B-II cross sections seem to be better than other readily available sets.

As updated cross section data becomes available, the libraries of the spectrum codes should be revised. To facilitate validation of results from any further revision of LASER-M the data cards input to LASER-M for the criticals discussed in this chapter are listed in Appendix F.

Additionally, the merits of a certain cross section set and calculational procedure should be checked against experimentally determined isotopics as a function of burnup. Poncelet [16] has done a comparison of this type with LASER (using the original cross section set) and concludes that "for burnups ranging to 25,000 MWD/MTU (LASER) has shown generally very good agreement". Since a comparison of LASER-M with experimental data at various burnups was not

done in this study it is recommended that future works using LASER-M perform this analysis. Uotinen, et al., [2] list the references which contain available experimental data.

CHAPTER 5

GENERAL PROCEDURES - BEGINNING OF LIFE CALCULATIONS

5.1 Introduction

The starting point of reactor physics calculations is a set of reactor design characteristics, including material compositions, dimensions, temperatures, and thermal-hydraulic parameters. The overall problem of establishing the distribution of neutrons in three space dimensions, in time, and in neutron energy must be broken down into a number of smaller, related segments, each of which is small enough and simplified enough to be economically solvable with available techniques and computer codes.

In the present work the energy spectra of the neutrons in the various unit cells were determined using LASER-M and the spatial dependence of the neutrons was determined using PDQ-7 in two dimensions only. The basis of the two dimensional calculation was to essentially slice the assembly or core through the midplane, axially homogenize the grid structures, and use core average values for the various temperatures and power in each assembly. A detailed discussion of the procedure used is discussed in the following sections and all data is contained in TABLE 1.1 and Appendix A.

5.2 Few Group Spectrum Averaged Cross Sections (LASER)

5.2.1 Definitions of Various Unit Cells

The unit cells modeled in LASER-M consisted of fuel, clad, and associated moderator. Four basic unit cells were modeled from a San Onofre assembly and they are defined below.

5.2.1.1 Normal Cell

A normal unit cell was modeled such that the moderator volume (per unit length) contained in the square defined by the cell pitch was associated with the fuel rod. This definition is, of course, the standard definition of a unit cell.

5.2.1.2 Assembly Average Cell

An assembly average unit cell was defined such that the moderator volume (per unit length) associated with the fuel rod was an assembly average value. That is, the total moderator volume in the assembly (including water holes) is divided among the total number of fuel rods.

5.2.1.3 Cell Around Water Holes

A cell which was considered to model a fuel cell adjacent to a water hole (4 per water hole) was formed by adding a quarter of the moderator volume in the water hole to the moderator volume of the normal cell.

5.2.1.4 Unfueled Cell

An unfueled cell was modeled to represent the 16 water holes for the control rods (commonly called RCC cells) in the assembly. Basically, the cell was modeled by using the moderator volume of the RCC cell in conjunction with the metal volume contained in the control rod sheaths present in the cell. Since LASER-M has no automatic provision for an unfueled calculation the input is not as straightforward as would be hoped. The unfueled cell is discussed further in subsection 5.2.4.

5.2.2 Input Quantities

5.2.2.1 Cell Geometry

The input of the cell geometry is relatively simple. Notable points are that the clad and gap were smeared together to obtain a pseudo clad thickness, and that the volume of the grid assemblies was subtracted from the volume available to the moderator.

5.2.2.2 Cell Expansion

Although it is difficult to determine specific dimensions for individual hot cells the following procedure was used to determine the thermally expanded dimensions of an average cell. The spacer grid assemblies were considered to be at the average moderator temperature and expanded accordingly,

increasing the pitch of the cell. Average temperatures where used to expand the fuel and clad. It is of interest to note that LEOPARD can be used to expand the cell by inputting basic geometry and temperature data. LEOPARD was used as a check on the expansion calculations done in the present study and very good agreement was found.

5.2.2.3 Atom Number Densities

Expanded number densities were calculated using the data shown in APPENDIX A. A heavy metal loading of 1.335 MTM[40] in the four mixed oxide (MOX) assemblies was used. Three other sets of loading data (from Ref. 3) were also available for the calculation of the MOX number densities. The first set of information was the percent of theoretical density, the second was 806 lbs. of MOX per assembly and the third was 45 Kg of plutonium in the four MOX assemblies. It should be pointed out that this is not a consistent set of data. The 1.335 MTM gave the most plutonium in the assembly with the percent of theoretical density yielding a value 1.8% lower, the 806 lbs. a value 3.3% lower and the 45 Kg loading yielding 4.4% less plutonium than the 1.335 MTM value. Since the value of 1.335 MTM for the MOX assembly loading was the most current it was used to calculate the MOX fuel number densities. Additionally, the effect of the 5000 ppm of Am-241 (per plutonium) was determined

to be negligible and was ignored.

Since LASER-M does not allow metal in the moderator region the grid assemblies had to be approximated by adding an equivalent amount of boron to the moderator. The equivalency was based on thermal absorptions only and was calculated by assuming the grid material (inconel) is a 1/v absorber in the thermal range. By equating the 2200 m/sec macroscopic absorption cross sections of the inconel to that of an undetermined amount of boron it was calculated that about 5 ppm of boron should be added to the moderator to account for the grid assembly absorption (by convention, ppm of boron refers to weight parts of natural boron per weight parts of water).

5.2.2.4 Effective Fuel Temperature (EFTEMP) and Temperature To Doppler Broaden the 1.056 eV PU-240 Resonance (TEMP)

The effective fuel temperature, EFTEMP, (used to Doppler broaden the U-238 resonances) is defined as that temperature which gives the correct experimental power coefficient of reactivity for the reactor.[39] The LASER-M variable TEMP would be defined in an analogous fashion except that it would be concerned with the Pu-240 effect on the power coefficient.

The experimental information needed to accurately determine these two quantities was not available so the average fuel temperature, $\overline{T}_f$, was used as an approximate value. Ref. 39 gives calculated data for the effective fuel temperature and average fuel temperature, $\overline{T}_f$, as a function of heat flux at the fuel surface (proportional to power) for the SAXTON reactor. This information shows the effective fuel temperature to be about 22% higher than the average fuel temperature at full power. By using this information, a 3.85 w/o MOX normal cell was run in LASER-M with EFTEMP and TEMP 22% higher than $\overline{T}_f$. This run yielded a 0.7% decrease in k_{inf} from the same cell with EFTEMP and TEMP input as the average fuel temperature. Although this difference is not insignificant the estimated value of EFTEMP and TEMP being 22% higher than $\overline{T}_f$ may be as much in error as using $\overline{T}_f$. Therefore, due to the uncertainty involved, the average fuel temperature was used for the effective fuel temperature and for the temperature at which the Pu-240 1.056 eV resonance is broadened.

5.2.2.5 Buckling

LASER-M requires the input of a buckling and this is often a point of confusion. In order to understand how to determine an input buckling and whether or not to search for a buckling, a determination of how LASER-M treats the buckling

was carried out. It was verified that the input buckling is the geometric buckling, B_g^2, used in the equation for k_{eff} to calculate the leakage terms $(\bar{D}^g B_g^2)$ in each group g, where $\bar{D}^g$ is the spectrum averaged diffusion coefficient of group g. That is, in subroutine BONE, k_{eff} is calculated using the following equation.

$$k_{eff}(2\ \text{group}) = \frac{\overline{\nu\Sigma}_f^1}{\bar{\Sigma}_a^1 + \bar{\Sigma}_r^1 + \bar{D}^1 B_g^2} + \frac{\bar{\Sigma}_r^1 \overline{\nu\Sigma}_f^2}{(\bar{\Sigma}_a^1 + \bar{\Sigma}_r^1 + \bar{D}^1 B_g^2)(\bar{\Sigma}_a^2 + \bar{D}^2 B_g^2)}, \tag{5.1}$$

where B_g^2 = group independent geometric buckling (input)

$\bar{\Sigma}_\alpha^g$ = spectrum average macroscopic cross section for reaction α and group g

$\bar{D}^g$ = diffusion coefficient for group g

g = 1 is the fast plus epithermal group

g = 2 is the thermal group.

The LASER-M calculation essentially assumes that the modeled unit cell is infinitely long and is in an infinite sea of like assemblies (thus it assumes that there is no net leakage from the system). Thus the input geometric buckling should be the total geometric buckling to describe the total leakage. Additionally, if one is interested only in k_{inf} and/or the spectrum averaged cross sections of the cell it does not matter what geometric buckling is input since it only effects k_{eff}.

The buckling which is, at option, searched by LASER-M is, of course, the material buckling, B_m^2, for the specific composition in the unit cell. The material buckling enters the calculation mainly in the fast groups. This is because the equation solved by LASER-M in the fast groups is the B-1 approximation to the transport equation (dependent on B_m^2) and in the thermal groups LASER-M solves the integral transport equation (independent of B_m^2). The searched material buckling is used to calculate the fast spectrum but if B_m^2 is not searched, the input geometric buckling is used.

The material buckling is also used in the calculation of the fast group diffusion coefficients and macroscopic removal cross sections as well as the groupwise leakage edited in LASER-M. In subroutine BONE the fast group diffusion coefficients are calculated using

$$\bar{D}^g = \int_{\Delta E_g} J(E)\,dE/(\bar{\phi}^g * (B_m^2)^{1/2}), \qquad (5.2)$$

where ΔE_g = energy interval of group g

$J(E)$ = neutron current

$\bar{\phi}^g$ = total flux for group g

B_m^2 = searched material buckling.

The group removal cross sections, $\bar{\Sigma}_r^g$, are calculated using neutron conservation arguments. That is,

$$\bar{\Sigma}_r^1 = \frac{SUMF}{\bar{\phi}^1} - \bar{\Sigma}_a^1 - \bar{D}^1 B_m^2 \quad , \tag{5.3}$$

$$\bar{\Sigma}_r^2 = \bar{\Sigma}_r^1 * \frac{\bar{\phi}^1}{\bar{\phi}^2} - \bar{\Sigma}_a^2 - \bar{D}^2 B_m^2 \quad , \tag{5.4}$$

and

$$\bar{\Sigma}_r^3 = \frac{SUMF}{\bar{\phi}^3} - \bar{\Sigma}_a^3 - \bar{D}^3 B_m^2 \quad , \tag{5.5}$$

where SUMF = neutron production rate due to fissions (fission neutrons are produced in the fast range only)

group 1 = fast range (5.53 KeV to 10 MeV)

group 2 = epithermal range (1.855 eV to 5.53 KeV0

group 3 = fast plus epithermal range (1.855 eV to 10 MeV).

Additionally, the group leakages which are edited in LASER-M are calculated in the fast groups (groups 1 and 2, as above) using

$$\text{Group g leakage} = \int_{\Delta E_g} J(E)\,dE * (B_m^2)^{1/2} * V_c \quad , \tag{5.6}$$

and in the thermal region using

$$\text{Thermal leakage} = \bar{D}^{th} * B_m^2 * \bar{\phi}^{th} * V_c \quad , \tag{5.7}$$

where V_c = volume of the cell.

Note that combining the expression for $\bar{D}^g$ (Eq. 5.2) with the expression for the group leakage (Eq. 5.6) and with Eq. 5.7 yields, in general,

$$\text{Group g leakage} = \bar{D}^g B_m \bar{\phi}^g V_c, \qquad g = \text{all groups}, \quad (5.8)$$

which is, of course, the standard expression for leakage. As mentioned, the group leakages calculated by Eqs. 5.6 and 5.7 are edited but are not used to calculate k_{eff} (Eq. 5.1).

In order to determine the effect of the material buckling on the fast spectrum and on the spectrum averaged fast cross sections a LASER-M calculation was done by inputting a very small (10^{-6} cm^{-2}) value of geometric buckling and not searching for B_m^2. This run was compared to one for the same cell in which B_m^2 was searched and found to be .003336 cm^{-2}. It was found that k_{inf} without searching B_m^2 was less than 0.2% higher than the value obtained from the calculation that searched B_m^2. Additionally, the thermal macroscopics were identical for the two runs, but the non-thermal averaged values of $\bar{D}, \bar{\Sigma}_a, \bar{\Sigma}_r$, and $\overline{\nu\Sigma}_f$ were increased by 1.64%, 2.45%, 4.5%, and 1.86%, respectively, when the buckling was not searched.

Also, to determine the effect of not searching buckling on a depletion calculation, a 3.6 w/o MOX cell was depleted. In one run the material buckling was searched and in another it was not, with both runs having the total geometric buckling

as input. It was found that although the searched buckling varied from 93% of the input buckling at time zero to 36% at 12,500 hours the values of k_{inf} for the two runs matched to within 0.13% for the whole depletion. Additionally, the isotopic concentrations at 12,500 hours were also very close for the two runs (within 0.4%) with the fast macroscopic (in the order listed above) differing by 1.3%, 1.0%, 3.4%, and 1.21% respectively.

From the above discussion it can be concluded that the material buckling does not have a large effect on the cell calculation. However, since B_m^2 varies greatly during cell depletion (going to zero when $k_{inf} = 1.0$) it was decided to search for the material buckling in the calculations done in this study.

5.2.3 Options Selected

In almost all of the LASER-M calculations done in the present study the material buckling was searched and the Nelkin scattering kernel for water was used since it has been shown to be more accurate.[7,10] Additionally, the U-238 L factor was searched (L factors for the other nuclides input as 1.0) and the standard THERMOS iteration without extrapolation was used since the extrapolated iteration has been found not to converge in some plutonium systems.[8]

5.2.4 Unfueled Cell

The unfueled cell (RCC cell) was modeled without the presence of a control rod. The cell has water in the center surrounded by a metal sheath and water and grid structure in the outer region. Since LASER-M does not allow moderator in the center region or metal in the outer region and has no provisions for an unfueled cell calculation (fuel must be present) the unfueled cell was modeled approximately. A very small fuel region (0.05 cm) was specified containing only dilute U-235 (0.00001 atom/b-cm) to minimize the effect of the fuel on the calculation. The sheath was assumed to have the same dimensions as the fuel cladding and 304 stainless steel (SS 304) was assumed for its composition. SS 304 was placed in the cladding region of the cell model such that the total amount of SS 304 in the unfueled cell was contained in the clad at its actual atom number density. Then the total amount of water and adjusted boron in the unfueled cell was placed in the moderator region, again using the actual number densities and adjusting the cell outer radius accordingly.

The results from a LASER-M unfueled calculation modeled as above were compared to a LEOPARD unfueled calculation and showed very good agreement. In comparing isotopic region averaged thermal absorption cross sections (0.625 eV edit in

LASER-M) it was found that the values for hydrogen, oxygen, and boron-10 differed by only 0.4% (identical to the difference when comparing two fueled runs). The difference in the values for SS 304 was 2.3% indicating that the lumping of the metal next to the dilute fuel causes a larger, but still acceptable, difference. Thus it was concluded that modeling the RCC cell in LASER-M gave reasonable results which were, in turn, used throughout the present work.

It should be noted that LASER-M now edits the thermal diffusion coefficient over the moderator region only, designated as $\bar{D}_{mod}$ (see subsection 3.3.4). From $\bar{D}_{mod}$ an approximate transport cross section for hydrogen, $\tilde{\sigma}^{H,mod}_{tr}$, is calculated. In an unfueled run the use of $\tilde{\sigma}^{H,mod}_{tr}$ would be more accurate since it does not contain any effects of the fuel. However, in practice, there is little difference between the approximate transport cross section for hydrogen obtained by averaging over the whole cell and averaging only over the moderator.

5.2.5 Output Quantities

TABLE 5.1 lists the calculated values of k_{inf} for a number of cells modeled at beginning of life (BOL). It is interesting to note the differences between the plutonium and uranium cells when adding more water to the cell. In going

TABLE 5.1

BASIC RESULTS FOR BEGINNING OF LIFE LASER-M CALCULATIONS

RUN DESCRIPTION	k_{inf}
Normal 4 w/0 uranium cell	1.20445
Normal 4 w/0 uranium cell around a water hole	1.24024
Assembly average 4 w/o uranium cell	1.22272
Normal 3.85 w/o plutonium cell	1.18996
Normal 3.6 w/o plutonium cell	1.18544
Normal 3.3 w/o plutonium cell	1.17956
Normal 3.6 w/o plutonium cell around water hole	1.25275
Normal 3.3 w/o plutonium cell around water hole	1.24630
Assembly average of graded enrichment plutonium assembly (3.53 w/o Pu)	1.21377
Assembly average of 3.6 w/o plutonium constant enrichment assembly	1.21516

Boron concentration in all runs was 1000 appm.

from a normal to an assembly average cell, the increase in k_{inf} is 1.5% for the uranium cells and 2.4% for the plutonium cells. When going from normal cells to cells around water the increase in k_{inf} is 3.0% for the uranium and 5.7% for the plutonium. Basically, the added water effects the plutonium cells more than the uranium cells because the plutonium cells are much more undermoderated than the uranium cells. This is, of course, due to the much higher thermal absorption in the plutonium cells. Additionally, it is interesting to note the small effect that the increases in enrichment of plutonium has on k_{inf}. For a 17% increase in plutonium enrichment an increase of only 0.9% is obtained in k_{inf}. In general, an increase in enrichment of plutonium cells has less of an effect on k_{inf} that an equivalent increase for uranium cells due to the larger thermal absorption of plutonium.[4]

LASER-M outputs spectrum averaged microscopic and macroscopic parameters for the thermal range, the epithermal range, the fast range, and a combination of the fast and epithermal range. It also edits one group macroscopic parameters. From this information it is seen that one, two, or three group parameters can be obtained from LASER-M for use in a diffusion code. In the present work <u>two-group</u> parameters were used exclusively since the improvements in going to three groups were not expected to be significant.[41]

When using normal cell calculations macroscopic parameters could be used in PDQ but when using assembly average cells or cells around water holes microscopics had to be used to conserve the volume of water in the assembly.

Most of the output of LASER-M is straightforward and is adequately described in Ref. 16. It should, however, be noted that the macroscopic removal cross section is not calculated on a neutron conservation argument in the thermal region as stated in Ref. 16. It is actually calculated on neutron conservation arguments in the fast region using Eq. 5.3 to 5.5.

5.3 Two Group Diffusion Equation Theory Calculations (PDQ-7)

5.3.1 Input Quantities

The input to PDQ when using macroscopics is relatively straightforward once the unique terminology of PDQ is understood. Basically, in the present study, two groups eigenvalue problems were run. When doing assembly calculations zero current boundary conditions were used, implying the assemblies were in an infinite sea of like assemblies, and a convergence criteria of 10^{-4} was used in all problems. In the unit assembly calculations 2 mesh points per cell were used.

When inputting microscopics the input is more complicated since not only do number densities and microscopics have to be input but the compositions must be made depletable even in a non-depletion calculation. Depletable compositions imply that fission product and nuclide depletion chains must be specified. However, these can be made into one simple dummy chain.

The standard procedure of determining the adequacy of a finite difference calculation such as PDQ is to decrease the mesh spacing and observe the effect on the calculated eigenvalue. A PDQ run using 4 mesh points per cell was done with only a 0.048% change in k_{eff}. Although water cell peaking was increased with the increased mesh the difference in the two runs was not considered to be significant.

When specifying microscopic cross sections in PDQ, microscopic removal and transport cross sections must be specified and they are now output by LASER-M (see Section 3.3). When used in PDQ the approximate microscopic removal cross section for hydrogen only is specified with the microscopic removal cross section for all other nuclides set equal to zero. Also, the approximate transport cross section for hydrogen, output by LASER-M, is used for the transport cross section of hydrogen in PDQ. The absorption cross section of all other nuclides is used as the transport cross section in PDQ. LASER-M has a special condensed cross section output which prints fast,

thermal, and GMND microscopic cross sections in a form consistent with the input requirements of PDQ. Additionally, effective thermal microscopics were used in PDQ (see Section 2.1).

5.3.2 Output Quantities

The output quantities in PDQ are straightforward and are explained in Ref. 26 and 27. Numerous edit sets can be specified in PDQ which allow the user to edit various quantities in different parts of the problem. k_{inf} and k_{eff} as well as volume and flux weighted macroscopics can be edited in the desired edit sets. Additionally, pointwise flux and power for the whole problem or selected parts may be edited by the user. Of primary importance in the present work was the average power density edits which were carried out over each cell of the quarter assembly which was modeled. Additionally, PDQ edits the average flux (both fast and thermal) for each of the specified edit sets. The reader should consult ANCR-1061[28] for a summary of the edits available in PDQ.

CHAPTER 6

COMPARISON OF CALCULATIONS WITH REFERENCE CALCULATIONS - TWO DIMENSIONAL BEGINNING OF LIFE (BOL) POWER DISTRIBUTIONS

6.1 Uranium Assembly

The reference WCAP report [3] gives cell power distributions in a quarter assembly of 4 w/o UO_2 fuel of the type used in region 4 of the San Onofre PWR. This power distribution was used as the first basis of comparison of the Westinghouse results with the results of the present study.

Excellent agreement with the reference WCAP results was obtained by using normal cell GMND cross sections from LASER (see Section 5.2.1 for definition of unit cells) as input to PDQ and modeling the inter-assembly water gap. The cross sections for the water holes and gap were obtained from an unfueled cell calculation as described in subsection 5.2.1.4. The results obtained are listed in Table 6.1 and for comparative purposes additional results from another calculation (using the same normal cell GMND but not modeling the water gap) are included as well as calculated values obtained with the use of regular normal cell cross sections. The deviations in pin power are calculated using

$$\text{Deviation in Pin Power} = \frac{(P_{calc} - P_{ref}) \times 100\%}{P_{ref}} \qquad (6.1)$$

where P_{ref} = relative power density of the cell as given in the reference WCAP report

P_{calc} = relative power density of the cell as calculated in the present study

and the average difference in cell power is calculating using

$$\text{Average Difference in Cell Powers} = \frac{1}{N} \sum_{i}^{N} \left| \frac{P^i_{calc} - P^i_{ref}}{P^i_{ref}} \right| \times 100\% \ , \qquad (6.2)$$

where N = number of cells.

As can be seen from Table 6.1, the addition of the water gap improved the results considerably in addition to the use of the GMND cross sections. Figure 6.1 shows the cell powers calculated in the present study using the normal cell GMND cross sections with the water gap. Also included are the reference powers and the percent deviation of the calculated results from the reference powers. The agreement shown in Table 6.1 and Figure 6.1 is considered excellent for the normal GMND calculation. It should, however, be noted that since the relative power densities of the cells in any calculation will

TABLE 6.1

URANIUM ASSEMBLY - COMPARISON OF CALCULATED AND REFERENCE POWERS

Model Description*	Maximum Pin Deviation	Deviation in Peak Pin	Average Difference
Normal GMND with water gap	+0.4%	-0.3%	0.18%
Normal GMND without water gap	-2.2%	+0.3%	0.60%
Normal cell without water gap	+2.8%	-2.0%	1.02%

*NOTE: See subsection 5.2.1 for cell definitions

have values near 1.0, a deviation of over 1.0% in cell powers is not considered a very good match.

For additional comparative purposes other calculations done in the present study are listed in Table 6.2. Except where otherwise noted, the cross sections for the water holes were obtained from an unfueled cell calculation and the inter-assembly water gap was not modeled.

From the information in Table 6.2 it is seen that no other model gave nearly as good an agreement as the normal cell GMND calculation listed in Table 6.1. It is interesting to note that only the model which used fuel cross sections from cells around water holes gave a higher assembly peaking than the reference calculation. Additionally, the effect of using water hole cross sections from an assembly average cell and a cell around water can be seen from Table 6.2. In both cases the results were worse than when the water hole cross sections obtained from an unfueled calculation were used. Finally, the improvement when using GMND cross sections is again seen when applied to assembly average cells.

TABLE 6.2

URANIUM ASSEMBLY - COMPARISON OF SUPPLEMENTARY CALCULATED POWERS WITH REFERENCE POWERS

Model Description*	Maximum Pin Deviation	Deviation in Peak Pin	Average Difference
Assy. Ave. cell	+2.8%	-2.1%	1.06%
Assy. Ave. cell with water hole c/s from Assy Ave cell	+3.9%	-3.4%	1.63%
Assy. Ave. GMND with water hole GMND c/s from Assy. Ave. cell	+2.7%	-2.1%	0.97%
Normal cell with water hole c/s from fuel cell around water	+3.7%	-3.2%	1.52%
Normal cell with cells around water modeled	+2.9%	+1.5%	1.75%

*NOTE: See subsection 5.2.1 for cell definitions

6.2 3.6 w/o Plutonium Assembly Surrounded by Uranium

6.2.1 Reference Power Distributions

Figure 6.2 shows the reference power distributions contained in Ref. 3 for a constant enrichment 3.6 w/o PuO_2-UO_2 cell surrounded by 4 w/o UO_2 assemblies (design specifications for these cells are given in Table 1.1 and Appendix A). Upon inspection of Figure 6.2 it is seen that the power peak shown in the center (lower left on Figure 6.2) of the plutonium assembly is not consistent with the other available information. Additionally, in cell calculations done in the present work a power depression was obtained in the center of the plutonium assembly. Therefore, it was decided that the power in the lower left cell of the plutonium should be adjusted to a more consistent value. The adjustment was done using the peak to average assembly power given in Ref. 3. A relative power density of 0.901 (versus 1.045 in Ref. 3) was calculated. Additionally, the uranium assembly pictured next to the plutonium assembly in the reference figure (Figure 6.2) is not actually in this position. This can be seen by comparing the cell powers of the uranium assembly in Figure 6.2 to the uranium cell powers for the assembly in an infinite sea of like assemblies shown in Figure 6.1. This comparison is

shown in Figure 6.3 where the first number in each cell is the reference power for the uranium assembly next to the 3.6 w/o PuO_2 - UO_2 assembly (Figure 6.2). The second number is the difference from the cell power in the uranium assembly in the sea of uranium assemblies (Figure 6.1). That is,

$$\text{Difference} = P_{\text{in U assy. next to Pu}} - P_{\text{in U assy. in sea of U assy.}} \tag{6.3}$$

It is seen from Figure 6.3 that the cell powers in the uranium assembly, which is pictured next to the plutonium assembly, have about the same distribution (with the exception of the upper left corner) as the uranium assembly in an infinite sea of uranium. Since the plutonium assembly will greatly reduce the power in the uranium cells near it (due to the effect on the uranium of the lower thermal flux in the plutonium) it was concluded that the uranium assembly shown in Figure 6.2 is not located as pictured. Further investigation showed that the assembly is probably the uranium assembly in the upper righthand corner of the 2 x 2 array of quarter assemblies shown below.

1/4 U Assy	1/4 U* Assy
1/4 Pu Assy	1/4 U Assy

Center of Pu Assy

It should be noted that in the present work this 2 x 2 array of quarter assemblies was modeled in PDQ and the upper right uranium assembly powers were compared to the uranium powers given in the reference WCAP report.

6.2.2 Results of Basic Calculations

A number of calculations were performed to try to match the power distribution given in the reference WCAP report (Figure 6.2). In all cases the plutonium assembly power was found to be considerably lower than that calculated by Westinghouse, although the relative power distribution within the plutonium and within the uranium assemblies was generally in good agreement with the published results.

Table 6.3 shows a comparison between the reference calculations and three basic calculations done in the present study. These calculations used cross sections from an unfueled cell calculation for all water holes and the following parameters for the fuel cells:

1. Assembly average cross sections for both the plutonium assembly and the uranium assembly.
2. Assembly average GMND cross sections for both the plutonium and uranium assembly.
3. Assembly average GMND cross sections for both the plutonium and the uranium assemblies with an additional region in the uranium cells directly surrounding the plutonium assembly. This additional region of uranium had an interface value of the GMND diffusion coefficient formed by considering the spectrums of both the plutonium and uranium assemblies as discussed in subsection 1.4.3.

The maximum pin deviation and the average difference in cell powers are defined as discussed in Section 6.1. The assembly power, $\bar{P}$, is the average of all cell powers in the assembly and the difference in assembly power is calculated using

$$\text{Difference in Assembly power} = \frac{\bar{P}_{calc} - \bar{P}_{ref}}{\bar{P}_{calc}} \times 100\% , \qquad (6.3)$$

where P_{ref} = 1.049 for the plutonium assembly and 0.992 for the uranium assembly.

TABLE 6.3

3.6 w/o PuO_2-UO_2 ASSEMBLY - COMPARISON OF CALCULATED POWERS WITH REFERENCE POWERS

Model Description	Assy	Maximum Pin Dev.	Average Difference	Assy Power	Difference in Assy Power
Assy. Ave. c/s	Pu	-7.0%	4.34%	1.003	-4.39%
	U	+5.3%	2.50%	1.017	+2.45%
	Total	-	3.42%	-	-
Assy. Ave. GMND c/s	Pu	-6.7%	4.87%	0.998	-4.89%
	U	+3.7%	2.67%	1.019	+2.67%
	Total	-	3.77%	-	-
Assy. Ave. GMND c/s with interface	Pu	-6.6%	4.32%	1.004	-4.33%
	U	+3.7%	2.57%	1.018	+2.58%
	Total	-	3.45%	-	-

In order to ease the evaluation of the relative power distribution within the assemblies the calculated assembly power in each assembly was forced to the reference value. Table 6.4 shows a comparison between the reference values and the same calculations discussed above after the powers had been adjusted such that the calculated assembly power equaled the reference assembly power.

The power distributions in the plutonium assembly calculations discussed above are shown in Figures 6.4 to 6.6. The adjusted plutonium power distributions are shown in Figures 6.7 to 6.9.

It can be seen from Table 6.3 that the plutonium assembly powers were from 4.39% to 4.89% lower than the reference values with the assembly average GMND cross sections giving the largest discrepancy. However, as seen in Table 6.4 when the calculated assembly powers were adjusted to the reference powers the relative power distributions match fairly well with the reference values, the assembly average GMND calculation giving the best results. This is seen by comparing the adjusted average difference in cell powers for each calculation. In the plutonium cell the value is 1.07% using the assembly average cross sections, 0.80% using the assembly average GMND cross sections, and 1.13% using assembly average GMND with interface uranium. From further comparison of

TABLE 6.4

3.6 w/o PuO_2 ASSEMBLY - COMPARISON OF ADJUSTED CALCULATED POWERS WITH REFERENCE POWERS

Model Description	Assy	Maximum Pin Dev.	Average Difference	Peak to Average Power (Ref. = 1.124)
Assy. Ave. c/s	Pu	+2.8%	1.07%	1.118
	U	-2.8%	1.16%	-
	Total	-	1.12%	-
Assy. Ave. GMND c/s	Pu	+2.3%	0.80%	1.128
	U	-2.1%	0.50%	-
	Total	-	0.65%	-
Assy. Ave. GMND c/s with interface	Pu	+2.5%	1.13%	1.135
	U	-2.4%	0.57%	-
	Total	-	0.85%	-

the adjusted average differences in cell power for the three calculations shown in Table 6.4, it is seen that the GMND cross sections effect the uranium assembly much more than the plutonium assembly. That is, for the uranium assembly the value goes from 1.16% to 0.50% (a 57% reduction), but for the plutonium assembly it only goes from 1.07% to 0.80% (a 25% reduction). This implies that the relative power distribution for the plutonium assembly is less affected by the GMND cross sections than the uranium assembly.

Also, as seen from Table 6.3, the addition of an interface region improves the assembly power match. The difference in assembly powers goes from -4.89% to -4.32% for assembly average GMND cross sections with the addition of the interface region. However, the relative power distributions were not as good when the interface GMND values were used. This is seen from Table 6.4 and by inspecting Figure 6.9 which gives the cell powers for the plutonium assembly as calculated by using interface GMND values in the uranium immediately adjacent to the plutonium assembly. From Figure 6.9 it is seen that the powers in the plutonium cells next to the uranium assembly (right hand column) are higher than the adjusted powers for the other calculations. This is to be expected since the interface

GMND cross sections have the effect of allowing more neutrons to leak from the uranium assembly to the plutonium assembly.

Additionally, assembly average cross sections yielded better results than using normal cross sections (discussed below) so it was concluded that assembly average GMND cross sections should be used for the remainder of the study. It should be noted that when depleting a unit cell an assembly average cell should be modeled since, on the average, a fuel rod will be associated with an assembly average amount of water.

6.2.3 Supplemental Calculations

As discussed in the previous section the best match between calculated and reference powers in the 3.6 w/o PuO_2-UO_2 fuel assembly was obtained using assembly average cross sections. However, the plutonium assembly power was well below (about 4.5%) the reference value. In an attempt to obtain better results many different calculations were done, none of which yielded any substantial improvement in the results discussed in subsection 6.2.2. Table 6.5 shows the results, for the plutonium assembly only, of two of these supplemental calculations. As seen by comparing Table 6.3 to Table 6.5, the results obtained

TABLE 6.5

3.6 w/o PuO_2 ASSEMBLY - COMPARISON OF SUPPLEMENTAL CALCULATIONS WITH REFERENCE POWERS (PLUTONIUM ASSEMBLY ONLY)

Model Description	Maximum Pin Dev.	Average Difference	Assy Power	Difference in Assy Pw	Peak to Ave. Pw (Ref. = 1.124)
All Normal c/s	-7.9%	5.13%	0.995	-5.16%	1.123
Normal GMND with interface in uranium	-7.4%	4.83%	0.998	-4.81%	1.146

by using normal cross sections were worse than those obtained from the assembly average cross sections. Additionally, calculations were done using LEOPARD cross sections, cold cell dimensions, and an adjusted value of ν (neutrons per fission) for U-235 to better match the value in the LEOPARD thermal library. None of these calculations improved the results significantly. Also, all atom number densities and cell dimensions were independently recalculated and found to be correct. Thus, the large discrepancy in plutonium assembly power could not be explained.

6.3 Graded Enrichment Plutonium Assembly Surrounded by Uranium

Due to the large (1.124) peak to average assembly power obtained when using constant enrichment plutonium assemblies the enrichments within a plutonium assembly were graded to reduce the power peak. The reference power distribution for a graded enrichment plutonium assembly, the specifications of which are given in Chapter 1, is presented in Figure 6.10 (from Ref. 3). Basically, the results of the calculations on this assembly done in the present study were very similar to the results for the constant enrichment plutonium assembly discussed in Section 6.2. Table 6.6 shows a comparison of the basic calculations done in the present study with the reference values, where the adjusted average difference in cell powers (discussed in Section 6.2) are listed.

As seen from Table 6.6, when using assembly average GMND cross sections a power deficiency in the plutonium assembly of 4.55% is obtained which was worse than the 4.03% deficiency when using straight assembly average cross sections. However, when the powers were adjusted the average difference in cell powers was 0.77% for the assembly average GMND calculation and 1.05% for the straight assembly average, implying that the GMND cross sections yield a better relative power distribution. Also, the interface GMND values gave the best assembly power match (a deficiency of 3.99%) but the largest discrepancy in relative power distribution (the average difference in cell powers was 1.17% in the plutonium assembly).

Table 6.7 shows the results from a number of supplemental calculations. By comparing Table 6.6 and 6.7 it is seen that the use of normal cross sections did not match the reference results as well as using assembly average cross sections. Additionally, the run labeled 3 x 3 array was performed to see the effect of adding more uranium assemblies around the plutonium assembly. As mentioned in Section 6.2 in all the previous calculations done in the present study a 2 x 2 array of quarter assemblies was modeled in PDQ. Since zero current (reflective) boundary conditions were used, the array modeled for the majority of calculations was essentially a checkerboard of plutonium and uranium assemblies. That is, moving

TABLE 6.6

GRADED ENRICHMENT PuO_2-UO_2 ASSEMBLY - COMPARISON OF CALCULATED POWERS WITH REFERENCE POWERS

Model Description	Assy	Maximum Pin Dev.	Average Difference (Adjusted)	Assy Power	Difference in Assy Pw	Peak to Ave. Pw (Ref. = 1.069)
Assy. Ave. c/s	Pu	-7.0%	0.98%	0.999	-4.03%	1.082
	U	+5.1%	1.13%	1.018	+2.31%	-
	Total	-	1.05%	-	-	-
Assy. Ave. GMND c/s	Pu	-7.5%	1.01%	0.994	-4.55%	1.085
	U	+3.6%	0.52%	1.020	+2.54%	-
	Total	-	0.77%	-	-	-
Assy. Ave. GMND with interface U	Pu	-7.3%	1.17%	1.000	-3.99%	1.090
	U	+3.6%	0.60%	1.019	+2.45%	-
	Total	-	0.87%	-	-	-

TABLE 6.7

GRADED ENRICHMENT PuO_2-UO_2 ASSEMBLY - COMPARISON OF SUPPLEMENTAL CALCULATED POWERS WITH REFERENCE POWERS

Model Description	Assy	Maximum Pin Dev.	Average Difference (Adjusted)	Assy Power	Difference In Assy Pw	Peak to Ave. Pw (Ref. = 1.069)
All Normal c/s	Pu	-8.1%	1.11%	0.992	-4.78%	1.087
	U	+5.6%	1.12%	1.022	+2.74%	-
	Total	-	1.12%	-	-	-
Normal GMND c/s	Pu	-8.6%	1.16%	0.986	-5.32%	1.091
	U	+4.2%	0.60%	1.025	+3.00%	-
	Total	-	0.88%	-	-	-
Assy. Ave. GMND c/s in 3 x 3 array	Pu	-9.0%	1.02%	0.978	-6.06%	1.085
	U	+2.1%	0.54%	1.004	0.98%	-
	Total	-	0.78%	-	-	-

in each of the two dimensions, the array of assemblies would be Pu - U - Pu - U -, etc. With a 3 x 3 array of assemblies one plutonium assembly is surrounded by 8 uranium assemblies thus separating the plutonium assemblies more than the 2 x 2 array of quarter assemblies. Therefore, in the 3 x 3 array, moving in each of the two dimensions, the array of assemblies would be Pu - U - U - Pu - U - U, etc. As shown in Table 6.7 the 3 x 3 array of assembly average GMND cross sections yielded an even larger discrepancy (the plutonium assembly power was 6.06% lower than the reference power).

6.4 Conclusions

It has been found that excellent agreement with reference power distributions for a uranium assembly in a sea of uranium assemblies is obtained using normal cell GMND cross sections. However, in all cases, when trying to match the relative power of a plutonium assembly surrounded by uranium assemblies the calculated power in the plutonium assembly was much lower (about 4.5%) than the reference value. Thorough checks of all input parameters and numerous different cell models did not improve the results. It was found that the relative cell powers within the plutonium and uranium assemblies showed reasonable agreement (an average of about 0.8% difference) with the reference values, the assembly average GMND cross sections giving the best results.

.945 .944 (-.1%)						
.949 .948 (-.1%)	.976 .973 (-.3%)					
.957 .958 (.1%)	1.019 1.015 (-.4%)					
.956 .958 (.2%)	.994 .994 (0%)	1.055 1.054 (-.1%)	1.057 1.058 (.1%)			
.958 .960 (.2%)	.996 .997 (.1%)	1.060 1.060 (0.0%)	1.090 1.087 (-.3%)			
.961 .964 (.3%)	1.026 1.023 (-.3%)		1.076 1.072 (-.4%)	1.042 1.041 (-.1%)	.983 .983 (0%)	
.957 .959 (.2%)	.993 .993 (0%)	1.044 1.042 (-.2%)	1.009 1.010 (.1%)	.970 .974 (.4%)	.944 .947 (.3%)	.928 .930 (.2%)

Center of Assy

Key:

Ref. Power Calc. Power (% Diff.)

FIGURE 6.1 4 w/o UO_2 Assembly-Calculated Versus Reference Powers for Normal Cell GMND c/s and Water Gap

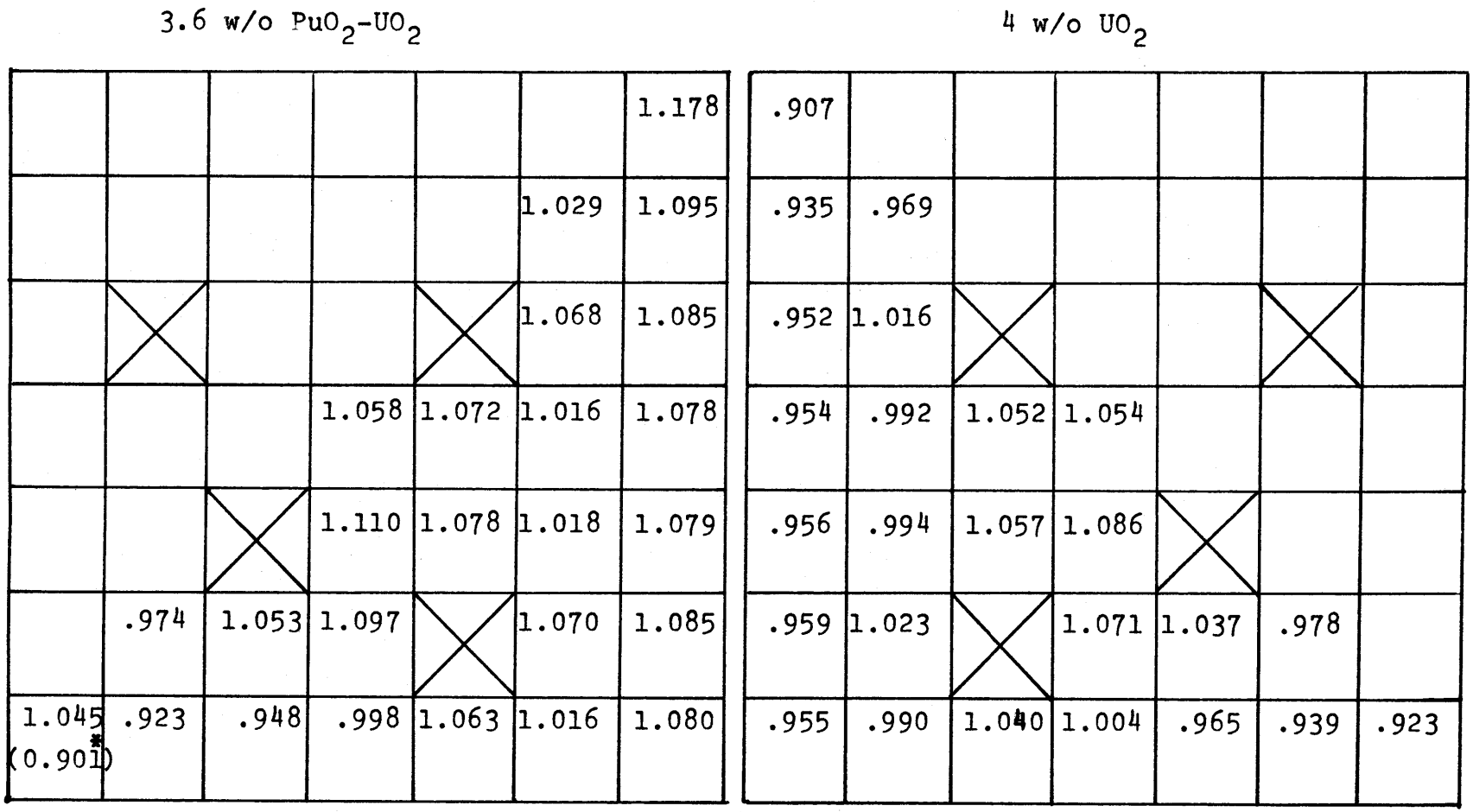

Figure 6.2 Reference Power Distribution in 3.6 w/o PuO_2-UO_2 Assembly Surrounded by 4 w/o UO_2. (Ref. 3)

*Adjusted Value

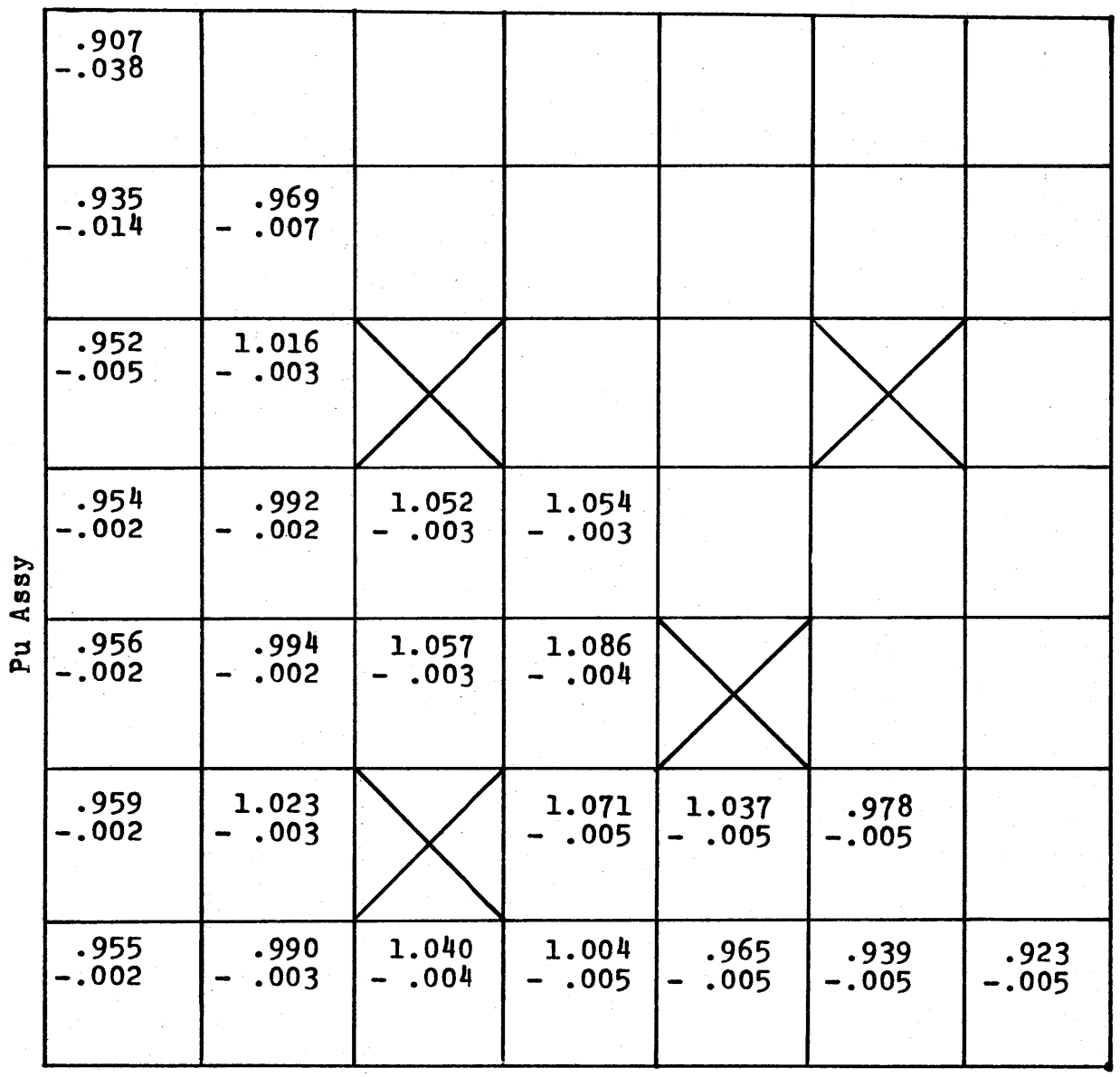

Figure 6.3 Comparison of Uranium Cell Powers for an Assembly Pictured Next to a Pu Assembly and an Uranium Assembly in an Infinite Sea of Uranium Assemblies

						1.178 1.121 (-4.8)
					1.029 1.011 (-1.7)	1.095 1.062 (-3.0)
					1.068 1.027 (-3.8)	1.085 1.049 (-3.3)
			1.058 1.008 (-4.7)	1.072 1.020 (-4.9)	1.016 .991 (-2.5)	1.078 1.040 (-3.5)
			1.110 1.036 (-6.7)	1.078 1.022 (-5.2)	1.018 .989 (-2.8)	1.079 1.038 (-3.8)
	.974 .922 (-5.3)	1.053 .983 (-6.6)	1.097 1.020 (-7.0)		1.070 1.018 (-4.9)	1.085 1.040 (-4.1)
.901 .867 (-3.8)	.923 .883 (-4.3)	.948 .911 (-3.9)	.998 .953 (-4.5)	1.063 1.001 (-5.8)	1.016 .984 (-3.1)	1.080 1.035 (-4.2)

Center of Assy

P_{ref}
P_{calc}
(% Diff.)

Figure 6.4 Calculated Power Distribution in 3.6 w/o PuO_2-UO_2 Assembly Using Assembly Average Cross Sections.

						1.178 1.125 (-4.5)
					1.029 1.001 (-2.7)	1.095 1.056 (-3.6)
					1.068 1.023 (-4.2)	1.085 1.041 (-4.1)
			1.058 1.006 (-4.9)	1.072 1.019 (-4.9)	1.016 .981 (-3.4)	1.078 1.031 (-4.4)
			1.110 1.040 (-6.3)	1.078 1.022 (-5.2)	1.018 .980 (-3.7)	1.079 1.030 (-4.5)
	.974 .913 (-6.3)	1.053 .983 (-6.6)	1.097 1.023 (-6.7)		1.070 1.015 (-5.1)	1.085 1.033 (-4.8)
.901 .855 (-5.1)	.923 .872 (-5.5)	.948 .901 (-5.0)	.998 .946 (-5.2)	1.063 1.000 (-5.9)	1.016 .974 (-4.1)	1.080 1.027 (-4.9)

Center of Assy

Key:

P_{ref}
P_{calc}
(% Diff.)

Figure 6.5 Calculated Power Distribution in 3.6 w/o PuO_2-UO_2 Assembly Using Assembly Average GMND Cross Sections

						1.178 1.139 (-3.3)
					1.029 1.009 (-1.9)	1.095 1.069 (-2.4)
					1.068 1.029 (-3.7)	1.085 1.053 (-2.9)
			1.058 1.008 (-4.7)	1.072 1.022 (-4.7)	1.016 .987 (-2.9)	1.078 1.043 (-3.2)
			1.110 1.043 (-6.0)	1.078 1.025 (-4.9)	1.018 .985 (-3.2)	1.079 1.041 (-3.5)
	.974 .915 (-6.1)	1.053 .984 (-6.6)	1.097 1.025 (-6.6)		1.070 1.020 (-4.7)	1.085 1.044 (-3.8)
.901 .857 (-4.9)	.923 .874 (-5.3)	.948 .903 (-4.7)	.998 .948 (-5.0)	1.063 1.003 (-5.6)	1.016 .979 (-3.6)	1.080 1.039 (-3.8)

Center of Assy

Key:

P_{ref}
P_{calc}
(% Diff.)

Figure 6.6 Calculated Power Distribution in 3.6 w/o PuO_2-UO_2 Assembly Using Assembly Average GMND Cross Sections with Interface GMND in Uranium Assembly.

						1.178 1.172 (-0.5)
					1.029 1.057 (2.8)	1.095 1.111 (1.4)
					1.068 1.074 (0.6)	1.085 1.097 (1.1)
			1.058 1.054 (-0.4)	1.072 1.067 (-0.5)	1.016 1.036 (2.0)	1.078 1.088 (0.9)
			1.110 1.084 (-2.4)	1.078 1.069 (-0.8)	1.018 1.034 (1.6)	1.079 1.086 (0.6)
	.974 .964 (-1.0)	1.053 1.028 (-2.4)	1.097 1.067 (-2.8)		1.070 1.065 (-0.5)	1.085 1.088 (0.3)
.901 .907 (0.6)	.923 .924 (0.1)	.948 .953 (0.5)	.998 .997 (-0.1)	1.063 1.047 (-1.5)	1.016 1.029 (1.3)	1.080 1.082 (0.2)

Center of Assy

Key:

P_{ref}
P_{calc}
(% Diff)

Figure 6.7 Calculated Power Distribution (ADJUSTED) in 3.6 w/o PuO_2 - UO_2 Assembly Using Assembly Average Cross Sections.

						1.178 1.183 (0.4)
					1.029 1.052 (2.3)	1.095 1.110 (1.4)
					1.068 1.076 (0.7)	1.085 1.095 (0.9)
			1.058 1.058 (0.0)	1.072 1.071 (-0.1)	1.016 1.031 (1.5)	1.078 1.084 (0.6)
			1.110 1.094 (-1.5)	1.078 1.075 (-0.3)	1.018 1.030 (1.2)	1.079 1.083 (0.4)
	.974 .960 (-1.4)	1.053 1.034 (-1.8)	1.097 1.076 (-1.9)		1.070 1.067 (-0.3)	1.085 1.086 (0.1)
.901 .899 (-0.2)	.923 .917 (-0.7)	.948 .947 (-0.1)	.998 .995 (-0.3)	1.063 1.051 (-1.1)	1.016 1.029 (0.8)	1.080 1.080 (0.0)

Center of Assy

Key:

P_{ref}
P_{calc}
(% Diff.)

Figure 6.8 Calculated Power Distribution (ADJUSTED) in 3.6 w/o PuO_2-UO_2 Assembly Using Assembly Average GMND Cross Sections.

						1.178 1.191 (1.1)
					1.029 1.055 (2.5)	1.095 1.117 (2.0)
					1.068 1.076 (0.7)	1.085 1.101 (1.4)
			1.058 1.054 (-0.4)	1.072 1.068 (-0.3)	1.016 1.032 (1.5)	1.078 1.090 (1.1)
			1.110 1.090 (-1.8)	1.078 1.071 (-0.6)	1.018 1.030 (1.1)	1.079 1.088 (0.8)
	.974 .956 (-1.8)	1.053 1.029 (-2.3)	1.097 1.071 (-2.3)		1.070 1.068 (-0.4)	1.085 1.091 (0.6)
.901 .896 (-0.6)	.923 .914 (-1.0)	.948 .944 (-0.4)	.998 .991 (-0.7)	1.063 1.048 (-1.4)	1.016 1.023 (0.7)	1.080 1.086 (0.6)

Center of Assy

Key:

P_{ref}
P_{calc}
(% Diff)

Figure 6.9 Calculated Power Distribution (ADJUSTED) in 3.6 w/o PuO_2-UO_2 Assembly Using Average Assembly GMND with Interface GMND in Uranium.

Graded Enrichment Plutonium

						1.113
					1.047	1.108
	X			X	1.018	1.096
			1.029	1.034	1.037	1.086
		X	1.075	1.038	1.038	1.087
	1.015	.999	1.053	X	1.019	1.094
.923	.945	.988	1.015	1.017	1.034	1.087

4 w/o Uranium

.911						
.937	.972					
.955	1.019	X			X	
.957	.994	1.055	1.057			
.958	.997	1.050	1.089	X		
.962	1.026	X	1.075	1.040	.981	
.957	.993	1.043	1.007	.967	.941	.926

Center of
Pu Assy

Figure 6.10 Reference Power Distribution for Graded Enrichment PuO_2-UO_2 Assembly Surrounded by 4 w/o UO_2 (Ref. 3)

CHAPTER 7

ZERO-DIMENSIONAL DEPLETION CALCULATIONS (LASER)

7.1 Introduction

The depletion of unit cells for the various enrichments of uranium and plutonium fuels was carried out using LASER-M. In this way the effects of the changing nuclide concentrations on the neutron spectrum were calculated. The output from a LASER-M depletion calculation, in the form of changing microscopic and macroscopic cross sections was then used in PDQ-7/HARMONY to calculate the behaviour of the San Onofre PWR during cycle 2, which was the first cycle the plutonium assemblies, described in Chapter1, were present. As discussed in Chapter 6, it was decided to deplete assembly average unit cells in LASER-M. This procedure is similar to the commonly used depletion of a "super-cell" in LEOPARD.

Since the spectrum in the various enrichments of uranium and plutonium is significantly different, an assembly average unit cell of each enrichment, shown in TABLE 7.1, was depleted.

As an example of the variation in spectrum, and thus the variation in cell averaged cross sections, TABLE 7.2 lists the variation in the cross sections of a number of nuclides for BOL calculations done for the 3.3 w/o PuO_2-UO_2 and the 3.85 w/o PuO_2-UO_2 fuel. In TABLE 7.2 the percent

TABLE 7.1

VARIOUS ENRICHMENTS (WITH LOADINGS) PRESENT DURING CYCLE 2 OF SAN ONOFRE - I (Ref. 40)

Region	Enrichment	Number of Assemblies	Total Loading (MTM)
1	3.15 w/o U-235	1	0.366
2	3.40 w/o U-235	52	19.084
3	3.85 w/o U-235	52	18.810
4U	4.0 w/o U-235	48	17.455
4Pu	Graded (See TABLE 1.1)	4	1.335

variation of the cross sections is calculated using

$$\text{Percent Variation} = \frac{\sigma(3.3\ \text{w/o}) - \sigma(3.85\ \text{w/o})}{\sigma(3.3\ \text{w/o})} \times 100\% \qquad (7.1)$$

As seen from TABLE 7.2, a number of cross sections are considerably different (5.0 to 7.0% different) in the two enrichments. This is especially true in the thermal energy range although the difference in the fast cross sections for the two enrichments is not inconsequential. It should be noted, however, that all three plutonium enrichments are located near one another (all are in one assembly) and thus a relatively large amount of spectrum overlap can be expected. This fact may make it possible to approximate the whole plutonium assembly as a constant enrichment assembly for zero-dimensional depletion purposes. That is, it may be possible to accurately approximate the depletion characteristics of the plutonium assembly by depleting only one plutonium unit cell with the average enrichment of plutonium (3.53 w/o Pu) to obtain spectrum averaged cross sections as a function of burnup. This approach was not attempted in the present study but its investigation is recommended for future work on graded enrichment plutonium assemblies of the type analysed in the present study.

7.2 Depletion Procedure

7.2.1 General Description

As mentioned in Section 7.1, assembly average unit cells were depleted for each enrichment of uranium and plutonium that was present in the San Onofre PWR during

TABLE 7.2

PERCENT VARIATION IN MICROSCOPIC CROSS SECTIONS BETWEEN 3.3 W/O PUO_2-UO_2 and 3.85 W/O PUO_2-UO_2 FUEL

	Microscopic Absorption Cross Section		Microscopic Fission Cross Section	
Nuclide	Fast	Thermal	Fast	Thermal
H	+1.7%	+1.4%	—	—
O	-0.3%	+2.9%	—	—
Zr	-0.1%	+2.3%	—	—
U-235	+1.0%	+6.2%	+0.9%	+6.1%
U-236	+1.6%	—	-0.4%	—
U-238	+0.5%	+5.1%	-0.4%	—
Pu-239	+2.2%	+6.7%	+1.9%	+6.7%
Pu-240	+1.1%	+3.5%	-0.4%	+3.5%
Pu-241	+1.6%	+7.1%	+1.5%	+7.0%
Pu-242	+2.8%	+4.5%	-0.4%	—
Xe-135	+2.2%	—	—	—
Sm-149	+1.6%	—	—	—
F.P.	+0.9%	—	—	—
B-10	+1.7%	+1.4%	—	—

NOTES: 1. Percent Variation $= \frac{\sigma(3.3\ w/o) - \sigma(3.85\ w/o)}{\sigma(3.3\ w/o)} \times 100\%$

2. Fast cross section denotes fast plus epithermal edit in LASER.

cycle 2. In all depletions, time steps of 2000 hours were used preceded by short time steps of 75 and 425 hours to accurately represent the Xe-135 and Sm-149 buildup, respectively. In all cases the total geometric buckling was input and the material buckling searched (see subsection 5.2.2.5). Additionally, the L-factor for U-238 was not searched in the depletion calculations but the searched, beginning of life (BOL) L-factor was used as input. The L-factor for U-238 was not searched since it was found that when searched, L-238 changed by only 0.12% after 12,500 hours of full power operation. Thus, the searched BOL L-factor for U-238 is an accurate approximation to the L-factor throughout depletion.

7.2.2 Resonance Capture of U-238

LASER-M requires the spatial distribution of epithermal captures in U-238 as input. This distribution accounts for the non-uniform buildup of Pu-239 in the fuel and is normalized by LASER-M such that the cell total capture rate using the input distribution is equal to the cell total capture rate calculated with MUFT. It is generally acceptable to use the results of a Monte Carlo calculation presented in Ref. 16 for the spatial distribution. The volume averaged values (using 5 points in the fuel) of the epithermal capture rate distribution from Ref. 16 were calculated by Mertens[5] and these values were used in the present study.

7.2.3 Pseudo Fission Product Cross Section Representation

LASER-M seperates the fission products into Xe-135, the directly produced Sm-149, and all other fission products

lumped into one pseudo fission product. The cross sections for the lumped fission product are defined such that one fission product is produced per fission event. The cross sections for the lumped fission products are represented by polynomials in the burnup since they may vary significantly during depletion. The coefficients to the polynomials are required as input to LASER-M for a depletion calculation. One method of obtaining the coefficients is to do a CINDER[20] calculation to obtain the effective cross sections of the pseudo fission product as a function of burnup and then perform a polynomial fit on this data to obtain the coefficients for input to LASER-M. Since the CINDER code is difficult to set up and expensive to run it is only used sparingly. Another method of obtaining the codfficients is to use data published by Celnik, et al.,[42] for the pseudo fission product, thermal, and epithermal cross sections as a function of burnup for typical water-moderated power reactors. This procedure was used by Mertens[5] and Rim[29] in work done at M.I.T.

As seen from the article by Celnik[42] and the information in Ref. 43, the pseudo fission product cross section in the thermal range is very dependent upon enrichment and water to metal ratio. Additionally, Celnik states that the cumulative reactivity worth of the fission products at 25,000 MWD/MTM is 10.2% $\Delta k_{inf}/k_{inf}$ for a UO_2 fueled PWR. However, it is shown in Ref. 43 that varying the fission product cross section versus burnup changes the values

obtained by a constant fission product cross section by a maximum difference in k_{inf} versus burnup of only about 0.5% up to 20,000 MWD/MTM. This latter information may be somewhat misleading since it is generally accepted that the pseudo fission product cross sections must be calculated as accurately as possible. Additionally, as seen in the article by Celnik[42] that the pseudo fission product cross sections are significantly larger in plutonium fuels than in uranium fuels. Uotinen, et al.,[2] state that for plutonium cells the burnup slope is very sensitive to the pseudo fission product cross section. Additionally, Uotinen concludes that only a small fraction of the neutron absorptions in the pseudo fission product nuclei occur at thermal energies and thus the "non-thermal fission product cross sections lead to the largest uncertainty" in calculating reactivity versus burnup in plutonium cells. Therefore, it was concluded that for the work done in the present study the pseudo fission product cross sections should be calculated as accurately as possible.

Information supplied by NUS[4] was used in the present study to determine pseudo fission product cross sections. This information consisted of plots of the 2200 m/sec cross section and constant epithermal cross sections of the pseudo fission product versus burnup for average enrichment and average metal to water ratio of the UO_2 and the PuO_2-UO_2 fuel present in cycle 2 of the San Onofre PWR. The data were obtained by NUS by performing a CINDER calculation using

cross sections with a thermal cutoff of 0.625 eV as input.

Since the data received from NUS had a thermal cutoff of 0.625 eV, a conversion to the 1.855 eV cutoff of LASER was necessary. Basically, this was done by ensuring that the total absorption by the fission products remained the same. That is, since the pseudo fission product is assumed by LASER-M to be a 1/v absorber in the thermal range and the epithermal absorption is assumed by LASER-M to be independent of energy, one can equate the fission product absorptions for the two cutoffs by writing:

$$\sigma_{a_o} \frac{v_o}{\bar{v}}(\bar{\phi}^{th}) + \sigma_a^{epi}\,\bar{\phi}^{epi} = \sigma_{a_o}' \frac{v_o}{\bar{v}'}(\bar{\phi}^{th'}) + \sigma_a^{epi'}\,\bar{\phi}^{epi'} \qquad (7.2)$$

where the primed quantaties indicate the 1.855 eV cutoff, the unprimed indicate the 0.625 eV cutoff and,

σ_{a_o} = 2200 m/sec absorption

v_o = reference neutron velocity (2200m/sec)

$\bar{v}$ = cell average neutron velocity

$\bar{\phi}^{th}$ = cell averaged total thermal flux

σ_a^{epi} = epithermal absorption cross section (not a function of energy)

$\bar{\phi}^{epi}$ = cell average total epithermal flux

The fluxes in Eq. 7.2 were then normalized by the total thermal flux for the 0.625 eV cutoff and since the 2200 m/sec value of the absorption cross section is not effected by the cutoff, σ_{a_o} was set equal to σ_{a_o}'. It is seen that this step results in Eq. 7.2 having only one unknown, $\sigma_a^{epi'}$. It should be noted that identical BOL cell calculations done with

LEOPARD and LASER for a UO_2 and PuO_2 cell were used to evaluate the other parameters in Eq. 7.2.

Thus, $\sigma_a^{epi'}$ was calculated as a function of burnup in the manner described above and the following polynomial fits were obtained by using a standard least squares curve fitting procedure:

1. URANIUM RESULTS (3.85 w/o U-235)

$$\sigma_{a_o} = 104.97 - 2.7292 \times 10^{-3} B + 6.4398 \times 10^{-8} B^2 - 5.417 \times 10^{13} B^3$$

$$\sigma_a^{epi} = 26.974 - 1.8190 \times 10^{-4} B - 1.5975 \times 10^{-9} B^2 + 4.0129 \times 10^{-14} B^3$$

2. PLUTONIUM RESULTS (3.53 w/o PU)

$$\sigma_{a_o} = 195.14 - 1.0865 \times 10^{-2} B + 3.9174 \times 10^{-7} B^2 - 5.3322 \times 10^{-12} B^3$$

$$\sigma_a^{epi} = 31.422 + 1.1693 \times 10^{-4} B - 2.4423 \times 10^{-8} B^2 + 4.5934 \times 10^{-13} B^3$$

where σ_{a_o} = 2200 m/sec absorption cross section of the pseudo fission product

σ_a^{epi} = constant epithermal absorption cross section of the pseudo fission product

B = burnup in MWD/MTM.

In an attempt to verify the method used to shift from the 0.625 eV cutoff to the 1.855 eV cutoff a 3.4 w/o uranium cell was depleted using LASER-M and LEOPARD. The LASER depletion used the polynomial fit for the uranium cell shown above and the LEOPARD calculation used a fission product multiplication factor of 0.85 (found to be required to

adjust the built in polynomial fit of LEOPARD to the NUS uranium cell results).

It was found that at 14,500 MWD/MTM, the $\Delta k_{inf}/k_{inf}$ for the fission products was -4.82% for the LASER-M calculation and -4.78% for the LEOPARD calculation. Thus, it was concluded that the method used to adjust the pseudo fission product epithermal cross section yielded acceptable results. It is of interest to also note that in the LASER calculation the pseudo fission product accounted for 7.3% of all fast absorptions and 3.2% of all thermal absorptions.

7.2.4 Boron Concentration

A Pressurized Water Reactor (PWR) is controlled through the cycle life by varying the boron concentration in the moderator. Boron-10, which has a large 1/v thermal absorption cross section, has a noticable effect on the neutron spectrum. To illustrate this point the effect of a 64% increase in boron concentration (from 600 ppm to 1000ppm) on a uranium and plutonium cell is shown in TABLE 7.3.

Note that the boron increase has more of an effect on the uranium cell than the plutonium cell (due to the lower boron worth in the harder spectrum plutonium cell). Although the effect of boron is not extremely large, it is significant enough to make it desirable to accurately model the boron concentration in the cell as a function of burnup. However, LASER-M has no provision for changing the boron concentration.

TABLE 7.3

EFFECT OF ADDING BORON ON SPECTRUM AVERAGED CROSS SECTIONS FOR URANIUM AND PLUTONIUM CELL

Cross Section	Uranium	Plutonium Cell
Fast + Epithermal		
D	+0.2%	+0.2%
Σ_a	+0.3%	+0.2%
Σ_f	+0.2%	+0.1%
Σ_r	+0.5%	+0.2%
Thermal		
D	+0.2%	+0.1%
Σ_a	-0.8%	-0.2%
Σ_f	-0.8%	-0.5%

NOTES:
1. Identical cells (except for boron concentration) were calculated by searching material buckling and L-238
2. Boron concentration was changed from 600 ppm to 1000 ppm.
3. Percentages were calculated using

$$\frac{\Sigma_{1000ppm} - \Sigma_{600ppm}}{\Sigma_{600ppm}} \times 100\%$$

4. The boron macroscopic absorption cross sections has been removed from the total macroscopic absorption cross sections.

Additionally, since an assembly is in the reactor for an average of three cycles, the boron concentration during the depletion of that assembly will be cycled three times. This leads to the practice of setting up cross section table sets in HARMONY which are a function of boron concentration as well as burnup. Since this is a relatively expensive and much more difficult procedure to set up, it was not employed in the present study.

From the information provided in the reference WCAP report[3] the average burnup through cycle 1 and 2 of each enrichment was known. It was also known that the average boron concentration was about 1000 ppm and about 500 ppm in cycles 1 and 2, respectively. Thus, it was decided to use the average boron concentration of cycle 1 in the depletion of an assembly to its average cycle 1 burnup, and the average boron concentration of cycle 2 for the rest of the depletion. This procedure, however, still requires the boron concentration to be changed during a LASER depletion.

The following procedure to change the boron concentration during a LASER depletion was developed and verified to work (by comparison with a LEOPARD depletion where the boron concentration was changed). The procedure simply employs the continuation option available in LASER-M and is basically as follows:

1. Input the initial natural boron concentration in the normal fashion and deplete the cell until it is desired to change the boron concentration.

2. By using the continuation deck which is output from step 1, change the boron concentration punched on the continuation cards. This must be done in three places on the continuation cards and to ease the location of the correct positions, subroutine MEMO (which causes the continuation deck to be punched) should be consulted. Specifically, the following variables should be changed:

   ENC(15) = pure atom density of B-10 (i.e. 0.198 times the atom density of natural boron)

   X1BARO(14) = volume averaged atom density of B-10 (i.e. f_m times ENC(15), where f_m= volume fraction of the moderator)

   X1BAR(11) = X1BARO(14)

3. Continue the depletion using the changed continuation deck.

7.3 Depletion Results

7.3.1 Changes in Cross Sections during Depletion

Because of the change in nuclide concentration as a function of burnup and resultant change in neutron spectrum, the spectrum averaged cross sections of a cell will change during depletion. Additionally, because of changing spatial effects in the fuel during depletion the disadvantage factors and thus the effective cross sections will also vary during depletion. The changes in the cross sections of various nuclides during depletion is discussed by

Celnik, et al.,[6] and results obtained in the present study from the depletion of a 3.4 w/o uranium cell are shown in TABLE 7.4, where the percentage change in σ was calculated using;

$$\text{Percentage change in microscopic cross section} = \frac{\sigma(\text{at 16500 hrs}) - \sigma(\text{at 2500 hrs})}{\sigma(\text{2500 hrs})} \times 100\% \qquad (7.3)$$

The information shown in TABLE 7.4 is given to show the wide range of cross section variation during depletion and to suggest that the changing cross sections of certain nuclides may have a significant effect on the diffusion calculation. Two other factors, however, need to be considered before it is decided to set up complicated cross section table sets in PDQ/HARMONY for a particular nuclide. In addition to the percentage change in cross section during depletion, the magnitude of the cross section and the amount of the specific nuclide must be evaluated. That is, in order to decide if a cross section should be varied during depletion using PDQ/HARMONY, the magnitude of the particular macroscopic cross section ($\overline{N}\ \overline{\sigma}$) needs to be evaluated, and found to be significant. This criteria was used in the present study to decide how to set up the cross section table sets for the two dimensional depletions (discussed in Chapter 8).

Additionally, once it has been decided that the cross sections for a particular nuclide should be varied with depletion, the method of modeling must be determined. That is, some cross sections vary almost linearly with burnup

TABLE 7.4

PERCENTAGE CHANGE IN MICROSCOPIC CROSS SECTIONS DURING DEPLETION (3.4 W/O URANIUM CELL)

Nuclide	Fast Absorption	Fast Fission	Thermal Absorption	Thermal Fission
H	+0.8%	–	-0.1%	–
O	+1.0%	–	-0.6%	–
SS	+0.9%	–	-0.6%	–
U-235	+3.1%	+2.6%	-1.6%	-1.5%
U-236	+0.02%	-0.4%	-1.1%	–
U-238	+1.1%	-0.2%	-1.0%	–
Pu-239	-1.1%	-0.8%	-7.0%	-6.6%
Pu-240	-0.8%	-0.7%	-30.0%	-29.0%
Pu-241	+0.8%	-0.7%	-4.5%	-4.3%
Pu-242	+3.2%	-0.8%	-0.5%	–
Xe-135	+0.7%	–	-0.1%	–
Sm-149	+0.8%	–	-0.4%	–
F.P.	-9.6%	–	-24.0%	–
B-10	+0.8%	–	+0.1%	–

NOTE:

$$\text{Percentage change} = \frac{\sigma(\text{at } 16500 \text{ hrs}) - \sigma(\text{at } 2500 \text{ hrs})}{\sigma(\text{at } 2500 \text{ hrs})} \times 100\%$$

while others exhibit a more complex behavior and, therefore, require more detailed representation in the table sets.

7.3.2 Comparison of LASER-M and LEOPARD-R Depletions

Throughout the present study the various differences between LEOPARD-R and LASER-M have been discussed. Additionally, it was mentioned in Chapter 4 that agreement with an experimental value of k_{eff} does not necessarily imply agreement with corresponding experimental isotopics (i.e. a match in k does not necessarily imply a match in isotopics). These two points can be clarified by a comparison between a LEOPARD-R and LASER-M calculation of k and isotopics during depletion. Although the points would best be made with the depletion of a plutonium cell, only a 3.4 w/o uranium cell was depleted in the present work using LEOPARD-R and LASER-M. A comparison of the two depletions is presented below.

It was found that k_{inf} versus time (to 14500 hours) for the LEOPARD-R and LASER-M depletion of the 3.4 w/o uranium cell were nearly identical. Notable differences were: 1) during the build up of Xe-135 and Sm-149 (time 0 to 500 hours), LASER-M calculated a value of k_{inf} about 0.4% lower than LEOPARD-R, and, 2) at 14500 hours LASER-R calculated a value of k_{inf} of 0.3% higher than LEOPARD-R.

TABLE 7.5 shows the difference in calculated isotopics at three time (4500, 8500, and 14500 hours) during the depletion, where the difference has been calculated using

$$\text{Percent Difference} = \frac{\bar{N}^i_{Leop} - \bar{N}^i_{Laser}}{\bar{N}^i_{Laser}} \times 100\% \qquad (7.4)$$

which means that a negative value of percent difference implies that the number density of nuclide i calculated by LEOPARD-R is lower than that calculated by LASER-M. Although k_{inf} versus burnup for the two calculations matched very well (to within 0.4% at all times) it is seen from TABLE 7.5 that the isotopics for the two calculations are fairly different. Notably, the atom densities at 14500 hours of U-235 (-2.2% different), Pu-239 (+4.1%), Pu-240 (+10.3%), and Sm-149 (-16.5%).

7.3.3 Comparison of Uranium and Plutonium Cell Depletions

As discussed in Chapter 1, one of the basic differences between a uranium and a plutonium cell is the rate at which the cell reactivities decrease (i.e. the slope of the k_{inf} versus burnup curve). FIGURE 7.1 and TABLE 7.6 show a comparison of k_{inf} versus time for a LASER-M depletion of a 4.0 w/o uranium cell and a 3.6 w/o plutonium cell. It is seen from Figure 7.2 that the plutonium reactivity decreases at a slower rate than the uranium. From TABLE 7.6 it is seen that the change in k_{inf} for the uranium cell is -7.9% $\Delta k_{inf}/k_{inf}$ per 1000 hours whereas it is -6.9% $\Delta k_{inf}/k_{inf}$ per 1000 hours for the plutonium cell. Additionally, it is interesting to note that the change in k_{inf} from 0 to 75 hours is also different for the two cells. For the uranium cell $\Delta k_{inf}/k_{inf}$ from time 0 to 75 hours is -2.33% and for the plutonium cell it is -1.69%. This is, of course, due to the reduced Xe-135 worth in the plutonium cell as discussed in Chapter 1.

TABLE 7.5

COMPARISON OF ISOTOPICS VERSUS BURNUP FOR A LEOPARD-R AND LASER-M DEPLETION OF A 3.4 W/O URANIUM CELL

Nuclide	Percent Difference 4500 hours	8500 hours	14500 hours
U-235	-0.6%	-1.23%	-2.2%
U-236	+2.1%	+2.9%	+1.84%
U-238	-0.02%	-0.03%	-0.04%
Pu-239	+3.55%	+3.88%	+4.1%
Pu-240	+6.3%	+8.44%	+10.3%
Pu-241	-7.8%	-6.3%	-4.1%
Pu-242	+14.4%	+4.1%	+0.9%
Xe-135	-3.3%	-2.9%	-2.6%
Sm-149	-11.0%	-14.0%	-16.5%
F.P.	+4.7%	+4.6%	+4.7%
Burnup	+0.02%	+0.02%	+0.02%

NOTE:

$$\text{Percent Difference} = \frac{\bar{N}^i_{Leop} - \bar{N}^i_{Laser}}{\bar{N}^i_{Laser}} \times 100\%$$

TABLE 7.6

COMPARISON OF K_{inf} VERSUS TIME FOR A 4.0 W/O URANIUM CELL AND A 3.6 W/O PLUTONIUM CELL

TIME (hours)	K_{inf}(4 w/o U)	K_{inf}(3.6 w/o Pu)	Difference
0	1.23268	1.22094	+0.96%
75	1.20398	1.20024	+0.31%
500	1.19311	1.18384	+0.78%
2500	1.17573	1.16425	+0.99%
4500	1.15586	1.14619	+0.84%
6500	1.13586	1.12947	+0.56%
8500	1.11676	1.11386	+0.26%
10500	1.09886	1.09894	-0.01%
12500	1.0826	1.08507	-0.23%

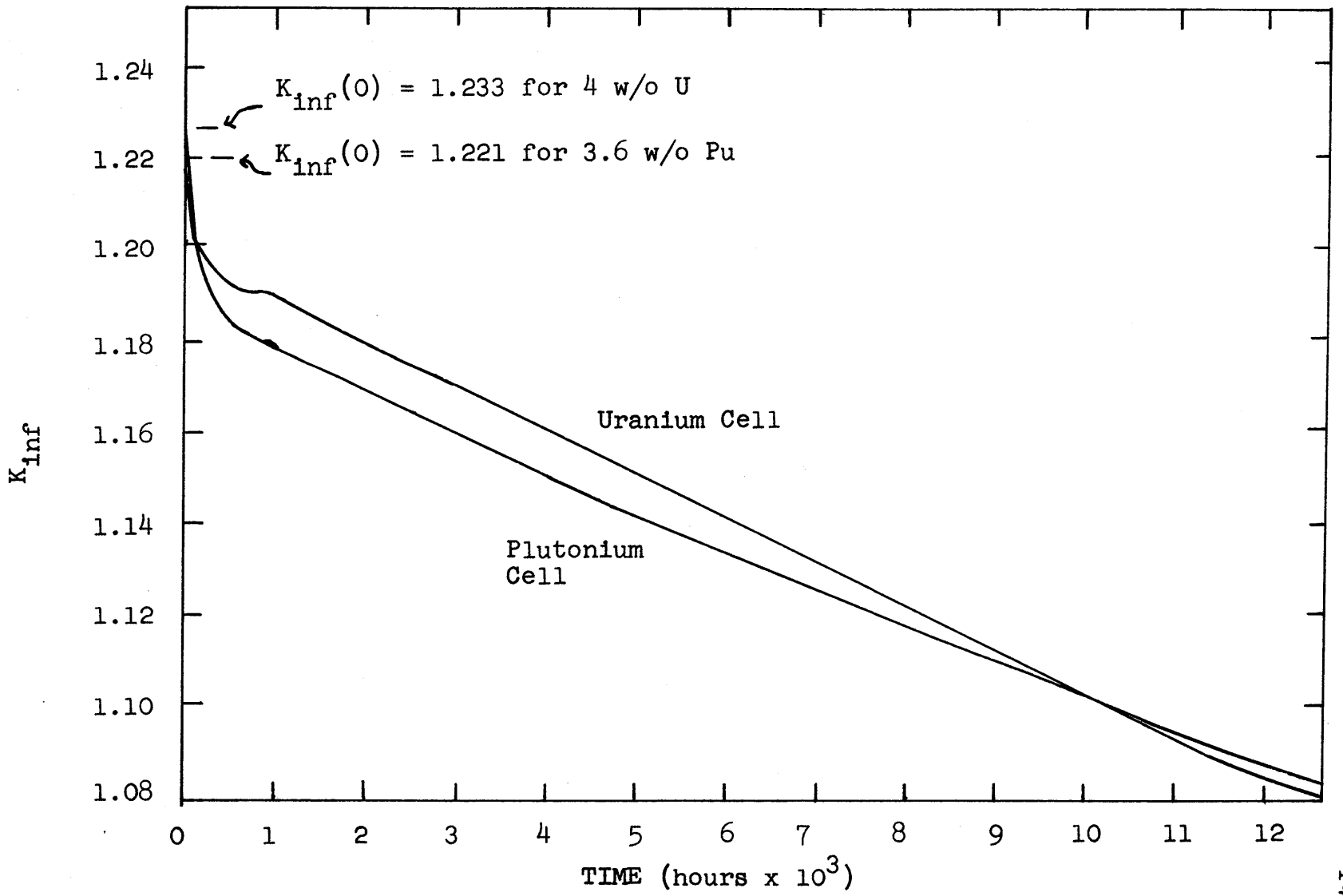

FIGURE 7.1 Comparison of K_∞ versus Burnup for a 4.0 w/o Uranium Cell and a 3.6 w/o Plutonium Cell

CHAPTER 8

TWO DIMENSIONAL DEPLETION CALCULATIONS (PDQ-7)

8.1 Introduction

The PDQ-7/HARMONY computer code package was used to do two dimensional depletion calculations in the present study. Cross sections as a function of burnup for input into PDQ-7 were obtained from the zero-dimensional depletions done using LASER-M (see Chapter 7).

As discussed in the following sections, two dimensional depletions were done for the unit cell and for the quarter core. The purpose of the unit cell depletions was: 1) to verify the validity of the depletion and fission product chains, 2) to verify the validity of the method used to represent cross sections as a function of burnup in PDQ-7/HARMONY, and 3) to verify that no mistakes had been made when setting up the complicated cross section table sets.

After having verified the validity of the table sets and chains, they were used in the quarter core depletion in an attempt to match reference assembly powers during depletion of cycle 2 of the San Onofre PWR.

8.2 Unit Cell Depletions

The preparation of cross sections versus burnup for PDQ-7/HARMONY is a very tedious and error prone process.

The usual procedure used in industry is to employ a processing type code which essentually takes the cross sections from the spectrum code and processes them into the desired form for direct input into PDQ. However, in the present study the cross section table sets had to be set up by hand since no processing code for LASER was available.

As discussed in subsection 7.3.1, the magnitude of the particular macroscopic cross sections as well as the percent change during depletion was evaluated to determine how to set up the cross section table sets. For example, for the particular case cited in TABLE 7.4, the fast absorption cross section of U-235 was found to change by 3.1% during depletion. By using the initial cell averaged number density of U-235 and the fast microscopic cross section at BOL, it was found that U-235 accounted for about 32% of the fast absorptions. Thus it was concluded that the 3.1% change in the U-235 fast absorption would have about a 1% effect on the total fast macroscopic absorption cross section and probably should be modeled in the cross sections table sets. Conversely, again from TABLE 7.4, it is seen that the fast absorption cross section of Pu-242 also changes by about 3% during depletion but it accounts for only about 0.4% of all fast absorptions (late in life where its effect is largest) and therefore the changing cross section need not be modeled in the PDQ table set.

Additionally, because of the various effects on the spectrum averaged cross sections that occur during depletion

(discussed in subsection 7.3.1) the slopes of the cross section versus burnup curves for the various nuclides are significantly different. This difference in shape along with the importance of the cross section variation can be used to determine if a cross section can be approximated as a constant, a straight line, or a more complicated function during depletion.

After setting up the cross section table sets for the different cells in cycle 2, an evaluation of the method used to model the cross sections versus burnup was performed by depleting a unit cell with PDQ using the applicable cross section table set. It was found that the value of k_{inf} obtained from the PDQ depletion was, on the average, less than 0.3% different than that obtained from the LASER-M depletion for the cell. Also, the isotopics as a function of time showed good agreement. Most nuclides were less than 0.5% different for the PDQ and LASER-M depletions although some of the less important, and therefore less accurately modeled nuclides such as Pu-242 in the uranium cell were as much as 10% different. It was therefore concluded that the table sets were a reasonable approximation to the actual cross section variation during burnup calculated by LASER-M.

8.3 Quarter Core Depletions

8.3.1 Reference Power Distribution

The reference WCAP report gives quarter core relative

power distributions and assembly burnups through cycle 2 for the San Onofre PWR. However, this information was not used in the present study since it is more desireable to use experimental values as a basis of comparison. However, there is no strictly experimental data available for assembly powers in power reactors since the usual practice is to use experimentally determined flux levels in incore detectors and process this information (with propietary computer codes) using calculated power distributions to obtain what is termed in the present study as quasi experimental power distributions. In the San Onofre PWR this process is carried out using the computer code INCORE which is a Westinghouse proprietary code. In work done at M.I.T. Herbin[47] found that for a 1% increase in input assembly power INCORE gave a 1% increase in output quasi experimental assembly power, independent of position in the core (i.e. regardless of instrumentation locations). This information shows that the assembly power distribution input to INCORE strongly influences the output power distribution. Additionally, however, Herbin also found that for an instrumented assembly that the output assembly power was significantly effected by the instrument data. For the specific case of the plutonium assemblies analysed in the present study, two of the four plutonium assemblies were instrumented, one had an instrumented assembly next to it and the fourth was at the corner of an instrumented assembly. Applying Herbin's work to the present study indicated that the quasi experimental power

output by INCORE would reflect the experimental data although it would be influenced by the calculated, PDQ assembly power distribution used as input.

Therefore, it was decided to use quasi experimental assembly powers supplied by SCE[48] which were output from INCORE as the reference values in the present study. This information was determined to be more accurate (on the basis of the work done by Herbin) than the calculated power distributions shown in the reference WCAP report. However, it should be noted that the calculated assembly powers used as input to the INCORE runs for cycle 2 were in error since they did not include the effect of the core barrel or take into account the increased assembly burnups at the start of cycle 2 due to the longer than expected life of cycle 1.

8.3.2 Calculated Power Distributions

The quarter core power distributions during cycle life calculated in the present study made use of the cross section table sets discussed in section 8.2. The mesh spacing used was 83 x 83, in which the uranium assemblies were represented with coarse mesh (4 mesh points per assembly) and the plutonium assemblies with fine mesh (one point per unit cell). Additionally, in the uranium around the plutonium assemblies a mesh spacing equivalent to one point per unit cell was used in an attempt to more accurately represent the thermal flux depression in these regions. Additionally, the mesh was set up to allow explicit representation of the core baffle immediately adjacent to the core.

The core barrel was well represented in the region near the plutonium and adjacent uranium assemblies and approximately represented with existing mesh lines in the rest of the problem. It is interesting to note that when the barrel was not modeled, the peripheral assembly power decreased by more than 5%, but the change in k_{eff} was not significant. This decrease in peripheral assembly powers is apparently due to the effect the barrel has on the fast flux (steel being a good reflector of fast neutrons). This effect is seen by comparing the flux at the core edge for runs with and without the barrel. It was found that without the barrel the fast flux is reduced by about 30% from the value obtained when modeling the barrel but the thermal flux is only reduced by 9% without the barrel.

Also, 10 inches of water was placed outside the barrel to allow the fast flux in the reflector to be accurately modeled.

Due to the differences in mesh in the uranium and plutonium assemblies, the uranium cell number densities corresponded to assembly average values (smeared over the entire assembly) and the plutonium number densities were normal cell values placed in each specific unit cell. The specific number densities for the individual assemblies which had been present in cycle 1 were obtained by using assembly burnup data and interpolating between LASER-M time steps to obtain the correct number densities. Also, the Xe-135 was removed for the start of cycle 2 and allowed to

build back in during depletion.

Assembly average GMND cross sections were used for all the fuel, and soft spectrum water cross sections (from an unfueled cell calculation) were used in the water surrounding the core as well as for the water holes in the plutonium assembly. Additionally, SS 304 absorption cross sections from a fueled cell were used in the baffle (adjacent to the core) and SS 304 cross sections from an unfueled cell were used in the barrel. The removal cross sections of the steel were input as zero in this two group representation although because of the inelastic scattering at high energies SS 304 would be much more accurately represented by 3 or 4 groups. Since LASER-M does not explicitly calculate a transport cross section for SS 304, adjusted LEOPARD values from a fueled and unfueled cell were used in the baffle and barrel, respectively.

The setup of the nuclide depletion and fission product chains was relatively straight forward once the terms used in PDQ were understood. It should, however, be pointed out that if burnups of various assemblies and/or unit cells are required that burnup must be made a fission product and be formed by a designated fission product chain. This method was used in the present study. Basically, the input quantity "fraction of fission yield"(designated as f_B in the present study) used in this special burnup chain is calculated using,

$$f_B = \frac{\nu}{L} \times 10^{24} \qquad (8.1)$$

where κ = energy per fission (MWD/fission)

L = Volumetric loading of heavy metal (MT/cm ^{3})

and f_B is in units of (MWD-cm^3)/(MTM - fission).

Since the energy per fission varies for the different nuclides and the volumetric loading varies for the different enrichments, special chains were setup for each enrichment of fuel present in cycle 2.

As mentioned in Section 7.2, the boron concentration in the moderator changes as a function of time through the cycle life. In the version of PDQ presently operable at M.I.T. (PDQ-7 Version 5) it is a simple matter to change only the boron concentration in each composition at any desired time step (by using the 01017s and 99cccs cards shown in Ref. 28). However, in the version used for the quarter core depletion (the CDC PDQ-7 Version 2) all of the nuclide concentrations must be entered at each time and for each composition in which any concentration is changed. This difficulty was by-passed by fractionally reducing the boron fast and thermal cross sections as a function of burnup. This reduction, of course, has the same effect as fractionally reducing the boron concentration for each time step.

The critical boron concentration as a function of burn-up during cycle 2 of the San Onofre PWR was supplied by Southern California Edison[48] and used to calculate the fractional reduction in the boron cross sections. The boron

data used indicated that at the start of the cycle the boron concentration was 1250 ppm (weight parts per million weight parts of water). The concentration dropped linearly to 970 ppm at 100 MWD/MTM and then essentially decreased linearly to zero at 8000 MWD/MTM.

PDQ allows the user to input a buckling for each composition in the problem. Since PDQ will, in effect, calculate the radial leakage it is obvious that the geometric axial buckling should be used as the input value to PDQ. However, the axial buckling, B^2_{axial}, calculated from the standard equation

$$B^2_{axial} = \left(\frac{\pi}{H_e}\right)^2, \qquad (8.2)$$

where H_e = The equivalent height of the core (approximately equal to the actual height),

implies a cosine shape for the flux along the axis which is strictly true only for a fresh, unburned core. Through the cycle life the axial flux shape will depart from a cosine shape. The flux will flatten and may even dip at the midplane of the core implying that there is a much steeper flux gradient at the top and at the bottom of the core than would be calculated with the cosine flux distribution.

Since the quarter core depletion done in the present study starts at cycle 2 (with a core average burnup of about 8900 MWD/MTM) the axial flux shape is considerably different from the fresh core cosine shape. Since the axial buckling effects the value of k_{eff} for the core and, to a lesser degree the power distribution, an approximate value of the

actual axial buckling (as a function of burnup) was used in the quarter core calculation. The value of the axial buckling versus burnup was obtained from information, supplied by Brian Kirschner of Yankee Atomic Electric Company,[45] for the Connecticutt Yankee PWR (which is similar to the San Onofre PWR). The values used at each time step are shown in TABLE 8.1 along with the total accumulated burnup and the cycle burnup at each time step. Note that the buckling values listed in TABLE 8.1 are considerably different from the value of 0.1×10^{-3} which is calculated using Eq. 8.2.

TABLE 8.1

AXIAL BUCKLING VERSUS BURNUP FOR CYCLE 2 DEPLETION

Axial Buckling* (cm^{-2})	Cycle Burnup (MWD/MTM)	Accumulated Burnup (MWD/MTM)	Time (hours)
0.316 - 3	0.0	8828.2	0.0
0.316 - 3	88.5	8916.7	100.0
0.332 - 3	1691.3	10519.4	1910.0
0.344 - 3	3300.4	12128.6	3755.0
0.356 - 3	4905.1	13733.3	5620.0
0.364 - 3	5905.1	14733.4	6792.0
0.372 - 3	7858.0	16686.0	9110.0

* From Ref. 45.

NOTE: The axial buckling calculated from Eq. 8.2 is about 0.1 -3 cm^{-2}.

The reference power distributions and assembly burnups at the start of cycle 2 are shown in FIGURE 8.1. As discussed in subsection 8.3.1, this information is to be considered quasi experimental. Additionally, the burnups provided by SCE reflect the actual cycle 1 life. The SCE data was for the whole core and was reduced in the present study to reflect the eighth core symmetry which is calculated using a quarter core representation of the entire reactor.

FIGURES 8.2 through 8.4 show the relative power distributions calculated in the present study and a comparison to the reference distribution for cycle burnups of 0 MWD/MTM, 3342 MWD/MTM, and 6045 MWD/MTM. Additionally, the value of k_{eff} obtained at each time step is shown in TABLE 8.2.

TABLE 8.2

CALCULATED K_{eff} VERSUS CYCLE BURNUP

Cycle Burnup (MWD/MTM)	k_{eff}
0.0	1.0065
88.5	1.0051
1691.3	1.0043
3300.4	1.0046
4905.1	1.0040
5905.2	1.0031
7858.0	1.0012

Since the changing boron concentration and axial buckling were input, the calculated value of k_{eff} should be compared to the actual operating condition of $K_{eff} = 1.0000$. As shown in TABLE 8.2, the calculated values are in excellent agreement with the actual value.

Also, the calculated power distributions shown in FIGURES 8.2 to 8.4 show excellent agreement with the reference values, with the average difference in assembly powers being less than 2.1% (considered excellent when comparing to INCORE results)[45] for each of the times calculated.

Note that in FIGURES 8.2 to 8.4 the percent difference in assembly powers and the average difference in assembly powers are calculated in a manner analogous to that shown in Eq. 6.3 and Eq. 6.2, respectively.

From FIGURE 8.2 it is seen that the calculated power in the plutonium assembly was higher than the reference value (by 0.8%) and the calculated power in the uranium assembly next to the plutonium assembly was lower than the reference value (by 3.9%). In effect, this shows that the calculations done in the present study, when compared to the quasi experimental powers, yield a higher assembly power difference for the adjacent uranium and plutonium assemblies. This result is just the reverse of what was found in the present study when comparing the calculations to those given in the reference WCAP report[3] for unit assemblies of plutonium surrounded by uranium (See Chapter 6).

From the above information it is concluded that excellent agreement is obtained when analysing the plutonium assemblies in the quarter core. It should be noted that Westinghouse states (in Ref. 46) that "cycle two INCORE runs show that the peripheral assemblies are operating at higher than predicted power levels," and that measurements exceed calculations by 10 to 20 percent (versus 0.8% high to 2.8% low found in the present study). It is important to note that this does not necessarily imply that the measured and predicted assembly powers are 10 to 20 % different since the percentage discrepancy is apparently based on predicted versus measured relative activations in the instrument thimbles.[49] This percentage discrepancy will not result in as large a percentage discrepancy in the assembly powers although it is a more accurate representation of the true agreement between measurements and calculations.

Additionally, since an incorrect set of calculated power distributions is biasing the reference values output from INCORE, a clear cut comparison of Westinghouse calculated results and/or experimental results versus the present study results is difficult.

However, it can be stated that, since the results of the present study show excellent agreement with the INCORE results the calculational method is thus shown to be as good or better than published calculations. Therefore, it is applicable for independent calculations to evaluate proposed plutonium recycle loadings.

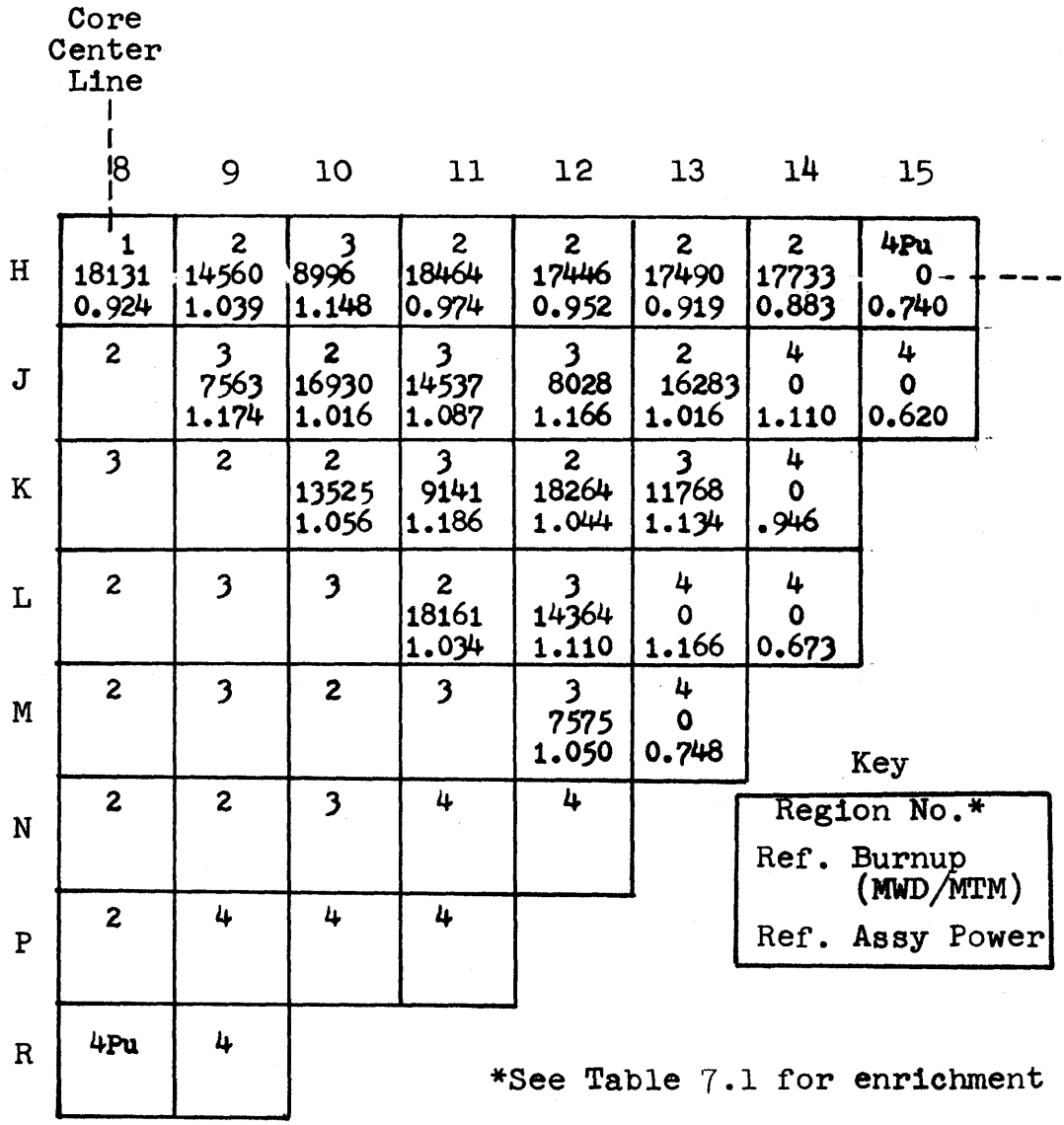

FIGURE 8.1 Reference Quarter Core Power Distribution and Assembly Burnups for Beginning of Cycle 2.

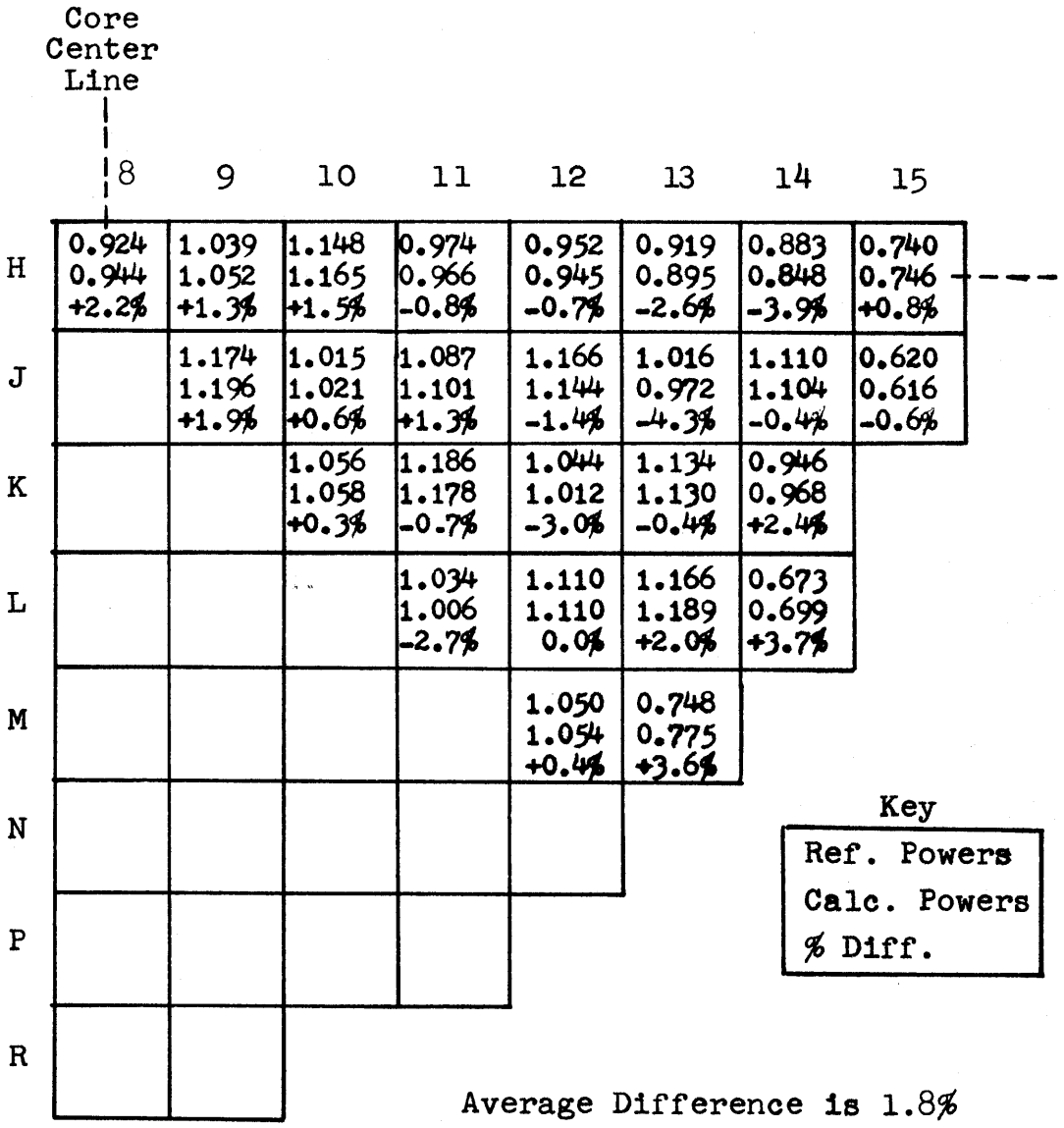

FIGURE 8.2 Calculated Versus Reference Powers for Beginning of Cycle 2.

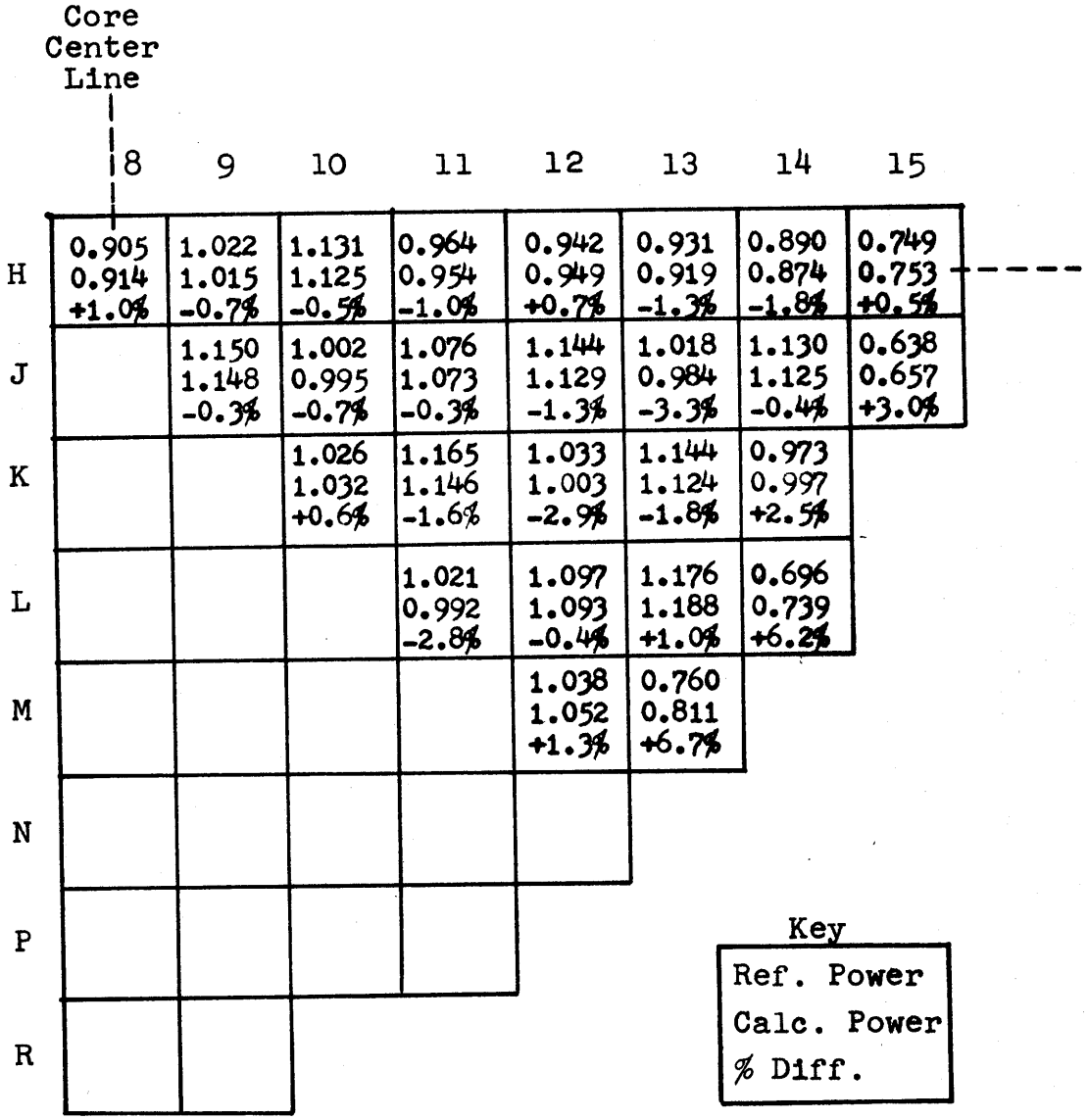

Average Difference is 2.0%

FIGURE 8.3 Calculated Versus Reference Powers at 3342 MWD/MTM

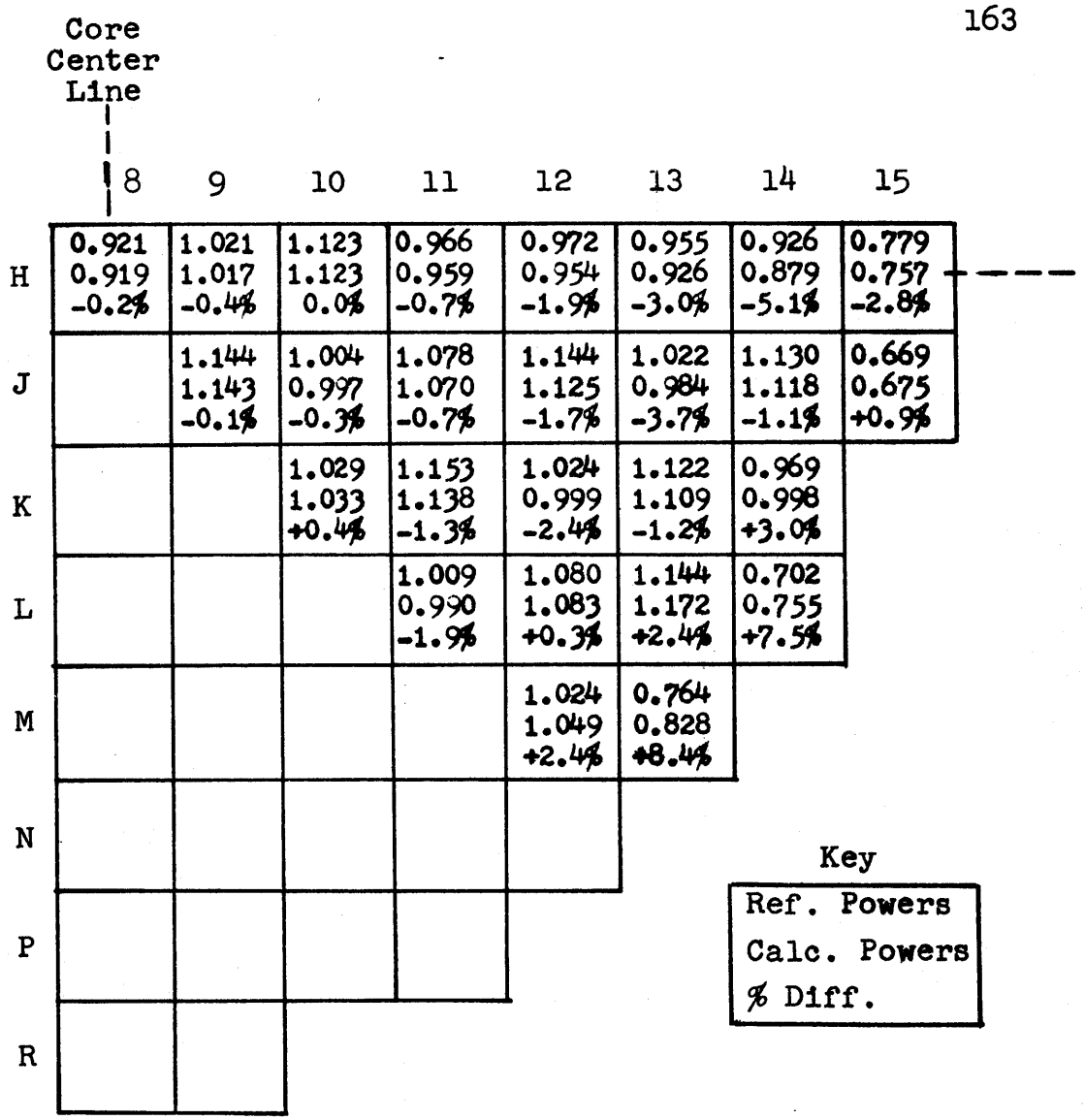

FIGURE 8.4 Calculated Versus Reference Powers at 6045 MWD/MTM

CHAPTER 9

CONCLUSIONS AND RECOMMENDATIONS

From the work done in the present study the following conclusions are made.

1. The revised version of LASER (designated LASER-M) shows better agreement with plutonium critical experiments than the old version of LASER and other published calculations as shown in Chapter 4.
2. As shown in Chapter 6, the use of LASER-M with Generalized Mixed Number Density (GMND) cross sections yields good agreement for cell power peaking in uranium and plutonium assemblies when compared to calculations published in the open literature (Ref. 3).
3. The use of GMND cross sections from LASER-M cell depletions in PDQ-7/HARMONY yields excellent agreement with quasi experimental power distributions for a quarter core containing plutonium assemblies as shown in Chapter 8.
4. The method used in the present study yields criticality and power distribution results that are as good or better than the published calculations. Therefore, this method is applicable for independent calculations to evaluate proposed plutonium recycle loadings.

The following recommendations are given for future work.

1. Further modification of the cross section library (both fast and thermal) of LASER-M is recommended as updated data becomes available.
2. Further modification of LASER-M to more accurately calculate the microscopic transport and removal cross sections (possibly as done in LEOPARD) and to allow for changing boron concentration as a function of burnup is recommended.
3. Comparison of LASER-M calculated isotopics versus burnup for plutonium systems with experimental values is recommended.
4. Comparison of actual experimental power distributions (possibly in critical experiments) in plutonium systems and plutonium - uranium interfaces with the results from a LASER-M and PDQ-7 calculation is recommended.
5. Further modification of LEOPARD and the LEOPARD cross section library to more accurately calculate plutonium systems is recommended.
6. Continuation of the present study to analyse the San Onofre plutonium assemblies during cycle 3 when they are no longer on the periphery of the core is recommended.
7. Calculation of reactivity parameters (temperature coefficients, control rod worths, void coefficients,

neutron lifetimes, effective delayed neutron fraction, etc.) for plutonium recycle cores is recommended.

REFERENCES

1. L. C. Schmid, "Preface - A Review of Plutonium Utilization in Thermal Reactors," Nucl. Technol., 18, 78 (1973).

2. V. O. Uotinen, B. R. Leonard Jr., R. C. Liikala, "The Neutronics of Plutonium Recycling," Nucl. Technol., 18, 115 (1973).

3. "EEI-Westinghouse Plutonium Recycle Demonstration Program Progress Report for the Period Ending December 1970," WCAP-4167-2, Westinghouse Electric Corporation (1971).

4. R. F. Barry, "LEOPARD - A Spectrum Dependent, Non-Spatial Depletion Code for the IBM-7094," WCAP-3269-26, Westinghouse Electric Corporation (1963).

5. P. G. Mertens, "Analysis of Conventional and Plutonium Recycle Unit-Assemblies for the Yankee (Rowe) PWR," MIT-134 (Draft Report), Department of Nuclear Engineering (1971).

6. J. Celnik, S. Kellman, J. R. Tomonto, J. Tulenko, W. Jager, "Evaluation of Plutonium Recycle Nuclear Calculation Methods by Comparison with Experimental Data," Topical Report for "Development of Plutonium Recycle in Thermal Reactors," UNC-5163 (1967).

7. E. G. Taylor, "SAXTON Plutonium Program Critical Experiments for the SAXTON Partial Plutonium Core," WCAP-3385-4, Westinghouse Electric Corporation (1965).

8. C. G. Poncelet, "LASER - A Depletion Program for Lattice Calculations Based on MUFT and THERMOS," WCAP-6073, Westinghouse Electric Corporation (1966).

9. R. L. Hellens, "Problems in Recycle of Plutonium in Pressurized Water Reactors," Paper presented at American Nuclear Society Winter Meeting, Miami Beach, Florida, October 17-21, 1971.

10. R. C. Liikala, V. O. Uotinen, U. P. Jenquin, "Lattices of Plutonium-Enriched Rods in Light Water - Part II: Theoretical Analysis of Plutonium-fueled Systems," Nucl. Technol., 15, 272 (1972).

11. V. O. Uotinen, J. H. Lauby, L. C. Schmid, W. P. Stinson, "Lattices of Plutonium-Enriched Rods in Light Water - Part 1: Experimental Results," Nucl. Technol., 15, 257 (1972).

12. E. G. Adensam, J. H. Bell, H. L. McCullough, M. Raber, "Computer Methods for Utility-Reactor Physics Analysis," Reactor and Fuel-Processing Tech., 13, 3 (Spring 1969).

13. J. Chernick, "Status of Reactor Physics Calculations for U. S. Power Reactors," Reactor Technol., 13, 4 (Winter 1970-71).

14. H. Bohl Jr., E. M. Gelbard, G. M. Ryan, "MUFT-4 Fast Neutron Spectrum Code for the IBM-704," WAPD-TM-72, (1957).

15. R. J. Breen, "A One Group Model for Thermal Activation Calculations," Nucl. Sci. Eng., 9, 91 (1961).

16. C. G. Poncelet, "Burnup Physics of Heterogeneous Reactor Lattices," WCAP-6069, Westinghouse Electric Corporation (1965).

17. H. C. Honeck, "THERMOS - A Thermalization Transport Theory Code for Reactor Lattice Calculations;" BNL-5826 (1961).

18. H. C. Honeck, "The Calculation of the Thermal Utilization and Disadvantage Factor in Uranium Lattices," Nucl. Sci. Eng., 18, 49 (1964).

19. L. E. Strawbridge, R. F. Barry, "Critical Calculations for Uniform Water-Moderated Lattices," Nucl. Sci. Eng., 23, 57 (1965)

20. T. R. England, "CINDER - A One-Point Depletion and Fission Product Program," WAPD-TM-334 (1962).

21. C. L. Beard, R. A. Dannels, "ETOT, A Fortran IV Program to Process Data form ENDF/B File to Thermal Library Format," WCAP-7363 (ENDF-146) (1971).

22. H. Amster, R. Suarez, "The Calculation of Thermal Constants Averaged over a Wigner-Wilkens Flux Spectrum: Description of the SOFOCATE Code," WAPD-TM-39 (1957).

23. A. Amoyal, P. Benoist, J. Horowitz, "New Method of Determining the Thermal Utilization Factor in a Unit Cell," J. Nucl. Energy, 6, 79 (1957).

24. H. Spierling, "The Value of Recycle Plutonium in Pressurized Water Reactors," PhD. Thesis, MIT, Department of Nuclear Engineering (1972).

25. D. L. Farrar, "A Comparison of Simple Calculational Methods for Boiling Water Reactor Fuel Assembly Analysis," Nucl. E. Thesis, MIT, Department of Nuclear Engineering (1971).

26. W. R. Cadwell, "PDQ-7 Reference Manual," USAEC Report WAPD-TM-678, Bettis Atomic Power Laboratory (1967).

27. R. Breen, O. J. Marlowe, C. J. Pfeifer, "HARMONY - System for Nuclear Reactor Depletion Computation," USAEC Report WAPD-TM-478, Bettis Atomic Power Laboratory (1965).

28. A. W. Brown, J. A. McClure, R. J. Wagner, "Summary of PDQ-7 (IBM-360-370 Version) Input Data Requirements and Operating Procedures," ANCR-1061, Aerojet Nuclear Company (1972).

29. C. S. Rim, "Neutronic and Thermal Analysis of Nuclear Fuels," Sc. D. Thesis, MIT, Department of Nuclear Engineering (1969).

30. R. Sher, J. Felberbaum, "Least Squares Analysis of the 2200 m/sec Parameters of U-233, U-235, and Pu-230," BNL-918 (1965).

31. C. H. Westcott, "Survey of Nuclear Data for Reactor Calculations," A/Conf. 28/p. 717 (1964).

32. Personnel Communication, C. S. Rim, April 1974.

33. H. C. Honeck, "ENDF/B - Specifications for an Evaluated Nuclear Data File for Reactor Applications," BNL 50066, USAEC (1966).

34. C. H. Westcott, K. Ekberg, G. C. Hanna, N. J. Pattenden, S. Sanatani, P. M. Attree, "A Survey of Values of the 2200 m/sec Constants for Four Fissile Nuclides," Atomic Energy Review, 3, No. 2 (1963).

35. R. A. Dannels, D. E. Kusner, "ETOM-1 - A Fortran Program to Process Data from the ENDF/B File to MUFT Format," WCAP-3688-1, Westinghouse Electric Corporation (1968).

36. Personnel Communication, Bill Flournoy, SCE, January 1973.

37. H. A. Risti, "Unit Cell Homogenization for Reactor Depletion Studies," WCAP-6060, Westinghouse Electric Corporation (1964).

38. L. C. Schmid, R. C. Liikala, W. P. Stinson, J. R. Worden, "Critical Masses and Bucklings of PuO_2-UO_2-H_2O Systems," Trans. Am. Nucl. Soc., 7, 216 (1964).

39. N. R. Nelson, "SAXTON Plutonium Program Quarterly Progress Report for the Period Ending December 31, 1964," WCAP-3385-2, Westinghouse Electric Corporation (1965).

40. Personnel communication, Southern California Edison, October 1972.

41. Personnel communication, P. G. Mertens, August 1973.

42. J. Celnik, J. R. Tomonto, J. S. Tulenko, "Representation of Fission Products in Thermal Power Reactors Containing UO_2 and Plutonium Recycle Fuel," Trans. Am. Nucl. Soc., 10, 516 (1967).

43. "Large Closed-Cycle Water Reactor Research and Development Program Progress Report, Oct. 1 - Dec. 31, 1963," Westinghouse Electric Corporation, WCAP-3750 (1964).

44. R. P. Sullivan, "Lumped Fission Product Representation for San Onofre Fuel," NUS Memo NA-548 (1973).

45. Personnel Communication, Yankee Atomic Electric Company, April 1974.

46. "EEI - Westinghouse Plutonium Recycle Demonstration Program Letter Progress Report, January - September 1971," WCAP-4167-3, Westinghouse Electric Corporation (1971).

47. H.C. Herbin, "Analysis of Operating Data Related to Power and Flow Distribution in a PWR," Nucl.E. Thesis, MIT, Department of Nuclear Engineering (1974).

48. Personnel Communication, Southern California Edison, February 1974.

49. Personnel Communication, Southern California Edison, May 1974.

50. Personnel Communication, A.F. Henry, MIT, April 1973.

APPENDIX A

REFERENCE DATA LIST (SUPPLEMENT TO TABLE 1.1)

The following list shows supplemental design and operating parameters for the San Onofre PWR.

Quantity	Value
Average moderator temperature (full power), ^{o}F.	578
Average Clad Temperature (full power), ^{o}F.	648
Average fuel temperature (full power), ^{o}F.	
Plutonium cell	1900
Uranium cell	1780
Power Density (full Power), kw/l	71.6
Grid (inconel) weight per assembly, pounds	
Plutonium Assembly	12
Uranium Assembly	12
Water Gap (between assemblies) half thickness, in.	0.02
Am-241 content in plutonium fuel, ppm	5000

APPENDIX B

COMPARISON OF SPECTRUM AVERAGED CROSS SECTIONS, ν, AND κ FROM LEOPARD-R AND LASER-M

The following data was obtained from LEOPARD-R and LASER-M calculations on the same cell. This comparison is presented to show the differences in cross section library values in the two codes and although it is obvious that even with the same cross section libraries LEOPARD-R and LASER-M would calculate different spectrum averaged cross sections, a number of differences shown below can not be explained by the difference in spectrum calculation. Note that in all cases the percent difference is calculated using

$$\text{Difference} = \frac{\text{LASER-M value - LEOPARD-R value}}{\text{LEOPARD-R value}} \times 100\%$$

Additionally, it should be pointed out that in some cases, because of the small magnitude of the cross section or the associated atom density of the nuclide, a large percent difference may have a relatively small effect on the total cell calculation.

For the thermal cross section comparison the 0.625 eV edit for the region averaged cross sections from LASER-M was used which is equivalent to the cross sections edited by LEOPARD-R.

For the non-thermal cross sections, flux weighting was employed to reduce the LEOPARD-R cross sections to an energy range identical to that edited in LASER-M.

1. Comparison of Thermal Cross Sections

Absorption Cross Sections

Nuclide	Percent Difference
U-235	-4.1%
U-236	-3.7%
U-238	-3.7%
Pu-239	+3.3%
Pu-240	+1.4%
Pu-241	+0.1%
Pu-242	-2.3%
Xe-135	-6.5%
Sm-149	-2.4%
B-10	-1.9%
H	-1.9%
O	-1.9%
SS 304	+0.1%

Fission Cross Sections

U-235	-4.6%
Pu-239	+3.9%
Pu-240	-2.8%
Pu-241	-0.2%

Nu Fission Cross Sections

U-235	-3.9%
Pu-239	+3.9%
Pu-240	-2.9%
Pu-241	-0.2%

2. Comparison of Fast Cross Sections (5.53 Kev to 10 Mev)

Absorption Cross Sections

U-235	+0.1%
U-238	+0.08%
Pu-239	+13.5%
Pu-240	+115.3%
Pu-241	+31.0%
Sm-149	+0.4%
B-10	+0.2%

Fission Cross Sections

U-235	+0.1%
U-238	0.0%
Pu-239	+11.0%
Pu-240	+2.6%
Pu-241	+20.3%
Pu-242	-0.03%

3. Comparison of Thermal plus Epithermal Cross Sections (0 eV to 5.53 KeV)

Absorption Cross Sections

Nuclide	Percent Difference
U-235	-3.6%
U-236	-1.7%
U-238	-2.4%
Pu-239	+2.15%
Pu-240	+9.9%
Pu-241	-1.7%
Pu-242	-72.0%
Xe-135	-6.4%
Sm-149	-1.4%
B-10	-1.2%
H	-1.3%
O	+0.9%
SS 304	-3.9%

Fission Cross Sections

U-235	-4.0%
Pu-239	+2.8%
Pu-240	-41.2%
Pu-241	-2.1%
Pu-242	-74.0%

4. Comparison of Thermal Values of Nu (Neutrons per Fission)

Nuclide	Percent Difference
U-235	+0.8%
Pu-239	0.0%
Pu-240	0.0%
Pu-241	0.0%

5. Comparison of Values of Kappa (Energy per Fission)

U-235 +4.3%

Note that kappa in LEOPARD does not include energy released from radiative capture so the value used for this comparison was obtained from the spectrum averaged kappa fission macroscopic cross sections output from LEOPARD.

APPENDIX C

PROCESSED ENDF/B-II PLUTONIUM CROSS SECTIONS INPUT to the LASER-M THERMAL LIBRARY

This Appendix lists the thermal pointwise ENDF/B-II cross sections used to modify the LASER thermal cross section library as discussed in Chapter 3.

Also included is the energy group structure used in LASER-M. This structure, of course, also applies to the plutonium cross sections given here.

GROUP STRUCTURE IN LASER-M THERMAL LIBRARY

GROUP	ENERGY POINT (eV)	SPEED POINT (2200 m/sec)	ENERGY RANGE (eV)
1	.001012	.200000	.000253 - .002277
2	.004048	.400000	.002277 - .006325
3	.009108	.600000	.006325 - .012397
4	.016192	.800000	.012397 - .020439
5	.025300	1.000000	.020493 - .030613
6	.036432	1.200000	.030613 - .042757
7	.049588	1.400000	.042757 - .056925
8	.068879	1.650000	.056925 - .081972
9	.096203	1.950000	.081972 - .111570
10	.128081	2.250000	.111570 - .145730
11	.164513	2.550000	.145730 - .184440
12	.205499	2.850000	.184440 - .227700
13	.239227	3.075000	.227700 - .251040
14	.260694	3.210000	.251040 - .270530
15	.280549	3.330000	.270530 - .290750
16	.295919	3.420000	.290750 - .301130
17	.310811	3.505000	.301130 - .320640
18	.338909	3.660000	.320640 - .357680
19	.386789	3.910000	.357680 - .417040
20	.459134	4.260000	.417040 - .503260
21	.562450	4.715000	.503260 - .624930
22	.701322	5.265000	.624930 - .782110
23	.864350	5.845000	.782110 - .950700
24	.981966	6.230000	.950700 - 1.013740
25	1.028208	6.375000	1.013740 - 1.042770
26	1.047653	6.435000	1.042770 - 1.052540
27	1.057444	6.465000	1.052540 - 1.062360
28	1.067281	6.495000	1.062360 - 1.072220
29	1.085433	6.550000	1.072220 - 1.098730
30	1.132329	6.690000	1.098730 - 1.166450
31	1.236161	6.990000	1.166450 - 1.307910
32	1.381686	7.390000	1.307910 - 1.457480
33	1.325469	7.765000	1.457480 - 1.595000
34	1.659933	8.100000	1.595000 - 1.726160
35	1.789995	8.411350	1.726160 - 1.855000

Pu-239 Thermal Absorption Cross Section

```
.4166E&04 .2327E&04 .1604E&04 .1233E&04 .1013E&04 .8732E&03 .7810E&03A   79   2
.7174E&03 .7000E&03 .7635E&03 .9728E&03 .1586E&04 .2666E&04 .3867E&04A   79   3
.4909E&04 .5235E&04 .4860E&04 .3188E&04 .1340E&04 .4751E&03 .1996E&03A   79   4
.1017E&03 .6622E&02 .5277E&02 .4946E&02 .4809E&02 .4744E&02 .4680E&02A   79   5
.4567E&02 .4302E&02 .3815E&02 .3281E&02 .2869E&02 .2552E&02 .2289E&02A   79   6
```

Pu-240 Thermal Absorption Cross Section

```
.1210E&04 .6752E&03 .4643E&03 .3555E&03 .2901E&03 .2472E&03 .2173E&03A   81   2
.1921E&03 .1712E&03 .1576E&03 .1500E&03 .1469E&03 .1470E&03 .1482E&03A   81   3
.1501E&03 .1519E&03 .1540E&03 .1590E&03 .1705E&03 .1958E&03 .2598E&03A   81   4
.4611E&03 .1645E&04 .9693E&04 .5058E&05 .1369E&06 .1673E&06 .1167E&06A   81   5
.4421E&05 .8762E&04 .1524E&04 .3968E&03 .1763E&03 .1014E&03 .6610E&02A   81   6
```

Pu-241 Thermal Absorption Cross Section

```
.6278E&04 .3466E&04 .2327E&04 .1732E&04 .1375E&04 .1140E&04 .9834E&03A   80   2
.8679E&03 .8054E&03 .8406E&03 .1043E&04 .1608E&04 .2262E&04 .2336E&04A   80   3
.1938E&04 .1505E&04 .1135E&04 .6701E&03 .3109E&03 .1342E&03 .6980E&02A   80   4
.5016E&02 .4168E&02 .3787E&02 .3673E&02 .3630E&02 .3609E&02 .3588E&02A   80   5
.3550E&02 .3458E&02 .3279E&02 .3073E&02 .2903E&02 .2768E&02 .2678E&02A   80   6
```

Pu-242 Thermal Absorption Cross Section

```
.1292E&03 .7182E&02 .4906E&02 .3723E&02 .3001E&02 .2519E&02 .2175E&02A   82   2
.1873E&02 .1605E&02 .1410E&02 .1266E&02 .1154E&02 .1089E&02 .1055E&02A   82   3
.1027E&02 .1007E&02 .9929E&01 .9706E&01 .9376E&01 .8964E&01 .8632E&01A   82   4
.8560E&01 .8811E&01 .8759E&01 .7537E&01 .7647E&01 .7706E&01 .7766E&01A   82   5
.7881E&01 .8202E&01 .9058E&01 .1066E&02 .1292E&02 .1602E&02 .2051E&02A   82   6
```

Pu-239 Thermal Fission Cross Section

```
.3168E&04 .1760E&04 .1203E&04 .9144E&03 .7421E&03 .6310E&03 .5560E&03F   79   16
.5006E&03 .4724E&03 .4903E&03 .6014E&03 .9537E&03 .1584E&04 .2290E&04F   79   17
.2907E&04 .3100E&04 .2878E&04 .1890E&04 .8250E&03 .3118E&03 .1364E&03F   79   18
.7227E&02 .4736E&02 .3777E&02 .3545E&02 .3456E&02 .3414E&02 .3373E&02F   79   19
.3300E&02 .3128E&02 .2815E&02 .2476E&02 .2221E&02 .2030E&02 .1877E&02F   79   20
```

```
.2890E&01 Pu-239 Thermal Nu                                        NU   79   14
```

Pu-240 Thermal Fission Cross Section

```
.2418E&00 .1349E&00 .9273E-01 .7094E-01 .5785E-01 .4924E-01 .4324E-01F   81   16
.3816E-01 .3394E-01 .3116E-01 .2958E-01 .2886E-01 .2882E-01 .2902E-01F   81   17
.2934E-01 .2967E-01 .3006E-01 .3098E-01 .3312E-01 .3793E-01 .5136E-01F   81   18
.8959E-01 .3153E&00 .1851E&01 .9655E&01 .2612E&02 .3193E&02 .2228E&02F   81   19
.8439E&01 .1674E&01 .2921E&00 .7684E-01 .3470E-01 .2037E-01 .1359E-01F   81   20
```

```
.2890E&01 Pu-240 Thermal Nu                                        NU   81   14
```

Pu-241 Thermal Fission Cross Section

```
.4355E&04 .2418E&04 .1649E&04 .1248E&04 .1008E&04 .8523E&03 .7484E&03F   80  16
.6720E&03 .6268E&03 .6473E&03 .7843E&03 .1160E&04 .1599E&04 .1638E&04F   80  17
.1343E&04 .1029E&04 .7680E&03 .4492E&03 .2086E&03 .9043E&02 .5046E&02F   80  18
.3970E&02 .3539E&02 .3271E&02 .3193E&02 .3170E&02 .3158E&02 .3146E&02F   80  19
.3125E&02 .3073E&02 .2959E&02 .2800E&02 .2664E&02 .2553E&02 .2481E&02F   80  20

.2936E&01 Pu-241 Thermal Nu                                             NU  80  14
```

APPENDIX D

INPUT INSTRUCTIONS FOR LIBP AND LIST OF CARDS USED TO CHANGE LASER THERMAL LIBRARY

The version of LIBP at MIT is LIBP-IV with a few modifications. The user is encouraged to consult the code listing to enable complete understanding of the input. Listed in this Appendix for future users is the deck which was used to change the thermal library of LASER.

```
//STEP1 EXEC PGM=IEFBR14
//DD2 DD DSNAME=PV.M10121.10840.LASER.THERMNU,DISP=(NEW,CATLG),
//  UNIT=2314,VOL=SER=234019,SPACE=(TRK,(50,2)),
//  DCB=(RECFM=VS,LRECL=4946,BLKSIZE=4950)
//STEP2 EXEC PGM=IEHMOVE
//SYSPRINT DD SYSOUT=A
//SYSUT1 DD UNIT=SYSDA,SPACE=(CYL,(20,2)),DISP=NEW
//DD1 DD UNIT=2314,VOL=SER=234136,DISP=OLD
//DD2 DD UNIT=2314,VOL=SER=234019,DISP=OLD
//SYSIN DD *
 COPY PDS=PV.M7514.10581.LASER.THERMLIB,TO=2314=234019,                X
               RENAME=PV.M10121.10840.LASER.THERMNU
//STEP2 EXEC FORCLG,PARM.C='DECK'
//C.SYSIN DD *,DCB=(RECFM=FB,LRECL=80,BLKSIZE=2000)
```

LIBP SOURCE DECK

```
//G.FT09F001 DD DSNAME=PV.M10121.10840.LASER.THERMNU,
//       DISP=(OLD,KEEP)
//G.FT02F001 DD UNIT=SYSDA,DISP=(NEW,DELETE),SPACE=(TRK,(50,10)),
//       DCB=(RECFM=VS,LRECL=4946,BLKSIZE=5000)
//G.SYSIN DD *,DCB=(RECFM=FB,LRECL=80,BLKSIZE=2000)
1 LASER THERMLIB - '65 SHER DATA(235), ENDF/B-II DATA (PU-39,40,41,42)
  -1    35    7    7
```

```
23994   0
24094   0
24194   0
24294   0
2399400100
2409400100
2419400100
23994   0      0      0
 .4166E&04 .2327E&04 .1604E&04 .1233E&04 .1013E&04 .8732E&03 .7810E&03A    79    2
 .7174E&03 .7000E&03 .7635E&03 .9728E&03 .1586E&04 .2666E&04 .3867E&04A    79    3
 .4909E&04 .5235E&04 .4860E&04 .3188E&04 .1340E&04 .4751E&03 .1996E&03A    79    4
 .1017E&03 .6622E&02 .5277E&02 .4946E&02 .4809E&02 .4744E&02 .4680E&02A    79    5
 .4567E&02 .4302E&02 .3815E&02 .3281E&02 .2869E&02 .2552E&02 .2289E&02A    79    6
24094   0      0      0
 .1210E&04 .6752E&03 .4643E&03 .3555E&03 .2901E&03 .2472E&03 .2173E&03A    81    2
 .1921E&03 .1712E&03 .1576E&03 .1500E&03 .1469E&03 .1470E&03 .1482E&03A    81    3
 .1501E&03 .1519E&03 .1540E&03 .1590E&03 .1705E&03 .1958E&03 .2598E&03A    81    4
 .4611E&03 .1645E&04 .9693E&04 .5058E&05 .1369E&06 .1673E&06 .1167E&06A    81    5
 .4421E&05 .8762E&04 .1524E&04 .3968E&03 .1763E&03 .1014E&03 .6610E&02A    81    6
24194   0      0      0
 .6278E&04 .3466E&04 .2327E&04 .1732E&04 .1375E&04 .1140E&04 .9834E&03A    80    2
 .8679E&03 .8054E&03 .8406E&03 .1043E&04 .1608E&04 .2262E&04 .2336E&04A    80    3
 .1938E&04 .1505E&04 .1135E&04 .6701E&03 .3109E&03 .1342E&03 .6980E&02A    80    4
 .5016E&02 .4168E&02 .3787E&02 .3673E&02 .3630E&02 .3609E&02 .3588E&02A    80    5
 .3550E&02 .3458E&02 .3279E&02 .3073E&02 .2903E&02 .2768E&02 .2678E&02A    80    6
24294   0      0      0
 .1292E&03 .7182E&02 .4906E&02 .3723E&02 .3001E&02 .2519E&02 .2175E&02A    82    2
 .1873E&02 .1605E&02 .1410E&02 .1266E&02 .1154E&02 .1089E&02 .1055E&02A    82    3
 .1027E&02 .1007E&02 .9929E&01 .9706E&01 .9376E&01 .8964E&01 .8632E&01A    82    4
 .8560E&01 .8811E&01 .8759E&01 .7537E&01 .7647E&01 .7706E&01 .7766E&01A    82    5
 .7881E&01 .8202E&01 .9058E&01 .1066E&02 .1292E&02 .1602E&02 .2051E&02A    82    6
2399400100   0      0
```

```
 .3168E&04 .1760E&04 .1203E&04 .9144E&03 .7421E&03 .6310E&03 .5560E&03F   79  16
 .5006E&03 .4724E&03 .4903E&03 .6014E&03 .9537E&03 .1584E&04 .2290E&04F   79  17
 .2907E&04 .3100E&04 .2878E&04 .1890E&04 .8250E&03 .3118E&03 .1364E&03F   79  18
 .7227E&02 .4736E&02 .3777E&02 .3545E&02 .3456E&02 .3414E&02 .3373E&02F   79  19
 .3300E&02 .3128E&02 .2815E&02 .2476E&02 .2221E&02 .2030E&02 .1877E&02F   79  20
 .2880E&01                                                          NU   79  14
2409400100  0     0
 .2418E&00 .1349E&00 .9273E-01 .7094E-01 .5785E-01 .4924E-01 .4324E-01F   81  16
 .3816E-01 .3394E-01 .3116E-01 .2958E-01 .2886E-01 .2882E-01 .2902E-01F   81  17
 .2934E-01 .2967E-01 .3006E-01 .3098E-01 .3312E-01 .3793E-01 .5136E-01F   81  18
 .8959E-01 .3153E&00 .1851E&01 .9655E&01 .2612E&02 .3193E&02 .2228E&02F   81  19
 .8439E&01 .1674E&01 .2921E&00 .7684E-01 .3470E-01 .2037E-01 .1359E-01F   81  20
 .2890E&01                                                          NU   81  14
2419400100  0     0
 .4355E&04 .2418E&04 .1649E&04 .1248E&04 .1008E&04 .8523E&03 .7484E&03F   80  16
 .6720E&03 .6268E&03 .6473E&03 .7843E&03 .1160E&04 .1599E&04 .1638E&04F   80  17
 .1343E&04 .1029E&04 .7680E&03 .4492E&03 .2086E&03 .9043E&02 .5046E&02F   80  18
 .3970E&02 .3539E&02 .3271E&02 .3193E&02 .3170E&02 .3158E&02 .3146E&02F   80  19
 .3125E&02 .3073E&02 .2959E&02 .2800E&02 .2664E&02 .2553E&02 .2481E&02F   80  20
 .2936E&01                                                          NU   80  14
```

APPENIDX E

LISTING OF CHANGED SUBROUTINES IN LASER-M

The changes to LASER to form LASER-M that were carried out in the present study were confined to a few LASER subroutines. The subroutines which contain the majority of the revisions are listed on the following pages.

```
C     LASER  PONCELET,WAPD                                                    EDIT
C     LINK 11,DECK 33   THERMOS OUTPUT                                        EDIT
      SUBROUTINE EDIT                                                         EDIT
      COMMON NCONT,NBUR,DUMMY1,KF,DUMMY2(5),NX,MX                             EDIT
      COMMON MTBL(14),NXA,ENC(17),UPU,RN(14),RO(14),DUMMY3(4),VOLUME(14)EDIT
      COMMON DUMMY4(67),QTH,CT,NUMBER                                         EDIT
      COMMON DUMMY5(1546),KCLAD,KMOD,DUMMYF(130)                              EDIT
      COMMON DUMMY7(50),DUMMYD(21),MM                                         EDIT
      COMMON DUMMY8(51),SS(14,35),DUMMY9(255),IX,DUMMYA,SCARIN                EDIT
      COMMON DUMMYB(2),Z,DUMMYC(570),MOD,NCLAD,DUMMYE(3),BM2,ELF(7),DTH EDIT
      COMMON DUMMY6(5),TMOD,TCLAD,TFUEL,NFUEL,DUMMYG(3),NIT,IY,DTHY,DCPMEDIT
      COMMON ANT(4),BNT(4),LAT,EFTEMP,CAT(5)                                  EDIT
      COMMON OME25,OME28                                                      EDIT
      COMMON/LINK6/T(14,14,35),S(14,35),FVSTR,CONCTA(17,4),DV(35),V(35) EDIT
      COMMON/LINK6/XATE(20,35),P(35,35,4),XAM(14,35),XTM(14,35)               EDIT
      COMMON/LINK6/XST(17,35),XAT(17,35),CONCTC(10,5),F(14,35)                EDIT
      COMMON/MODIF1/NOFLUX,NORATE,NO625,NOMISC,NODECK,MINBRN,DTHYMR,DTH
     1MR
      DIMENSION SUMA(20,14),XTR(14,35),SUMK(35),SUML(35)                      EDIT
      DIMENSION SUMKMR(35),SUMLMR(35)
C                                                                             EDIT
      ISOXE=20                                                                EDIT
      IP=IY                                                                   EDIT
      IF(NUMBER.EQ.1) IP=IX                                                   EDIT
    2 CONTINUE                                                                EDIT
      DO5N=1,NX                                                               EDIT
      DO5J=1,ISOXE                                                            EDIT
    5 SUMA(J,N)=0.0                                                           EDIT
      DO15N=1,NX                                                              EDIT
      DO15J=1,ISOXE                                                           EDIT
      DO10I=1,IP                                                              EDIT
   10 SUMA(J,N)=SUMA(J,N)+F(N,I)*V(I)*DV(I)*XATE(J,I)                         EDIT
```

```
   15 CONTINUE                                                          EDIT
      WRITE(4) SUMA                                                     EDIT
      IF(NUMBER.EQ.1) GOTO40                                            EDIT
C                                                                       EDIT
C     CALCULATION OF THERMAL DIFFUSION COEFFICIENT                      EDIT
C                                                                       EDIT
      IF(NFUEL.NE.2) SPOT=0.9583                                        EDIT
      IF(NFUEL.EQ.2) SPOT=0.9753                                        EDIT
      DO20K=1,KF                                                        EDIT
      DO20I=1,IP                                                        EDIT
   20 XTR(K,I)=XAM(K,I)+CONCTA(15,1)*XST(15,I)*0.9972+CONCTA(11,1)*XST(1EDIT
     11,I)*SPOT                                                         EDIT
      KF1=KF+1                                                          EDIT
      BMU=0.9879                                                        EDIT
      IF(NCLAD.EQ.2) BMU=0.9753                                         EDIT
      IF(NCLAD.EQ.3) BMU=0.9927                                         EDIT
      DO25K=KF1,KCLAD                                                   EDIT
      DO25I=1,IP                                                        EDIT
   25 XTR(K,I)=XAM(K,I)+CONCTA(14,2)*XST(14,I)*BMU                      EDIT
      KCL1=KCLAD+1                                                      EDIT
      BMU=1.0                                                           EDIT
      DO30K=KCL1,KMOD                                                   EDIT
      DO30I=1,IP                                                        EDIT
   30 XTR(K,I)=XAM(K,I)+CONCTA(12,3)*XST(12,I)*0.9583+CONCTA(13,3)*XST(1EDIT
     13,I)*BMU+CONCTA(16,3)*XST(16,I)*0.9394+CONCTA(17,3)*XST(17,I)     EDIT
      SUM1=0.0                                                          EDIT
      SUM2=0.0                                                          EDIT
      SUM1MR=0.0
```

```
      SUM2MR=0.0
      DO35I=1,IP                                                    EDIT
      SUMK(I)=0.0                                                   EDIT
      SUML(I)=0.0                                                   EDIT
      SUMKMR(I)=0.0
      SUMLMR(I)=0.0
      DO32K=1,KMOD                                                  EDIT
      SUMK(I)=SUMK(I)+F(K,I)*XTR(K,I)*V(I)*VOLUME(K)                EDIT
      SUML(I)=SUML(I)+F(K,I)*V(I)*VOLUME(K)                         EDIT
   32 CONTINUE                                                      EDIT
      DO 33 N=KCL1,KMOD
      SUMKMR(I)=SUMKMR(I)+F(N,I)*XTR(N,I)*V(I)*VOLUME(N)
   33 SUMLMR(I)=SUMLMR(I)+F(N,I)*V(I)*VOLUME(N)
      SUMK(I)=SUMK(I)/SUML(I)                                       EDIT
      SUM2=SUM2+SUML(I)*DV(I)/SUMK(I)                               EDIT
      SUM1=SUM1+SUML(I)*DV(I)                                       EDIT
      SUMKMR(I)=SUMKMR(I)/SUMLMR(I)
      SUM2MR=SUM2MR+SUMLMR(I)*DV(I)/SUMKMR(I)
      SUM1MR=SUM1MR+SUMLMR(I)*DV(I)
   35 CONTINUE                                                      EDIT
      IF(IP.EQ.IY) DTHY=SUM2/(3.*SUM1)                              EDIT
      IF(IP.EQ.IY) DTHYMR=SUM2MR/(3.*SUM1MR)
      IF(IP.EQ.IX) DTH=SUM2/(3.*SUM1)                               EDIT
      IF(IP.EQ.IX) DTHMR=SUM2MR/(3.*SUM1MR)
   40 IF(IP.EQ.IX) GOTO45                                           EDIT
      IP=IX                                                         EDIT
      GOTO2                                                         EDIT
C                                                                   EDIT
   45 IF(NUMBER.EQ.1) GOTO55                                        EDIT
      Z=(1.+DTH*BM2*SUM1)/Z                                         EDIT
   55 RETURN                                                        EDIT
      END                                                           EDIT
```

```
C     LINK 7,DECK 25  DATA FOR DOPPLER-BROADENED PU CROSS SECTIONS
      BLOCK DATA                                                        DOPL
      COMMON/LINK7/B0,B2,B4,B6,B8,B10                                   DOPL
      COMMON/LINK7/C6,CSQ,ANS
      COMMON/LINK7/PPR(6),PPI(6),CR(6),CI(6),QR(6),QI(6),P6(2)          DOPL
      COMMON/LINK7/SIG0,E0,GAMMAN,GAMMAC,MASS,BOLK,GF                   DOPL
      COMMON/LINK7/S039P,S039N,E0P,E0N,GAMP,GAMN,GFP,GFN,MASS39         DOPL
      COMPLEX C6,CSQ,ANS,B0,B2,B4,B6,B8,B10                             DOPL
      REAL MASS,MASS39
      DATA B0/(2.5052367,.0)/,B2/(1.2831204,.0)/,B4/(.22647180,.0)/,B6/(DOPL
     1.13064690,.0)/,B8/(-.0202490,.0)/,B10/(.00391320,.0)/             DOPL
      DATA PPR(1),PPI(1),PPR(2),PPI(2),PPR(3),PPI(3)/
     1.0,6.1043246,-10.966304,1.131723,24.240703,-78.663636/
      DATA CR(1),CI(1),CR(2),CI(2),CR(3),CI(3)/
     1.0,1.322715,1.0914789,1.2908118,-2.3055569,1.1741668/
C        DATA FOR THE PU-240 RESONANCE HAS BEEN UPDATED AT MIT BY
C        S MOMSEN(1/17/73) TO REFLECT ENDF/B-II CROSS SECTION DATA.
      DATA SIG0,E0,GAMMAN,GAMMAC,MASS,BOLK,GF/.186225E6,1.056,.00244,.02
     X986,237.99,.8616656E-4,.19085E-3/
      DATA S039P,S039N,E0P,E0N,GAMP,GAMN,GFP,GFN,MASS39/.2120E4,
     1.1569E3,.296,.40,.099,.220,1.5385,9.695,236.999/                 DOPL
      END                                                               DOPL
```

```
C       LASER  PONCELET,WAPD                                                  BONE
C       LINK  1,DECK 7    OUTPUT IS EDITED (PART II)                         BONE
        SUBROUTINE BONE                                                      BONE
        COMMON NCONT,NBUR,NTT,KF,DT,PR,TON,EPSI,BUCKL,NX,MX,MTBL(14)         BONE
        COMMON NXA,ENC(17),UPU,RN(14),RO(14),SEARCH,NSCH,LPT,QEPI            BONE
        COMMON VOLUME(14),VOLC,VOLFU,VOLCLA,VOLMOD,X1BAR0(17),PHIR(5)        BONE
        COMMON XNU(7),KAPPA(7),YXE(7),YSM(7),DCXE,DC41,X1BAR(11),QTH,CT      BONE
        COMMON NUMBER,FASFLU(50),SAF(8,50),SAB1(17),SAB2(17),SFB1(7)         BONE
        COMMON SFB2(7),SB1(7),SB2(7),PST(14,35),SABTH(20,14),SFBTH(7,14)     BONE
        COMMON XLAMDA(5),U,A(9,5),C(9,5),FC(7,5),FS(7,5),KCLAD,KMOD          BONE
        COMMON XX(10,5),AD(9,5),CD(7,5),X(10,5),AW(7),A1B(7),C1B(7)          BONE
        COMMON MM,NT,ST(50),SS(14,35),DELTA(5),SFBTHP(7,14),SFB2P(7)         BONE
        COMMON SFB1P(7),A1(16),A2(16),A3(16),F1(7),F2(7),F3(7),A1T(16)       BONE
        COMMON A2T(16),A3T(16),F1T(7),F2T(7),F3T(7)                          BONE
        COMMON IX,IDEN,SCARIN,BURNUP,COBUR,Z                                 BONE
        COMMON STAN(50),FASCUR(50),SAFAN(8,50)                               BONE
        COMMON FCDD(7,5),FSDD(7,5),MOD,NCLAD,MAX,DIF,MOR,BM2,ELF(7),DTH      BONE
        COMMON NONLI,BM21,BM22,CRIT1,CRIT2                                   BONE
        COMMON TMOD,TCLAD,TFUEL,NFUEL,LSERCH,DTXE,DTSM,NIT,IY,DTHY,DCPM      BONE
        COMMON ANT(4),BNT(4),LAT,EFTEMP,CAT(5)                               BONE
        COMMON OME25,OME28                                                   BONE
        COMMON/LINK1/C28(5),NRP(5),NPP(5),THP(5),RI(14),TOTC                 BONE
        COMMON/LINK1/SOB1(17),SOB2(17),PTH(7),THFLUX(14,35),FRAC             BONE
        COMMON/LINK1/SPAFLU(14),SPADEN(14),POWER(7),ABSTH(16),FISTH(7)       BONE
        COMMON/LINK1/CAPTH(7),ABSEPI(16),ABSFAS(16),FISEPI(7),CAPEPI(7)      BONE
        COMMON/LINK1/FISFAS(7),CAPFAS(7),TABS(16),FIS(7),CAP(7),VBAR(14)     BONE
        COMMON/LINK1/TSHIFT(14),AVABX(16,14),AVFIX(7,5),ABSXFA(17)           BONE
        COMMON/LINK1/ABSXEP(17),ABSXFE(17),ABSXTH(16),FISXFA(7),NUFXFA(7)    BONE
        COMMON/LINK1/FISXFE(7),NUFXFE(7),FISXEP(7),NUFXEP(7),FISXTH(7)       BONE
        COMMON/LINK1/NUFXTH(7),EFFXA(16),EFFXF(7),EFFXNF(7),A25TH(5)         BONE
        COMMON/LINK1/A49TH(5),A41TH(5),XBAR(10),URA(5),PLU(5)                BONE
        COMMON/LINK1/ATOM(7,5),TAS(7),PTU(5),PTUM(5),AVATOM(7)               BONE
        COMMON/LINK1/U238R(5),DEPL25(5),TAU,PF1(7),PF2(7)                    BONE
        COMMON/LINK1/FP(50),DELTAE(50),VEL(35),DELV(35)                      BONE
        COMMON/LINK1/DIFU(4),SIGMAA(4),SIGMAF(4),SIGMAN(4),SIGMAR(4)         BONE
        COMMON/LINK1/AGE(4),QU(4)                                            BONE
        COMMON/LINK1/SABTHY(20,14),SFBTHY(7,14),SPADY(14),SPAFY(14)          BONE
        COMMON/LINK1A/FBARF,FBARC,FBARM,FBAR,NBARF,NBARC,NBARM,NBAR          BONE
```

```
      COMMON/LINK1A/TOTAL1,TOTAL2,TOTALF,TOTAL3,TOTC1,TOTC2                BONE
      COMMON/LINK1A/CEDFM,CEDFC                                            BONE
      COMMON/LINK1A/TOTALY,FBARFX,FBARCX,FBARMX,FBARX,NBARFX,NBARCX        BONE
      COMMON/LINK1A/NBARMX,NBARX,BR1,BR2,BR3,BR4                           BONE
      COMMON/LINK1A/ABSCEL,FISCEL,TOTLK                                    BONE
      COMMON/MODIF1/NOFLUX,NORATE,NO625,NOMISC,NODECK,MINBRN,DTHYMR,DTH
     1MR
      COMMON/MODIF2/VGRAD,FRACFU,FRACMD,FRACCL,NOPDQ
      DIMENSION EQITR(4),BB(4),EQITRS(4),EQIREM(4)
      DIMENSION GMNDXA(16),GMNDXF(7),GMNDNF(7),FASTNU(7),EPINU(7),FEPINU
     1(7),EFFXF1(7),TEM(7),XKSIGF(4),TEMFA(14),TEMFB(14),TEMFC(14),TEMFD
     2(14),TEMFE(14),TEMA(14),TEMB(14),TEMC(14),TEMD(14),TEME(14),TEMF(1
     34)
      REAL KAPPA
C                                                                          BONE
C     CALCULATION OF MICROSCOPIC PARAMETERS                                BONE
C                                                                          BONE
      THABS=0.0                                                            BONE
      DO200I=1,10                                                          BONE
  200 THABS=THABS+ABSTH(I)                                                 BONE
      THABSF=THABS+ABSTH(16)                                               BONE
      DO205I=11,16                                                         BONE
  205 THABS=THABS+ABSTH(I)                                                 BONE
      THERUT=THABSF/THABS                                                  BONE
      ETA=0.0                                                              BONE
      DO206I=1,7                                                           BONE
  206 ETA=ETA+XNU(I)*FISTH(I)                                              BONE
      ETA=ETA/THABSF                                                       BONE
      ETAF=ETA*THERUT                                                      BONE
      WRITE(6,2115)THERUT,ETA,ETAF                                         BONE
      DELT25=(FISEPI(1)+FISFAS(1))/FISTH(1)                                BONE
      SUM=FIS(3)*(ABSCEL+TOTLK)                                            BONE
      DELT28=SUM/(FISCEL-SUM)                                              BONE
      RHO28=(CAPFAS(3)+ABSEPI(3))/ABSTH(3)                                 BONE
      REAL MODCR                                                           BONE
      FISA=TABS(1)+TABS(4)+TABS(6)                                         BONE
      MODCR=CAP(3)/FISA                                                    BONE
      CR1=FIS(3)/FISA                                                      BONE
```

```
      CR2=CAP(3)/FIS(1)                                                 BONE
      CR3=(CAP(3)+CAP(5))/FISA                                          BONE
      IF(NOMISC.EQ.1) GO TO 209
      WRITE(6,2120)DELT25,DELT28,RH028                                  BONE
      WRITE(6,2122)                                                     BONE
      WRITE(6,2125)MODCR,CR1,CR2,CR3                                    BONE
  209 SUM=0.0
      DO210I=1,7                                                        BONE
  210 SUM=SUM+(XNU(I)*FISTH(I)+VOLC*X1BAR(I)*(SB2(I)+SB1(I)))           BONE
      CRIT=SUM/ABSCEL                                                   BONE
      WRITE(6,2130)CRIT                                                 BONE
      IF(LSERCH.EQ.1) WRITE(6,2136)(CAT(I),I=1,5),ELF(3)
      IF(LSERCH.EQ.2) WRITE(6,2141) ELF(1),ELF(3)                       BONE
C                                                                       BONE
      REAL NBARF                                                        BONE
      REAL NBARC                                                        BONE
      REAL NBARM                                                        BONE
      REAL NBAR                                                         BONE
      REAL NBARFX                                                       BONE
      REAL NBARCX                                                       BONE
      REAL NBARMX                                                       BONE
      REAL NBARX                                                        BONE
C                                                                       BONE
C     CALCULATION OF AVERAGE THERMAL SPEEDS AND NEUTRON TEMPERATURES    BONE
C                                                                       BONE
      KF1=KF+1                                                          BONE
      KCL1=KCLAD+1                                                      BONE
      WRITE(6,5000)
      SPEED=220000.0                                                    BONE
      DO215K=1,NX                                                       BONE
  215 VBAR(K)=(SPAFLU(K)/SPADEN(K))/SPEED                               BONE
      IF(NOMISC.EQ.1) GO TO 216
      WRITE(6,2132)                                                     BONE
      WRITE(6,2133)                                                     BONE
      WRITE(6,2135)(K,VBAR(K),K=1,NX)                                   BONE
  216 VBARFU=(FBARFX/NBARFX)/SPEED
      VBARCL=(FBARCX/NBARCX)/SPEED                                      BONE
```

```
      VBARMD=(FBARMX/NBARMX)/SPEED                                      BONE
      VCELL=(FBARX/NBARX)/SPEED                                         BONE
      WRITE(6,2137)                                                     BONE
      WRITE(6,2268)
      WRITE(6,2269)VBARFU,VBARCL,VBARMD,VCELL,VGRAD
      IF(NOMISC.EQ.0) WRITE(6,5000)
  219 DO 220K=1,NX
  220 TSHIFT(K)=298.0*((VBAR(K)/1.128)**2.-1.)                          BONE
      IF(NOMISC.EQ.1) GO TO 221
      WRITE(6,2142)                                                     BONE
      WRITE(6,2143)                                                     BONE
      WRITE(6,2145)(K,TSHIFT(K),K=1,NX)                                 BONE
  221 CONTINUE
      TSHIFF=298.0*((VBARFU/1.128)**2.-1.)                              BONE
      TSHIFC=298.0*((VBARCL/1.128)**2.-1.)                              BONE
      TSHIFM=298.0*((VBARMD/1.128)**2.-1.)                              BONE
      TSHCEL=298.0*((VCELL/1.128)**2.-1.)                               BONE
      IF(NOMISC.EQ.1) GO TO 222
      WRITE(6,2148)                                                     BONE
      WRITE(6,2138)                                                     BONE
      WRITE(6,2140)TSHIFF,TSHIFC,TSHIFM,TSHCEL                          BONE
  222 IF(NO625.EQ.0) WRITE(6,5000)
C                                                                       BONE
C     SPECIAL EDIT      0.0EV-0.625EV                                   BONE
C                                                                       BONE
      IF(NO625.EQ.0) WRITE(6,2041)
      SUM1=0.0                                                          BONE
      DO105I=1,10                                                       BONE
      DO105K=1,KF                                                       BONE
  105 SUM1=SUM1+SABTHY(I,K)*XX(I,K)*VOLUME(K)                           BONE
      DO110K=1,KF                                                       BONE
      IF(NFUEL.NE.2) SUM1=SUM1+SABTHY(15,K)*ENC(11)*VOLUME(K)           BONE
      IF(NFUEL.EQ.2) SUM1=SUM1+SABTHY(16,K)*ENC(17)*VOLUME(K)           BONE
  110 CONTINUE                                                          BONE
      SUM2=0.0                                                          BONE
      DO125I=11,15                                                      BONE
      J=0                                                               BONE
      L=0                                                               BONE
      KX=KCL1                                                           BONE
      KY=KMOD                                                           BONE
```

```
      IF(I.EQ.11) J=4                                                    BONE
      IF(I.EQ.14) J=2                                                    BONE
      IF(I.EQ.15) L=1                                                    BONE
      IF(I.NE.13) GOTO115                                                BONE
      KX=KF1                                                             BONE
      KY=KCLAD                                                           BONE
  115 IJ=I+J-L                                                           BONE
      DO120K=KX,KY                                                       BONE
  120 SUM2=SUM2+SABTHY(I,K)*ENC(IJ)*VOLUME(K)                            BONE
  125 CONTINUE                                                           BONE
      SUM2=SUM1+SUM2                                                     BONE
      THERUT=SUM1/SUM2                                                   BONE
      ETA=0.0                                                            BONE
      DO130I=1,7                                                         BONE
      DO130K=1,KF                                                        BONE
  130 ETA=ETA+XNU(I)*SFBTHY(I,K)*XX(I,K)*VOLUME(K)                       BONE
      ETA=ETA/SUM1                                                       BONF
      ETAF=ETA*THERUT                                                    BONE
      IF(NO625.EQ.1) GO TO 223
      WRITE(6,2115) THERUT,ETA,ETAF                                      BONE
      WRITE(6,2137)                                                      BONE
      WRITE(6,2138)                                                      BONE
  223 SUM1=(FBARF/NBARF)/SPEED
      SUM2=(FBARC/NBARC)/SPEED                                           BONE
      SUM3=(FBARM/NBARM)/SPEED                                           BONE
      SUM4=(FBAR/NBAR)/SPEED                                             BONE
      IF(NO625.EQ.0) WRITE(6,2140) SUM1,SUM2,SUM3,SUM4
      WRITE(6,5000)                                                      BONE
      DO230K=1,KMOD                                                      BONE
      DO225I=1,16                                                        BONE
      AVABX(I,K)=SABTH(I,K)/SPAFLU(K)                                    BONE
      IF(I.GT.7) GOTO225                                                 BONE
      AVFIX(I,K)=SFBTH(I,K)/SPAFLU(K)                                    BONE
  225 CONTINUE                                                           BONE
  230 CONTINUE                                                           BONE
C                                                                        BONE
C     CALCULATION OF AVERAGE MICROSCOPIC CROSS SECTIONS                  BONE
C                                                                        BONE
      IF(NOMISC.EQ.1) GO TO 243
```

```
      WRITE(6,2152)                                                     BONE
      WRITE(6,2153)                                                     BONE
      WRITE(6,2154)(K,(AVABX(I,K),I=1,7),K=1,KMOD)                      BONE
      IF(MOD.EQ.3) GOTO235                                              BONE
      WRITE(6,2155)                                                     BONE
      WRITE(6,2156)(K,(AVABX(I,K),I=8,12),AVABX(15,K),K=1,KMOD)         BONE
      GOTO240                                                           BONE
  235 WRITE(6,2157)                                                     BONE
      WRITE(6,2154)(K,(AVABX(I,K),I=8,12),AVABX(15,K),AVABX(14,K),K=1,KMBONE
     1OD)                                                               BONE
  240 CONTINUE                                                          BONE
      WRITE(6,5000)                                                     BONE
      WRITE(6,2152)                                                     BONE
      IF(NCLAD.NE.2) GOTO241                                            BONE
      WRITE(6,2158)                                                     BONE
      WRITE(6,2159)(K,AVABX(13,K),K=1,KMOD)                             BONE
      GOTO242                                                           BONE
  241 IF(NCLAD.EQ.1) WRITE(6,2160)                                      BONE
      IF(NCLAD.EQ.3) WRITE(6,2161)                                      BONE
      WRITE(6,2162)(K,(AVABX(I,K),I=13,16,3),K=1,KMOD)                  BONE
  242 CONTINUE                                                          BONE
      WRITE(6,2164)                                                     BONE
      WRITE(6,2153)                                                     BONE
      WRITE(6,2154)(K,(AVFIX(I,K),I=1,7),K=1,KMOD)                      BONE
      WRITE(6,5000)                                                     BONE
  243 DO 245I=1,17
      ABSXFA(I)=SAB1(I)/TOTAL1                                          BONE
      ABSXEP(I)=SAB2(I)/TOTAL2                                          BONE
  245 ABSXFE(I)=(SAB1(I)+SAB2(I))/TOTALF                                BONE
      DO255I=1,10                                                       BONE
      ABSXTH(I)=0.0                                                     BONE
      DO250K=1,KF                                                       BONE
  250 ABSXTH(I)=ABSXTH(I)+SABTH(I,K)*VOLUME(K)                          BONE
      ABSXTH(I)=ABSXTH(I)/(FBARFX*VOLFU)                                BONE
  255 CONTINUE                                                          BONE
      DO257I=11,15                                                      BONE
      ABSXTH(I)=0.0                                                     BONE
      IF(I.EQ.13) GOTO257                                               BONE
      DO256K=KCL1,KMOD                                                  BONE
```

```
256 ABSXTH(I)=ABSXTH(I)+SABTH(I,K)*VOLUME(K)                                    BONE
    ABSXTH(I)=ABSXTH(I)/(FBARMX*VOLMOD)                                        BONE
257 CONTINUE                                                                   BONE
    DO258K=KF1,KCLAD                                                           BONE
258 ABSXTH(13)=ABSXTH(13)+SABTH(13,K)*VOLUME(K)                                BONE
    ABSXTH(13)=ABSXTH(13)/(FBARCX*VOLCLA)                                      BONE
    IJ=15                                                                      BONE
    IF(NFUEL.EQ.2) IJ=IJ+1                                                     BONE
    ABSXTH(16)=0.0                                                             BONE
    DO259K=1,KF                                                                BONE
259 ABSXTH(16)=ABSXTH(16)+SABTH(IJ,K)*VOLUME(K)                                BONE
    ABSXTH(16)=ABSXTH(16)/(FBARFX*VOLFU)                                       BONE
    WRITE(6,2168)                                                              BONE
    WRITE(6,2023)                                                              BONE
    WRITE(6,2170)(ABSXFA(I),ABSXEP(I),ABSXFE(I),ABSXTH(I),I=1,7)               BONE
    WRITE(6,2171)(ABSXFA(I),ABSXEP(I),ABSXFE(I),ABSXTH(I),I=8,11)              BONE
    DO261I=1,6                                                                 BONE
261 ABSXTH(I)=0.1*10.**21.                                                     BONE
    ABSXTH(1)=ABSXTH(14)                                                       BONE
    ABSXTH(2)=ABSXTH(15)                                                       BONE
    IF(MOD.EQ.3) ABSXTH(3)=ABSXTH(12)                                          BONE
    IF(NCLAD.EQ.1) ABSXTH(4)=ABSXTH(13)                                        BONE
    IF(NCLAD.EQ.2) ABSXTH(5)=ABSXTH(13)                                        BONE
    IF(NCLAD.EQ.3) ABSXTH(6)=ABSXTH(13)                                        BONE
    WRITE(6,2172)(ABSXFA(I),ABSXEP(I),ABSXFE(I),ABSXTH(I-11),I=12,17)          BONE
    IF(NFUEL.EQ.1) WRITE(6,2173) ABSXFA(13),ABSXEP(13),ABSXFE(13),ABSXBONE
   1TH(16)                                                                     BONE
    IF(NFUEL.EQ.2) WRITE(6,2174) ABSXFA(16),ABSXEP(16),ABSXFE(16),ABSXBONE
   1TH(16)                                                                     BONE
    WRITE(6,2175)                                                              BONE
    WRITE(6,5000)                                                              BONE
C                                                                              BONE
    REAL NUFXFA                                                                BONE
```

```
      REAL NUFXFE                                                       BONE
      REAL NUFXEP                                                       BONE
      REAL NUFXTH                                                       BONE
      DO260I=1,7                                                        BONE
      FISXFA(I)=SFB1(I)/TOTAL1                                          BONE
      NUFXFA(I)=SB1(I)/TOTAL1                                           BONE
      FISXEP(I)=SFB2(I)/TOTAL2                                          BONE
      NUFXEP(I)=SB2(I)/TOTAL2                                           BONE
      FISXFE(I)=(SFB1(I)+SFB2(I))/TOTALF                                BONE
  260 NUFXFE(I)=(SB1(I)+SB2(I))/TOTALF                                  BONE
      DO270I=1,7                                                        BONE
      FISXTH(I)=0.0                                                     BONE
      DO265K=1,KF                                                       BONE
  265 FISXTH(I)=FISXTH(I)+SFBTH(I,K)*VOLUME(K)                          BONE
      FISXTH(I)=FISXTH(I)/(FBARFX*VOLFU)                                BONE
      NUFXTH(I)=XNU(I)*FISXTH(I)                                        BONE
  270 CONTINUE                                                          BONE
      WRITE(6,2177)                                                     BONE
      WRITE(6,2023)                                                     BONE
      WRITE(6,2170)(FISXFA(I),FISXEP(I),FISXFE(I),FISXTH(I),I=1,7)      BONE
      WRITE(6,2182)                                                     BONE
      WRITE(6,2023)                                                     BONE
      WRITE(6,2170)(NUFXFA(I),NUFXEP(I),NUFXFE(I),NUFXTH(I),I=1,7)      BONE
C
CALCULATION OF SPECTRUM AVERAGED - ISOTOPIC NU
C
      DO 466 K=1,7
      FASTNU(K)=NUFXFA(K)/FISXFA(K)
      IF(K.EQ.2.OR.K.EQ.3) GO TO 467
      EPINU(K)=NUFXEP(K)/FISXEP(K)
      GO TO 466
  467 EPINU(K)=0.0
  466 FEPINU(K)=NUFXFE(K)/FISXFE(K)
      WRITE(6,2232)
      WRITE(6,2023)
      WRITE(6,2170)  (FASTNU(I),EPINU(I),FEPINU(I),XNU(I),I=1,7)
      WRITE(6,5000)                                                     BONE
C                                                                       BONE
C     CALCULATION OF EFFECTIVE THERMAL MICROSCOPIC CROSS SECTIONS       BONE
C                                                                       BONE
```

```
      DO 20 I=1,10
   20 EFFXA(I)=0.0
      DO 21 I=1,7
   21 EFFXF(I)=0.0
      DO275I=1,10                                                    BONE
      IF(X1BAR(I).EQ.0.) GO TO 275
      EFFXA(I)=ABSTH(I)/(X1BAR(I)*TOTAL3*VOLC)
  275 CONTINUE
      DO272I=11,15                                                   BONE
      IF(I.EQ.13) GOTO272                                            BONE
      EFFXA(I)=ABSXTH(I)*CEDFM                                       BONE
  272 CONTINUE                                                       BONE
      EFFXA(13)=ABSXTH(13)*CEDFC                                     BONE
      EFFXA(16)=ABSXTH(16)*FBARFX/FBARX                              BONE
      DO280I=1,7                                                     BONE
      IF(X1BAR(I).EQ.0.) GO TO 280
      EFFXF(I)=FISTH(I)/(X1BAR(I)*TOTAL3*VOLC)                       BONE
  280 EFFXNF(I)=XNU(I)*EFFXF(I)                                      BONE
      WRITE(6,2187)                                                  BONE
      WRITE(6,2188)                                                  BONE
      WRITE(6,2189)(EFFXA(I),EFFXF(I),EFFXNF(I),I=1,7)               BONE
      WRITE(6,2190)(EFFXA(I),I=8,11)                                 BONE
      IF(MOD.NE.3) WRITE(6,2191) EFFXA(12)                           BONE
      IF(MOD.EQ.3) WRITE(6,2192) EFFXA(12),EFFXA(14)                 BONE
      WRITE(6,2193) EFFXA(15),EFFXA(13)                              BONE
      IF(NFUEL.EQ.1) WRITE(6,2194) EFFXA(16)                         BONE
      IF(NFUEL.EQ.2) WRITE(6,2195) EFFXA(16)                         BONE
      DO 283 K=1,7
  283 EFFXF1(K)=EFFXF(K)
      AVXA=(FRACFU*ENC(11)*EFFXA(16)+FRACMD*ENC(14)*EFFXA(15))/X1BAR0(11
     X)
      WRITE(6,2233) AVXA
C
CALCULATION OF GMND CROSS SECTIONS
C
      DO 281 K=1,7
      GMNDXA(K)=VCELL*EFFXA(K)
```

```
      GMNDXF(K)=VCELL*EFFXF(K)
  291 GMNDNF(K)=VCELL*EFFXNF(K)
      DO 282 K=8,16
  282 GMNDXA(K)=VCELL*EFFXA(K)
      WRITE(6,2231)
      WRITE(6,2188)
      WRITE(6,2189) (GMNDXA(I),GMNDXF(I),GMNDNF(I),I=1,7)
      WRITE(6,2190) (GMNDXA(I),I=8,11)
      IF(MOD.NE.3) WRITE(6,2191) GMNDXA(12)
      IF(MOD.EQ.3) WRITE(6,2192) GMNDXA(12),GMNDXA(14)
      WRITE(6,2193) GMNDXA(15),GMNDXA(13)
      IF(NFUEL.EQ.1) WRITE(6,2194) GMNDXA(16)
      IF(NFUEL.EQ.2) WRITE(6,2195) GMNDXA(16)
      GAVXA=AVXA*VCELL
      WRITE(6,2233)GAVXA
      WRITE(6,5000)                                                    BONE
C                                                                      BONE
C     CALCULATION OF CAPTURE-TO-FISSION RATIOS                         BONE
C                                                                      BONE
      DO285K=1,KF                                                      BONE
      A25TH(K)=(SABTH(1,K)-SFBTH(1,K))/SFBTH(1,K)                      BONE
      A49TH(K)=(SABTH(4,K)-SFBTH(4,K))/SFBTH(4,K)                      BONE
  285 A41TH(K)=(SABTH(6,K)-SFBTH(6,K))/SFBTH(6,K)                      BONE
      IF(NOMISC.EQ.1) GO TO 290
      WRITE(6,2197)                                                    BONE
      WRITE(6,2198)                                                    BONE
      WRITE(6,2200)(K,A25TH(K),A49TH(K),A41TH(K),K=1,KF)               BONE
  290 CONTINUE
      A25BTH=CAPTH(1)/FISTH(1)                                         BONE
      A25BEP=CAPEPI(1)/FISEPI(1)                                       BONE
      A25BFA=CAPFAS(1)/FISFAS(1)                                       BONE
      A25=CAP(1)/FIS(1)                                                BONE
      IF(NOMISC.EQ.1) GO TO 291
      WRITE(6,2202)                                                    BONE
      WRITE(6,2203)                                                    BONE
      WRITE(6,2205)A25BTH,A25BEP,A25BFA,A25                            BONE
  291 IF(FIS(4).EQ.0.) GO TO 295                                       00017760
```

```
      A49BTH=CAPTH(4)/FISTH(4)                                          BONE
      A49BEP=CAPEPI(4)/FISEPI(4)                                        BONE
      A49BFA=CAPFAS(4)/FISFAS(4)                                        BONE
      A49=CAP(4)/FIS(4)                                                 BONE
  295 IF(NOMISC.EQ.1) GO TO 292                                         00017810
      WRITE(6,2208)                                                     BONE
      WRITE(6,2205)A49BTH,A49BEP,A49BFA,A49                             BONE
  292 IF(FIS(6).EQ.0.) GO TO 296                                        00017840
      A41BTH=CAPTH(6)/FISTH(6)                                          BONE
      A41BEP=CAPEPI(6)/FISEPI(6)                                        BONE
      A41BFA=CAPFAS(6)/FISFAS(6)                                        BONE
      A41=CAP(6)/FIS(6)                                                 BONE
  296 IF(NOMISC.EQ.1) GO TO 293                                         00017890
      WRITE(6,2209)                                                     BONE
      WRITE(6,2205)A41BTH,A41BEP,A41BFA,A41                             BONE
      WRITE(6,5000)                                                     BONE
  293 CONTINUE
C
CALCULATION OF TEMPORARY THERMAL VARIABLES FOR PDQ PRINTOUT
C
      TEMA(2)=AVXA
      TEMA(3)=EFFXA(13)
      DO 521 J=4,14
  521 TEMA(J)=EFFXA(J-3)
      DO 507 J=1,14
      TEMB(J)=TEMA(J)
      TEMC(J)=0.0
      TEMD(J)=0.0
      TEME(J)=0.0
  507 TEMF(J)=0.0
      TEMB(1)=EFFXA(12)
      DO 508 J=4,10
      TEMD(J)=EFFXF(J-3)
      TEME(J)=XNU(J-3)
  508 TEMF(J)=KAPPA(J-3)
```

```
C                                                                       BONF
C     SPECIAL EDIT      0.0EV-0.625EV                                   BONE
C                                                                       BONE
      IF(NO625.EQ.0) WRITE(6,2041)
      DO410I=1,10                                                       BONE
      ABSXTH(I)=0.0                                                     BONE
      DO400K=1,KF                                                       BONE
  400 ABSXTH(I)=ABSXTH(I)+SABTHY(I,K)*VOLUME(K)                         BONE
      ABSXTH(I)=ABSXTH(I)/(FBARF*VOLFU)                                 BONE
      IF(I.GT.7) GOTO410                                                BONE
      FISXTH(I)=0.0                                                     BONE
      DO405K=1,KF                                                       BONE
  405 FISXTH(I)=FISXTH(I)+SFBTHY(I,K)*VOLUME(K)                         BONE
      FISXTH(I)=FISXTH(I)/(FBARF*VOLFU)                                 BONE
      NUFXTH(I)=XNU(I)*FISXTH(I)                                        BONE
  410 CONTINUE                                                          BONE
      DO440I=11,16                                                      BONE
      ABSXTH(I)=0.0                                                     BONE
      IF(I.EQ.13) GOTO420                                               BONE
      IF(I.EQ.16) GOTO430                                               BONE
      DO415K=KCL1,KMOD                                                  BONE
  415 ABSXTH(I)=ABSXTH(I)+SABTHY(I,K)*VOLUME(K)                         BONE
      ABSXTH(I)=ABSXTH(I)/(FBARM*VOLMOD)                                BONE
      EFFXA(I)=ABSXTH(I)*FBARM/FBAR                                     BONE
      GOTO440                                                           BONE
  420 DO425K=KF1,KCLAD                                                  BONE
  425 ABSXTH(I)=ABSXTH(I)+SABTHY(I,K)*VOLUME(K)                         BONE
      ABSXTH(I)=ABSXTH(I)/(FBARC*VOLCLA)                                BONE
      EFFXA(I)=ABSXTH(I)*FBARC/FBAR                                     BONE
      GOTO440                                                           BONE
  430 IJ=15                                                             BONE
      IF(NFUEL.EQ.2) IJ=IJ+1                                            BONE
      DO435K=1,KF                                                       BONE
  435 ABSXTH(I)=ABSXTH(I)+SABTHY(IJ,K)*VOLUME(K)                        BONE
      ABSXTH(I)=ABSXTH(I)/(FBARF*VOLFU)                                 BONE
      EFFXA(I)=ABSXTH(I)*FBARF/FBAR                                     BONE
  440 CONTINUE                                                          BONE
      DO455I=1,10                                                       BONE
```

```
      EFFXA(I)=0.0                                                    BONE
      DO445K=1,KE                                                     BONE
  445 EFFXA(I)=EFFXA(I)+SABTHY(I,K)*XX(I,K)*VOLUME(K)                 BONE
      IF(X1BAR(I).EQ.0.) GO TO 22
      EFFXA(I)=EFFXA(I)/(X1BAR(I)*TOTALY*VOLC)                        BONE
   22 IF(I.GT.7) GOTO455                                              BONE
      EFFXF(I)=0.0                                                    BONE
      DO450K=1,KE                                                     BONE
  450 EFFXF(I)=EFFXF(I)+SFBTHY(I,K)*XX(I,K)*VOLUME(K)                 BONE
      IF(X1BAR(I).EQ.0.) GO TO 23
      EFFXF(I)=EFFXF(I)/(X1BAR(I)*TOTALY*VOLC)                        BONE
   23 EFFXNF(I)=XNU(I)*EFFXF(I)                                       BONE
  455 CONTINUE                                                        BONE
C                                                                     BONE
      IF(NO625.EQ.1) GO TO 294
      WRITE(6,2230)                                                   BONE
      WRITE(6,2188)                                                   BONE
      WRITE(6,2189)(ABSXTH(I),FISXTH(I),NUFXTH(I),I=1,7)              BONE
      WRITE(6,2190)(ABSXTH(I),I=8,11)                                 BONE
      IF(MOD.NE.3) WRITE(6,2191) ABSXTH(12)                           BONE
      IF(MOD.EQ.3) WRITE(6,2192) ABSXTH(12),ABSXTH(14)                BONE
      WRITE(6,2193) ABSXTH(15),ABSXTH(13)                             BONE
      IF(NFUEL.EQ.1) WRITE(6,2194) ABSXTH(16)                         BONE
      IF(NFUEL.EQ.2) WRITE(6,2195) ABSXTH(16)                         BONE
      WRITE(6,5000)                                                   BONE
      WRITE(6,2041)                                                   BONE
      WRITE(6,2187)                                                   BONE
      WRITE(6,2188)                                                   BONE
      WRITE(6,2189)(EFFXA(I),EFFXF(I),EFFXNF(I),I=1,7)                BONE
      WRITE(6,2190)(EFFXA(I),I=8,11)                                  BONE
      IF(MOD.NE.3) WRITE(6,2191) EFFXA(12)                            BONE
      IF(MOD.EQ.3) WRITE(6,2192) EFFXA(12),EFFXA(14)                  BONE
      WRITE(6,2193) EFFXA(15),EFFXA(13)                               BONE
      IF(NFUEL.EQ.1) WRITE(6,2194) EFFXA(16)                          BONE
      IF(NFUEL.EQ.2) WRITE(6,2195) EFFXA(16)                          BONE
      WRITE(6,5000)                                                   BONE
C                                                                     BONE
C     MACROSCOPIC EDIT                                                BONE
C                                                                     BONE
  294 WRITE(6,2210)
```

```
      WRITE(6,2212)                                                    BONE
      DIFU(1)=TOTC1/(TOTAL1*SQRT(ABS(BM2)))                            BONE
      DIFU(2)=TOTC2/(TOTAL2*SQRT(ABS(BM2)))                            BONE
      DIFU(3)=(TOTC1+TOTC2)/((TOTAL1+TOTAL2)*SQRT(ABS(BM2)))           BONE
      DIFU(4)=DTH                                                      BONE
      DO286J=1,4                                                       BONE
      SIGMAA(J)=0.0                                                    BONE
      SIGMAF(J)=0.0                                                    BONE
  286 SIGMAN(J)=0.0                                                    BONE
      DO287I=1,16                                                      BONE
      SIGMAA(1)=SIGMAA(1)+ABSFAS(I)/(TOTAL1*VOLC)                      BONE
      SIGMAA(2)=SIGMAA(2)+ABSFPI(I)/(TOTAL2*VOLC)                      BONE
      SIGMAA(3)=SIGMAA(3)+(ABSFAS(I)+ABSEPI(I))/(TOTALF*VOLC)          BONE
  287 SIGMAA(4)=SIGMAA(4)+ABSTH(I)/(TOTAL3*VOLC)                       BONE
      DO288I=1,7                                                       BONE
      SIGMAF(1)=SIGMAF(1)+FISFAS(I)/(TOTAL1*VOLC)                      BONE
      SIGMAN(1)=SIGMAN(1)+SB1(I)*X1BAR(I)/TOTAL1                       BONE
      SIGMAF(2)=SIGMAF(2)+FISFPI(I)/(TOTAL2*VOLC)                      BONE
      SIGMAN(2)=SIGMAN(2)+SB2(I)*X1BAR(I)/TOTAL2                       BONE
      SIGMAF(3)=SIGMAF(3)+(FISFAS(I)+FISFPI(I))/(TOTALF*VOLC)          BONE
      SIGMAN(3)=SIGMAN(3)+((SB1(I)+SB2(I))*X1BAR(I))/TOTALF            BONE
      SIGMAF(4)=SIGMAF(4)+FISTH(I)/(TOTAL3*VOLC)                       BONE
  288 SIGMAN(4)=SIGMAN(4)+FISTH(I)*XNU(I)/(TOTAL3*VOLC)                BONE
      SUMF=0.0                                                         BONE
      DO300J=1,25                                                      BONE
  300 SUMF=SUMF+FP(J)*DELTAE(J)                                        BONE
      SUMF=U*SUMF                                                      BONE
      SIGMAR(1)=(SUMF/TOTAL1)-SIGMAA(1)-DIFU(1)*BM2                    BONE
      SIGMAR(2)=(SIGMAR(1)*TOTAL1/TOTAL2)-SIGMAA(2)-DIFU(2)*BM2        BONE
      SIGMAR(3)=(SUMF/(TOTAL1+TOTAL2))-SIGMAA(3)-DIFU(3)*BM2           BONE
      SIGMAR(4)=0.0                                                    BONE
      DO289J=1,3                                                       BONE
  289 AGE(J)=DIFU(J)/(SIGMAR(J)+SIGMAA(J))                             BONE
      AGE(4)=0.0                                                       BONE
      QU(1)=QFPI                                                       BONE
      QU(2)=QTH                                                        BONE
      QU(3)=QTH                                                        BONE
```

```
      QU(4)=0.0                                                          BONE
C
CALCULATION OF GROUP AVERAGED ENERGY/FISSION TIMES MACRO FISSION C/S
C
      DO 500 J=1,7
  500 TEM(J)=KAPPA(J)*X1BAR(J)
      DO 501 J=1,4
  501 XKSIGF(J)=0.0
      DO 502 J=1,7
      XKSIGF(1)=XKSIGF(1)+TEM(J)*FISXFA(J)
      XKSIGF(2)=XKSIGF(2)+TEM(J)*FISXEP(J)
      XKSIGF(3)=XKSIGF(3)+TEM(J)*FISXFE(J)
  502 XKSIGF(4)=XKSIGF(4)+TEM(J)*EFFXF1(J)
C
CALCULATION OF MACROSCOPIC GMND CROSS SECTIONS
C
      GDIFU=VGRAD*DTH
      GSIGA=VCELL*SIGMAA(4)
      GSIGR=0.0
      GSIGF=VCELL*SIGMAF(4)
      GSIGNF=VCELL*SIGMAN(4)
      GKSIGF=VCELL*XKSIGF(4)
C
      WRITE(6,2215)(DIFU(J),SIGMAA(J),SIGMAR(J),SIGMAF(J),SIGMAN(J),AGE(
     1J),QU(J),XKSIGF(J),J=1,4)
C                                                                        BONE
      SUMD=(DIFU(3)*TOTALF+DIFU(4)*TOTAL3)/(TOTALF+TOTAL3)               BONE
      SUMA=(SIGMAA(3)*TOTALF+SIGMAA(4)*TOTAL3)/(TOTALF+TOTAL3)           BONE
      SUMF=(SIGMAF(3)*TOTALF+SIGMAF(4)*TOTAL3)/(TOTALF+TOTAL3)           BONE
      SUMN=(SIGMAN(3)*TOTALF+SIGMAN(4)*TOTAL3)/(TOTALF+TOTAL3)           BONE
      SUMR=0.0                                                           BONE
      SUMKF=(XKSIGF(3)*TOTALF+XKSIGF(4)*TOTAL3)/(TOTALF+TOTAL3)
      WRITE(6,2217)  SUMD,SUMA,SUMR,SUMF,SUMN,SUMR,SUMR,SUMKF
      WRITE(6,2216)  GDIFU,GSIGA,GSIGR,GSIGF,GSIGNF,GKSIGF
      WRITE(6,2218)  DTHY                                                BONE
C                                                                        BONE
      REAL K3GR                                                          BONE
      REAL K2GR                                                          BONE
      REAL K1GR                                                          BONE
      SUMA1=SIGMAA(1)+SIGMAR(1)+DIFU(1)*BUCKL                            BONE
```

```
      SUM1=SIGMAN(1)/SUMA1                                                  BONE
      SUMA2=SIGMAA(2)+SIGMAR(2)+DIFU(2)*BUCKL                               BONE
      SUM2=SIGMAR(1)*SIGMAN(2)/(SUMA1*SUMA2)                                BONE
      SUM3=SIGMAR(1)*SIGMAR(2)*SIGMAN(4)/(SUMA1*SUMA2*(SIGMAA(4)+DIFU(4)BONE
     1*BUCKL))                                                              BONE
      K3GR=SUM1+SUM2+SUM3                                                   BONE
      SUMA1=SIGMAA(3)+SIGMAR(3)+DIFU(3)*BUCKL                               BONE
      SUM1=SIGMAN(3)/SUMA1                                                  BONE
      SUM2=SIGMAR(3)*SIGMAN(4)/(SUMA1*(SIGMAA(4)+DIFU(4)*BUCKL))            BONE
      K2GR=SUM1+SUM2                                                        BONE
      K1GR=SUMN/(SUMA+SUMD*BUCKL)                                           BONE
      WRITE(6,2220) K3GR,K2GR,K1GR                                          BONE
      WRITE(6,2270) CRIT
C
C  CALCULATION OF EQUIVALENT MICROSCOPIC TRANSPORT C/S (EQITR) FOR HYD.
C
      DO 460 I=1,4
      BB(I)=1./(3.*DIFU(I))-SIGMAA(I)
  460 EQITRS(I)=BB(I)/X1BAR0(12)
      EQITR(1)=EQITRS(1)+ABSXFA(12)
      EQITR(2)=EQITRS(2)+ABSXFP(12)
      EQITR(3)=EQITRS(3)+ABSXFE(12)
      EQITR(4)=EQITRS(4)+TEMB(1)
      TEMA(1)=EQITR(4)
C
C     CALC. OF EQUIVALENT MICROSCOPIC REMOVAL CROSS SECTION FOR HYDROGEN
C
      DO 465 I=1,4
  465 EQIREM(I)=SIGMAR(I)/X1BAR0(12)
C
CALCULATION OF TEMPORARY FAST VARIABLES TO BE PRINTED OUT IN PDQ OUTPUT
C
      DO 503 J=4,14
  503 TEMFA(J)=ABSXFE(J-3)
      DO 504 J=1,14
      TEMFD(J)=0.0
```

```
      TEMFE(J)=0.0
  504 TEMFC(J)=0.0
      DO 505 J=4,10
      TEMFD(J)=FISXFE(J-3)
  505 TEMFE(J)=FEPINU(J-3)
      TEMFA(1)=EQITR(3)
      TEMFA(2)=ABSXFE(13)
      IF(NCLAD.EQ.1) TEMFA(3)=ABSXFE(15)
      IF(NCLAD.EQ.3) TEMFA(3)=ABSXFE(17)
      IF(NCLAD.EQ.2) TEMFA(3)=0.0
      TEMFB(1)=ABSXFE(12)
      TEMFC(1)=EQIREM(3)
      DO 520 J=2,14
  520 TEMFB(J)=TEMFA(J)
C
      WRITE(6,2250)
      WRITE(6,2023)
      WRITE(6,2251) (EQITR(I),I=1,4)
      WRITE(6,2252)
      WRITE(6,2023)
      WRITE(6,2251) (EQIREM(I),I=1,4)
C
      SIGMD=ENC(12)*TEMB(1)+ENC(14)*TEMB(2)+ENC(15)*TEMB(14)
      EQITRM=(1/(3.*DTHMR)-SIGMD)/ENC(12)+TEMB(1)
      WRITE(6,2253) DTHMR
      WRITE(6,2254) DTHYMR
      WRITE(6,2280) EQITRM
C
      IF(NOPDQ.EQ.1) GO TO 999
      WRITE(6,2255)
      WRITE(6,2256)
      WRITE(6,2257)
      WRITE(6,2258)
      WRITE(6,2259)(TEMFA(I),TEMFB(I),TEMFC(I),TEMFD(I),TEMFE(I),TEMF(I)
     1,I=1,2)
      IF(NCLAD.EQ.1) WRITE(6,2260)TEMFA(3),TEMFB(3),TEMFC(3),TEMFD(3),TE
```

```
     1MFF(3),TEMF(3)
      IF(NCLAD.EQ.2) WRITE(6,2261)
      IF(NCLAD.EQ.3) WRITE(6,2262)TEMFA(3),TEMFB(3),TEMFC(3),TEMFD(3),TE
     1MFE(3),TEMF(3)
      WRITE(6,2263)(TEMFA(I),TEMFB(I),TEMFC(I),TEMFD(I),TEMFE(I),TEMF(I)
     1,I=4,14)
      WRITE(6,2264)
      WRITE(6,2258)
      WRITE(6,2259)(TEMA(I),TEMB(I),TEMC(I),TEMD(I),TEME(I),TEMF(I),I=1,
     12)
      IF(NCLAD.EQ.1) WRITE(6,2260) TEMA(3),TEMB(3),TEMC(3),TEMD(3),TEME(
     13),TEMF(3)
      IF(NCLAD.EQ.2) WRITE(6,2261)
      IF(NCLAD.EQ.3) WRITE(6,2262) TEMA(3),TEMB(3),TEMC(3),TEMD(3),TEME(
     13),TEMF(3)
      WRITE(6,2263)(TEMA(I),TEMB(I),TEMC(I),TEMD(I),TEME(I),TEMF(I),I=4,
     114)
      WRITE(6,2265)
C
CALCULATION OF TEMPORARY VALUES FOR THERMAL GMND PDQ PRINTOUT.
C
      DO 506 J=1,14
      TEMA(J)=TEMA(J)/VGRAD
      TEMB(J)=TEMB(J)*VCELL
  506 TEMD(J)=TEMD(J)*VCELL
      TEMA(1)=EDITR(4)/VGRAD
C
      WRITE(6,2255)
      WRITE(6,2266)
      WRITE(6,2256)
      WRITE(6,2267)
      WRITE(6,2258)
      WRITE(6,2259)(TEMA(I),TEMB(I),TEMC(I),TEMD(I),TEME(I),TEMF(I),I=1,
```

```
     12)
      IF(NCLAD.EQ.1) WRITE(6,2260) TEMA(3),TEMB(3),TEMC(3),TEMD(3),TEME(
     13),TEMF(3)
      IF(NCLAD.EQ.2) WRITE(6,2261)
      IF(NCLAD.EQ.3) WRITE(6,2262) TEMA(3),TEMB(3),TEMC(3),TEMD(3),TEME(
     13),TEMF(3)
      WRITE(6,2263)(TEMA(I),TEMB(I),TEMC(I),TEMD(I),TEME(I),TEMF(I),I=4,
     114)
      WRITE(6,2265)
C                                                                       BONE
 5000 FORMAT(1H1)                                                       BONE
 2023 FORMAT  (//28X,65H   FAST         EPITHERMAL     EPITHERMAL + FAST BONE
     1       THERMAL     )                                            BONE
 2041 FORMAT(///22X,68H*****  RESULTS ON THIS PAGE ARE BASED ON AVERAGESBONE
     1 TO 0.625 EV  *****)                                            BONE
 2115 FORMAT  ////1X, 29HTHERMAL UTILIZATION FACTOR = E10.5 /88H(NUMBERBONE
     1OF NEUTRONS PRODUCED BY THERMAL FISSION)/(NUMBER OF NEUTRONS ABSORBONE
     2BED IN FUEL) = E10.5  /89H(NUMBER OF NEUTRONS PRODUCED BY THERMAL BONE
     3FISSION)/(NUMBER OF NEUTRONS ABSORBED IN CELL) = E10.5)           BONE
 2120 FORMAT  ////1X,100HDELTA25 = (U-235 FISSIONS FOR NEUTRONS ABOVE 1BONE
     1.855EV)/(U-235 FISSIONS FOR NEUTRONS BELOW 1.855EV) = E10.5/51H DEBONE
     2LTA28 = (U-238 FISSIONS)/(NON U-238 FISSIONS) = E10.5/99H RHO28 = BONE
     3(U-238 CAPTURES FOR NEUTRONS ABOVE 1.855EV)/(U-238 CAPTURES FOR NEBONE
     4UTRONS BELOW 1.855EV) = E10.5)                                    BONE
 2122 FORMAT  (//10X,99HU-238 CAP/FISSILE ABS     U-238 FIS/FISSILE ABS BONE
     1    U-238 CAP/U-235 FIS     FERTILE CAP/FISSILE ABS)              BONE
 2125 FORMAT(/12X,E10.5,18X,E10.5,17X,E10.5,15X,E10.5)                  BONE
 2130 FORMAT(///1X,33HINFINITE MULTIPLICATION FACTOR = 1PE11.5)         BONE
 2132 FORMAT  (///21X,78HPOINTWISE   AVERAGE   THERMAL   NEUTRON   VELOCBONE
     1ITY(1 UNIT = 2200METERS/SECOND))                                  BONE
 2133 FORMAT  (//39X,42HPOINT NUMBER IN CELL     NEUTRON VELOCITY )     BONE
 2135 FORMAT  ( 48X,I2,17X,E10.5)                                       BONE
 2136 FORMAT(///1X,36HPARAMETERS USED IN L-FACTOR SEARCH -//22H SLOWING BONE
     1DOWN POWER = E10.5/18H DANCOFF FACTOR = E10.5/28H U-238 RESONANCE BONE
     2INTEGRAL = E10.5/38H U-238 RESONANCE ESCAPE PROBABILITY = E10.5/9HBONE
     3 OMEGA = E10.5/28H CONVERGED U-238 L-FACTOR = E10.5)              BONE
 2137 FORMAT  (///20X,79HREGIONWISE   AVERAGE   THERMAL   NEUTRON   VELOBONE
```

```
     1CITY(1 UNIT = 2200METERS/SECOND))                                    BONE
2138 FORMAT   (//32X,55H   FUEL            CLAD        MODERATOR          BONE
     1CELL    )                                                            BONE
2140 FORMAT   (/32X,E10.5,5X,F10.5,5X,E10.5,5X,E10.5)                      BONE
2141 FORMAT(///1X,32HCONVERGED L-FACTOR FOR U-235 IS E10.5/1X,32HCONVERBONE
     1GED L-FACTOR FOR U-238 IS E10.5)                                     BONE
2142 FORMAT   (///29X,62HPOINTWISE   THERMAL   NEUTRON   TEMPERATURE   SBONE
     1HIFT(DEGREES K))                                                     BONE
2143 FORMAT   (//39X,42HPOINT NUMBER IN CELL     TEMPERATURE SHIFT)       BONE
2145 FORMAT   ( 48X,I2,18X,E10.5)                                          BONE
2148 FORMAT   (///24X,73HREGIONWISE   AVERAGE   THERMAL   NEUTRON   TEMPBONE
     1ERATURE   SHIFT(DEGREES K))                                          BONE
2152 FORMAT   (///14X,91HISOTOPIC - POINTWISE - AVERAGE - THERMAL - MICRBONE
     1OSCOPIC - ABSORPTION   CROSS SECTIONS(BARNS))                        BONE
2153 FORMAT(//1X,107HPOINT NUMBER IN CELL    U-235        U-236          BONE
     1U-238       PU-239       PU-240       PU-241       PU-242)          BONE
2154 FORMAT(10X,I2,10X,E10.5,3X,E10.5,3X,E10.5,3X,E10.5,3X,E10.5,3X,E10BONE
     1.5,3X,E10.5)                                                         BONE
2155 FORMAT(///7X,94HPOINT NUMBER IN CELL   XE-135       SM-149       FIBONE
     1S.PRO.       B-10       HYDROGEN      OXIGEN)                       BONE
2156 FORMAT(16X,I2,10X,E10.5,3X,E10.5,3X,E10.5,3X,E10.5,3X,E10.5,3X,E10BONE
     1.5)                                                                  BONE
2157 FORMAT(///1X,108HPOINT NUMBER IN CELL   XE-135       SM-149       FBONE
     1IS.PRO.       B-10       DEUTERIUM      OXIGEN      HYDROGEN)      BONE
2158 FORMAT(//35X,34HPOINT NUMBER IN CELL              AL)                 BONE
2159 FORMAT(44X,I2,17X,E10.5)                                              BONE
2160 FORMAT(//26X,51HPOINT NUMBER IN CELL              SS                  ABONE
     1L)                                                                   BONE
2161 FORMAT(//26X,51HPOINT NUMBER IN CELL              ZR                  ABONE
     1L)                                                                   BONE
2162 FORMAT(35X,I2,17X,E10.5,7X,E10.5)                                     BONE
2164 FORMAT   (///16X,88HISOTOPIC - POINTWISE - AVERAGE - THERMAL - MICRBONE
     1OSCOPIC - FISSION   CROSS SECTIONS(BARNS))                           BONE
2168 FORMAT   (///15X,90HISOTOPIC - ENERGYWISE - REGION-AVERAGED - MICROBONE
     1SCOPIC - ABSORPTION   CROSS SECTIONS(BARNS))                         BONE
2170 FORMAT   (/18X,5HU-235,5X,E10.5,5X,E10.5,9X,E10.5,9X,E10.5/18X,5HU-BONE
     1236,5X,E10.5,5X,E10.5,9X,E10.5,9X,E10.5/18X,5HU-238,5X,E10.5,5X,E1BONE
     20.5,9X,E10.5,9X,E10.5/18X,6HPU-239,4X,E10.5,5X,E10.5,9X,E10.5,9X,EBONE
```

```
     310.5/18X,6HPU-240,4X,E10.5,5X,E10.5,9X,E10.5,9X,E10.5/18X,6HPU-241BONE
     4,4X,E10.5,5X,E10.5,9X,E10.5,9X,E10.5/18X,6HPU-242,4X,E10.5,5X,E10.BONE
     55,9X,E10.5,9X,E10.5)                                                BONE
2171 FORMAT(18X,6HXE-135,4X,E10.5,5X,E10.5,9X,E10.5,9X,E10.5/18X,6HSM-1BONE
     149,4X,E10.5,5X,E10.5,9X,E10.5,9X,E10.5/18X,8HFIS.PRO.,2X,E10.5,5X,BONE
     2E10.5,9X,E10.5,9X,E10.5/18X,4HB-10,6X,E10.5,5X,E10.5,9X,E10.5,9X,EBONE
     310.5)                                                               BONE
2172 FORMAT(18X,8HHYDROGEN,2X,E10.5,5X,E10.5,9X,E10.5,9X,E10.5/18X,6HO(BONE
     1MOD),4X,E10.5,5X,E10.5,9X,E10.5,9X,E10.5/18X,9HDEUTERIUM,1X,E10.5,BONE
     25X,E10.5,9X,E10.5,9X,E10.5/18X,6HSS-304,4X,E10.5,5X,E10.5,9X,E10.5BONE
     3,9X,E10.5/18X,8HAL(CLAD),2X,E10.5,5X,E10.5,9X,E10.5,9X,E10.5/18X,2BONE
     4HZR,8X,E10.5,5X,E10.5,9X,E10.5,9X,E10.5)                            BONE
2173 FORMAT(18X,7HO(FUEL),3X,E10.5,5X,E10.5,9X,E10.5,9X,E10.5)            BONE
2174 FORMAT(18X,8HAL(FUEL),2X,E10.5,5X,E10.5,9X,E10.5,9X,E10.5)           BONE
2175 FORMAT(////,18X,79HNOTE - A VALUE .10000E 21 APPEARS WHEN THE CROSBONE
     1S SECTION DATA ARE NOT AVAILABLE)                                   BONE
2177 FORMAT  (///16X,87HISOTOPIC - ENERGYWISE - REGION-AVERAGED - MICROBONE
     1SCOPIC - FISSION   CROSS SECTIONS(BARNS))                           BONE
2182 FORMAT  (///15X,89HISOTOPIC - ENERGYWISE - REGION-AVERAGED - MICROBONE
     1SCOPIC - NUFISSION   CROSS SECTIONS(BARNS))                         BONE
2187 FORMAT(///28X,56HISOTOPIC - EFFECTIVE - THERMAL - CROSS   SECTIONSBONE
     1(BARNS))                                                            BONE
2188 FORMAT(//46X,10HABSORPTION,7X,7HFISSION,7X,9HNUFISSION)              BONE
2189 FORMAT(/26X,5HU-235,15X,E10.5,5X,E10.5,5X,E10.5/26X,5HU-236,15X,E1BONE
     10.5,5X,E10.5,5X,E10.5/26X,5HU-238,15X,E10.5,5X,E10.5,5X,E10.5/26X,BONE
     26HPU-239,14X,E10.5,5X,E10.5,5X,E10.5/26X,6HPU-240,14X,E10.5,5X,E10BONE
     3.5,5X,E10.5/26X,6HPU-241,14X,E10.5,5X,E10.5,5X,E10.5/26X,6HPU-242,BONE
     414X,E10.5,5X,E10.5,5X,E10.5)                                        BONE
2190 FORMAT(26X,6HXE-135,14X,E10.5/26X,6HSM-149,14X,E10.5/26X,8HFIS.PROBONE
     1.,12X,E10.5/26X,4HB-10,16X,E10.5)                                   BONE
2191 FORMAT(26X,8HHYDROGEN,12X,E10.5)                                     BONE
2192 FORMAT(26X,9HDEUTERIUM,11X,E10.5/26X,8HHYDROGEN,12X,E10.5)           BONE
2193 FORMAT(26X,6HO(MOD),14X,E10.5/26X,4HCLAD,16X,E10.5)                  BONE
2194 FORMAT(26X,7HO(FUEL),13X,E10.5)                                      BONE
2195 FORMAT(26X,8HAL(FUEL),12X,E10.5)                                     BONE
```

```
2197 FORMAT  (///23X,74HISOTOPIC - POINTWISE - THERMAL - CAPTURE - TO -BONE
    1 THERMAL - FISSION   RATIOS)                                      BONE
2199 FORMAT  (//20X,80HPOINT NUMBER IN FUEL              ALPHA25       BONE
    1     ALPHA49              ALPHA41)                                BONE
2200 FORMAT  ( 29X,I2,21X,E10.5,10X,E10.5,10X,E10.5)                   BONE
2202 FORMAT  (///23X,73HISOTOPIC - REGION-AVERAGED - ENERGYWISE - CAPTUBONE
    1RE - TO - FISSION   RATIOS)                                       BONE
2203 FORMAT (//24X,73HALPHA25 THERMAL     ALPHA25 EPITHERMAL     ALPHA2BONE
    15 FAST     ALPHA25 TOTAL)                                         BONE
2205 FORMAT (/27X,E10.5,11X,E10.5,10X,E10.5, 7X,E10.5)                 BONE
2208 FORMAT  (//24X,73HALPHA49 THERMAL     ALPHA49 EPITHERMAL     ALPHABONE
    149 FAST     ALPHA49 TOTAL)                                        BONE
2209 FORMAT  (//24X,73HALPHA41 THERMAL     ALPHA41 EPITHERMAL     ALPHABONE
    141 FAST     ALPHA41 TOTAL)                                        BONE
2210 FORMAT(///48X,16HMACROSCOPIC EDIT)                                BONE
2212 FORMAT(//,2X,12HENERGY GROUP,3X,9HDIFFUSION,4X,10HABSORPTION,6X,7H
    1REMOVAL,7X,7HFISSION,6X,9HNUFISSION,8X,3HAGE,12X,1HQ,9X,'KFISSION'
    2)
2215 FORMAT(/6X,4HFAST,6X,8(E10.5,4X),/3X,10HEPITHERMAL,3X,8(E10.5,4X),
    1/3X,10HFAST + EPI,3X,8(E10.5,4X),/4X,7HTHERMAL,5X,8(E10.5,4X))
2216 FORMAT(//1X,'THERMAL(GMND)',2X,E10.5,4X,E10.5,4X,E10.5,4X,E10.5,4X
    1,E10.5,32X,E10.5)
2217 FORMAT(/5X,5HTOTAL,6X,8(E10.5,4X))
2218 FORMAT(//1X,63HTHERMAL DIFFUSION COEFFICIENT(BASED ON AVERAGES TO BONE
    10.625 EV) = E10.5)                                                BONE
2220 FORMAT(///1X,44HEFFECTIVE MULTIPLICATION FACTOR(3 GROUPS) = 1PE11.BONE
    15/1X,44HEFFECTIVE MULTIPLICATION FACTOR(2 GROUPS) = 1PE11.5/1X,44HBONE
    2EFFECTIVE MULTIPLICATION FACTOR(1 GROUP ) = 1PE11.5)               BONE
2230 FORMAT(//26X,60HISOTOPIC - REGION-AVERAGED - THERMAL   CROSS SECTIBONE
    1ONS(BARNS))                                                       BONE
2231 FORMAT(///28X,'ISOTOPIC - EFFECTIVE - THERMAL(GMND) CROSS SECTIONS
    1(BARNS*2200 M/SEC)')
2232 FORMAT(/////28X,'ISOTOPIC - SPECTRUM AVERAGED NU (THERMAL NU NOT S
    1PECTRUM AVERAGED)')
2233 FORMAT(//28X,'CELL AVERAGED THERMAL ABSORPTION C/S FOR OXYGEN = ',
```

```
     XE10.5)
2250 FORMAT(//1X,'APPROXIMATE MICROSCOPIC TRANSPORT C/S FOR HYDROGEN (B
     1ARNS)')
2251 FORMAT(/28X,E10.5,5X,F10.5,9X,E10.5,11X,E10.5)
2252 FORMAT(///1X,'APPROXIMATE MICROSCOPIC REMOVAL C/S FOR HYDROGEN (BA
     1RNS)')
2253 FORMAT(//' THERMAL DIFFUSION COEFFICIENT OF MODERATOR REGION ONLY
     1 = ',E10.5)
2254 FORMAT(1X,'THERMAL DIFFUSION COEFFICIENT OF MODERATOR REGION ONLY
     1(.625EV EDIT) = ',E10.5)
2255 FORMAT(1H1,38X,'***SPECIAL FORMATTED OUTPUT FOR USE WITH PDQ***')
2256 FORMAT (/10X,'MICROSCOPIC OUTPUT')
2257 FORMAT (/10X,'***GROUP 1 CROSS SECTIONS (FAST + EPITHERMAL) IN BAR
     1NS')
2258 FORMAT(//16X,49HNUCLIDE    'TRANSPORT'    ABSORPTION    'REMOVAL',
     18X,'FISSION',8X,'NU',10X,'KAPPA')
2259 FORMAT(/15X,'HYDROGEN',5X,6(E10.5,4X),/15X,'OXYGEN',7X,6(E10.5,4X)
     1)
2260 FORMAT (15X,'SS-304',7X,6(E10.5,4X))
2261 FORMAT (15X,'THIS OUTPUT IS NOT SET UP TO HANDLE AL CLAD')
2262 FORMAT (15X,'ZIRCONIUM',4X,6(E10.5,4X))
2263 FORMAT (/17X,'U-235',6X,6(E10.5,4X),/17X,'U-236',6X,6(E10.5,4X),/1
     17X,'U-238',6X,6(E10.5,4X),//16X,'PU-239',6X,6(E10.5,4X),/16X,'PU-2
     240',6X,6(E10.5,4X)/16X,'PU-241',6X,6(E10.5,4X),//16X,'PU-242',6X,6
     3(E10.5,4X),/16X,'XE-135',6X,6(E10.5,4X),/16X,'SM-149',6X,6(E10.5,4
     4X),//15X,'FIS. PRO.',4X,6(E10.5,4X),/15X,'BORON-10',5X,6(E10.5,4X)
     5)
2264 FORMAT (//10X,'***GROUP 2 CROSS SECTIONS (THERMAL) IN BARNS')
2265 FORMAT(//5X,'***NOTE*** THE TRANSPORT AND REMOVAL CROSS SECTIONS A
     1RE THOSE WHICH HAVE BEEN',/16X,'OBTAINED BY APPROXIMATE METHODS. S
     3EE MANUAL REVISION UNDER PDQ OUTPUT EDIT.')
2266 FORMAT(1H+,88X,'(PAGE 2)')
2267 FORMAT(/10X,'***GROUP 2 (GMND) CROSS SECTIONS IN BARNS*2200 M/SEC'
     1)
```

```
 2268 FORMAT   (//32X,'   FUEL            CLAD         MODERATOR
     1CELL          AVERAGED OVER GRADIENT SPECTRUM')
 2269 FORMAT(/32X,4(E10.5,5X),11X,E10.5)
 2270 FORMAT(1X,33HINFINITE MULTIPLICATION FACTOR = ,1PE11.5)
 2280 FORMAT(1X,'THERMAL APPROXIMATE MICRO TRANSPORT C/S FOR HYDROGEN FO
     1R MODERATOR ONLY = ',E10.5)
C                                                                       BONE
  999 RETURN
      END                                                               BONE
```

APPENDIX F

LASER-M INPUT DATA FOR 1.5 W/O PUO_2 - UO_2 and 6.6 W/O PUO_2 - UO_2 CRITICALS

For the convience of future users of LASER-M, the input decks for the criticals analysed in the present study are listed on the following pages.

```
 PU CRITICALS 1.5 W/O PU  PITCH = .55 IN.
  319     0     0
14 5 4 1 3 1 1 1 1 0 1 0 1 1 1 1
  144.       .0048      298.
  1.           1.       .64919       1.         1.         1.         1.
11111233333344
     1     5  .4724
     2     1  .0686
     3     6  .1925
     4     2  .0642
.000033623             .0209882  .000292601.000025018.000002333.96698E-07
                                  .042697   .033366   .0150542
 1  298.


 PU CRITICALS 1.5 W/O PU  PITCH = .60 INCHES
  320     0     0
14 5 4 1 3 1 1 1 1 0 1 0 1 1 1 1
  144.      .006513     298.
  1.           1.       .699         1.         1.         1.         1.
11111233333344
     1     5  .4724
     2     1  .0686
     3     6  .2592
     4     2  .0864
.000033623             .0209882  .000292601.000025018.000002333.96698E-07
                                  .042697   .033366   .0150542
 1  298.
```

```
 PU CRITICALS 1.5 W/O PU  PITCH = .71 INCHES
  321     0     0
14 5 4 1 3 1 1 1 1 0 1 0 1 1 1 1
  144.     .007853     298.
  1.          1.      .64919       1.        1.         1.        1.
11111233333344
     1     5  .4724
     2     1  .0686
     3     6  .4056
     4     2  .1352
.000033623            .0209882  .000292601.000025018.000002333.96698E-07
                                  .042697   .033366   .0150542
 1  298.


 PU CRITICAL EXPERIMENTS(6.6 W/O PU SAXTON) PITCH=.52 IN. BUCK&L SEARCH
  311     1     0
14 5 4 1 3 1 1 1 1 0 1 0 1 1 1 1
  144.      .01088     290.
  1.          1.       .699       1.        1.         1.        1.
11111233333344
     1     5  .4285
     2     1  .068
     3     6  .2487
     4     2  .0829
.000154265            .0213037  .00137205 .000129946.134967E-4.000000601
                                  .04596189 .0333723  .0378924
10  .000001
 0  290.
1
```

```
 PU CRITICAL EXPERIMENTS(6.6 W/O PU SAXTON) PITCH=.56 INCHES  L SEARCH
  326     0     0
14 5 4 1 3 1 1 1 1 0 1 0 1 1 1 1      1
  144.       .01215       289.
  1.           1.        .699        1.        1.         1.        1.
111111233333344
     1     5  .4285
     2     1  .068
     3     6  .306
     4     2  .102
.000154265              .0213037   .00137205 .000129946.134967E-4.000000601
                                   .04596189 .0333723   .0378924
 0  289.
1


 PU CRITICAL 6.6 W/O PU SAXTON PITCH = .735 IN. L SEARCH
  325     0     0
14 5 4 1 3 1 1 1 1 0 1 0 1 1 1        1
  144.      .01596     297.
  1.           1.        .699        1.        1.         1.        1.
111111233333344
     1     5  .4285
     2     1  .068
     3     6  .55679
     4     2  .1856
.000154265              .0213037   .00137205 .000129946.134967E-4.000000601
                                   .04596189 .0333723   .0378924
 0  297.
```

```
 PU CRITICAL - SAXTON - 6.6 W/O PU PITCH=.56 IN. **BORON=337 WPPM L SEAR
   328     0     0
14 5 4 1 3 1 1 1 1 0 1 0 1 1 1 1      1
   144.      .01123     291.
   1.          1.        .699        1.        1.         1.        1.
11111233333344
     1     5  .4285
     2     1  .068
     3     6  .306
     4     2  .102
.000154265             .0213037   .00137205 .000129946.134967E-4.000000601
                                  .04596189 .0333723  .0378924  .000018731
 0  291.
```

APPENDIX G

SUPPLEMENTAL DESCRIPTION OF LASER

The information contained in this Appendix, along with Sections 2.1 and 5.2, is included to give the reader a more complete understanding of the computer code LASER than is obtained from the normal code summary.

As mentioned in Section 2.1, LASER uses different treatments in the thermal energy range (up to 1.855 eV) and the fast energy ranges.

In the non-thermal range the slowing down of neutrons by inelastic scattering is assumed to be isotropic and is determined using inelastic scattering matrices included in the library (MLIB). No provision is made for explicitly calculating (n,2n) reactions, although library data may be obtained that has modified values of ν(neutrons per fission) to account for this contribution. Absorption resonance integrals are calculated using the narrow resonance infinite-mass approximation with resonance parameters from the library. Corrections for resonance self-shielding, the Dancoff effect, and Doppler broading is made by use of input "L factors" (self-shielding factors) for the various nuclides. An L factor is essentially used as a means to fractionally reduce the absorption in a specific nuclide in the non-thermal region to account for the effects mentioned above which are

caused, in part, by the lumping of the absorbers (something the non-thermal calculation does not treat since it does a homogeneous calculation).

LASER contains two options for the search of L factors. Both options are based on iterative procedures which converge on the parameter ω^i (ratio of nonthermal captures in nuclide i to neutrons thermalized). The first, and most often used option, allows for a calculation of the U-238 self-shielding factor according to the procedures described by Strawbridge.[19] Basically, the U-238 resonance escape probability, p^{238}, is calculated with a resonance integral correlation which matches the measurements of Hellstrand. A MUFT calculation is performed with zero leakage ($B^2=0$) and all capture cross sections set to zero, except for U-238. Iterations are performed on the L factor for U-238 until the value of ω^{238} calculated from the MUFT results agrees with the value of ω^{238} obtained from the formula

$$\omega^{238} = \frac{1 - p^{238}}{p^{238}} \quad . \tag{2.1}$$

The converged L factor is then used in a normal MUFT calculation.

In the thermal region the energy mesh (given in Appendix F) has been set up such that accurate representations of the 0.296 eV Pu-239 resonance and of the 1.056 eV Pu-240

resonance are obtained. In light water systems LASER allows the user a choice of either the Wigner-Wilkins free gas kernal, or the more exact bound proton scatter kernal of Nelkin. LASER calculates the thermal flux spectrum, $\bar{\phi}^{th}(E)$, at up to 14 points in the cell and at up to 5 points in the fuel. The cross sections of the various nuclides from the thermal cross section library are then averaged over the spectrum at each point, yielding pointwise spectrum averaged cross sections for each nuclide in the cell. This is an important calculation since the spectrum changes significantly through various parts of the cell.

Additionally, it should be noted that in the thermal energy range LASER calculates both region averaged microscopic cross sections and effective microscopic cross sections. Effective cross sections, $\bar{\sigma}^{i}_{eff}$, are defined such that when combined with a cell averaged isotopic concentration, $\bar{N}^{i}$, and the average cell thermal flux, $\bar{\phi}^{th}$, they yield the correct reaction rates. Thus the thermal macroscopic parameters output by LASER are, in effect, formed by

$$\bar{\Sigma}^{th}_{\alpha} = \sum_{i} \bar{N}^{i}\bar{\sigma}^{i}_{\alpha,eff} \quad , \tag{2.2}$$

where the sum over i is over all nuclides and α denotes absorption and fission. Effective cross sections take into account the flux depression in the fuel and are sometimes written as $\bar{g}^{\gamma}\bar{\sigma}^{\gamma}$, where $\bar{g}^{\gamma}$ is the disadvantage factor in

region γ (i.e. $\bar{\phi}^{th}_{\alpha}/\bar{\phi}^{th}_{cell}$) and $\bar{\sigma}^{\gamma}$ is the region averaged microscopic cross section in region γ (γ is typically taken as fuel, clad, and moderator).

Another important feature of the thermal calculation is that LASER Doppler broadens the large 1.056 eV Pu-240 resonance using resonance parameters from subroutine DOPL.

LASER provides for control searches by allowing the critical materials buckling to be searched or by searching for the critical poison (boron) concentration. In the buckling search the buckling is varied until the eigenvalue (λ) is one. Since the thermal spectrum calculation is independent of the buckling only the MUFT calculation is repeated at each iteration. The searched buckling, which is the material buckling of the cell, is then used to calculate the fast and epithermal spectrum. The input geometric buckling, however, is still used to calculate the total leakage from the cell. In the poison search the boron concentration is varied until λ=1. Since the thermal spectrum is sensitive to the boron concentration, both the THERMOS (thermal) and MUFT (non-thermal) calculations must be performed at each iteration. This increases the cost of the calculation considerably and, therefore, the poison search was not used in this work.

When performing a burnup calculation, LASER requires the spatial distribution of epithermal captures in U-238 as input. This distribution accounts for the non-uniform buildup of Pu-239 in the fuel and is normalized by LASER such that the cell total capture rate using the input distribution is equal to the cell total capture calculated with MUFT. It is generally acceptable to use the results of a Monte Carlo calculation for the spatial distribution presented in Ref. 16. The volume averaged values (using 5 points in the fuel) of the epithermal capture rate distribution from Ref. 4.6 were calculated by Mertens[5] and these values were used in the present study. Additionally, LASER requires cross sections for the pseudo fission product as a function of burnup as input for depletion calculations. In LASER, the fission products are separated into Xe-135, the directly produced Sm-149, and all other fission products are lumped into one pseudo fission product. The cross sections for the lumped fission products are defined such that one fission product is produced per fission. Calculation of the pseudo fission product cross sections are normally done with the CINDER[20] program (see Section 7.2 for further discussion).

As discussed in Chapter 1, LASER has been found to be more accurate than other commonly used spectrum codes. However, the standard version of LASER does have a number of

major limitations. In addition to being more costly than most other spectrum codes, LASER does not allow burnable poison to be placed in the fuel or grid structure to be placed in the moderator. LASER has no extra region such as in LEOPARD and there are no provisions for an "unfueled" cell to be calculated in a straightforward manner. Additionally, the standard version of LASER does not edit microscopic removal or transport cross sections. Also, during burnup, LASER has no provision to change the concentration of boron except with the very expensive poison search and time steps of constant length must be used.